Analyses of diurnal rhythms in human post-mortem tissues

Dissertation

zur Erlangung des Doktorgrades
der Naturwissenschaften

vorgelegt beim Fachbereich Biowissenschaften
der Johann Wolfgang Goethe-Universität
in Frankfurt am Main

von
Katrin Ackermann
aus Neunkirchen/Saar

Frankfurt 2007
(D30)

vom Fachbereich Biowissenschaften der Johann Wolfgang Goethe-Universität als Dissertation angenommen.

Dekan: Prof. Dr. Volker Müller

Gutachter: Prof. Dr. Jörg H. Stehle; Prof. Dr. Jürgen H. Bereiter-Hahn

Datum der Disputation:

‚Because the universe was full of ignorance all around and the scientist panned through it like a prospector crouched over a mountain stream, looking for the gold of knowledge among the gravel of unreason, the sand of uncertainty and the little whiskery eight-legged swimming things of superstition.
Occasionally he would straighten up and say things like "Hurrah, I´ve discovered Boyle`s Third Law." And everyone knew where they stood.'

from Terry Pratchett´s ‚Witches abroad'

...or in other words...

‚Still confused, but on a higher level.'

O. Vintermyr

Table of Contents

Abbreviations

A	Alanine
AANAT	arylalkylamine *N*-acetyltransferase
A/DSPS	advanced/delayed sleep phase syndrome
aMT6-s	6-sulfatoxymelatonin
APS	ammonium peroxodisulfate
BMAL1	brain and muscle ARNT-like 1 protein
BSA	bovine serum albumin
cAMP	cyclic adenosine monophosphate
CLOCK	circadian locomotor output cycles kaput
CRY	cryptochrome
DAB	diaminobenzidine
ddH_2O	double destilled water
DLMO	dim-light-melatonin-onset
DNA	2'-deoxyribonucleic acid
dNTPs	mix of 2'-deoxynucleosid-triphosphates
EDTA	ethylendiamine tetra-acetic acid
ELISA	enzyme-linked immunosorbent assay
FSH	follicle-stimulating hormone
HIOMT	hydroxyindole *O*-methyltransferase
ICER	inducible cAMP early repressor
kDa	kilodalton
M-MLV	moloney murine leukemia virus
NDS	normal donkey serum
NE	norepinephrine
NES	nuclear export signal
NGS	normal goat serum
NLS	nuclear localization signal
NPCP	nuclear pore complex proteins
NRS	normal rabbit serum
OD_{xxx}	optical density at xxx nm
p	phosphorylated

PBS	phosphate-buffered saline
PCR	polymerase chain reaction
pCREB	phosphorylated cAMP response element binding protein
PER	period
PK	protein kinase
PMI	post-mortem interval
RNA	ribonucleic acid
rpm	revolutions per minute
RHT	retinohypothalamic tract
RT	reverse transcription
S	serine
SCN	suprachiasmatic nucleus
SDS	sodium dodecylsulfate
SDS-PAGE	SDS-polyacrylamid gel electrophoresis
SMS	Smith-Magenis-Syndrome
SNP	single nucleotide polymorphism
T	threonine
TEMED	N,N,N´,N´-tetramethylendiamine
Tris	tris-(hydroxymethyl-)aminomethane
Triton-X 100	octylphenoxypolyethoxyethanol
UV	ultraviolet
v/v	volume per volume
w/v	weight per volume

Zusammenfassung

Für alle überwiegend oberirdisch lebenden Organismen bedeutet der regelmäßige Wechsel zwischen Licht und Dunkelheit, sowie die Änderung der Tageslänge im Verlauf der Jahreszeiten eine fundamentale Veränderung ihrer Lebensbedingungen und prägen damit ihre interne zeitliche Organisation. Um eine Anpassung von Aktivitäts- bzw. Ruhephasen in Stoffwechsel, Physiologie, Nahrungsaufnahme und Verhalten zu erreichen, ist eine innere Uhr notwendig, mit deren Hilfe Lebewesen die tageszeitlichen und saisonalen Veränderungen ihrer Umwelt antizipieren können.

Bei Säugern ist diese innere Uhr als zentraler endogener Oszillator, als ‚Schrittmacher' der zirkadianen Rhythmogenese, im Nucleus suprachiasmaticus (SCN) des Hypothalamus lokalisiert. Über den retino-hypothalamischen Trakt (RHT), einer neuronalen Verbindung der Retina des Auges mit dem SCN, erfolgt die Synchronisation des SCN mit der aktuellen Tages- und Jahreszeit. Neben der Retina und dem RHT ist weiterhin das Pinealorgan ein essenzieller Bestandteil des sogenannten photoneuroendokrinen Systems. Durch dieses System werden die beim endogenen Oszillator ankommenden photoperiodischen Reize über einen multi-synaptischen Signalweg letztendlich im Pinealorgan in die Synthese des Neurohormons Melatonin umgewandelt, einer wichtigen Signalsubstanz zur Vermittlung der Tageszeit. Über die Länge der Melatoninausschüttung wird die Dauer der Dunkelphase vermittelt, so dass Melatonin so als Zeitgeber für jahreszeitliche Veränderungen von Körperfunktionen fungiert. Darüber hinaus wirkt Melatonin in einer sogenannten Rückkopplungsschleife unter anderem auf die Aktivität des SCN selbst ein.

Der entscheidende Reiz zur Initiierung der Melatoninsynthese zu Beginn der Nacht ist die vom SCN gesteuerte erhöhte Freisetzung des Neurotransmitters Noradrenalin aus sympathischen Nervenfasern in das Pinealparenchym, von wo das gebildete Hormon sofort nach der Synthese in die Blutbahn und damit in den gesamten Organismus gelangt. Die so vermittelte Licht- bzw. Zeitinformation kann von allen Körperzellen, welche mit Melatoninrezeptoren ausgestattet sind, erkannt und dekodiert werden.

Das geschwindigkeitsbestimmende Enzym der Melatoninsynthese ist die Arylalkylamin *N*-acetyltransferase (AANAT), wohingegen dem letzten Enzym der Synthese, der Hydroxyindol *O*-methyltransferase (HIOMT), ein geringerer Einfluss auf die Syntheserate des Hormons zugeschrieben wird.

Die Regulation der AANAT ist artspezifisch und erfolgt bei Nagern auf der transkriptionalen, bei allen bislang untersuchten Ungulaten und Primaten auf der post-translationalen Ebene. Im Pinealorgan des Schafes konnte gezeigt werden, dass das Enzym vor dem Abbau durch proteasomale Proteolyse geschützt ist, indem es im Zytosol durch Komplexierung mit einem 14-3-3-Dimer gebunden wird. Diese Komplexierung setzt eine vorherige Phosphorylierung der AANAT an der Aminosäure Threonin an Position 31 der Aminosäuresequenz voraus.

Das Pinealorgan von Säugern besitzt selbst keine endogene Uhr, sondern ist abhängig von rhythmischen Signalen des SCN. Die Generierung eines endogenen Rhythmus mit einer Periodenlänge von zirka 24 h in dieser inneren Uhr basiert auf transkriptional-translationalen Rückkopplungsschleifen, welche durch Beeinflussung der Transkriptionsrate sogenannter Uhrengene durch deren als Transkriptionsfaktoren wirkenden Proteinprodukte aufgebaut werden. Zu Beginn eines solchen Zyklus aktivieren die beiden Uhrengenproteine CLOCK und BMAL1 als Heterodimer durch Bindung an ein hochspezifisches E-Box-Promotor-Element die Transkription der Uhrengene aus der Period-Familie (*Per1-3*) und der Cryptochrome (*Cry1-2*). Die Uhrengenprodukte PER und CRY bilden nach Translation im Zytosol ebenfalls Heterodimere, und blockieren nach Translokation in den Zellkern ihre eigene CLOCK-BMAL1-getriebene Transkription.

Neben der Uhrengenexpression im SCN konnten in allen bislang bei Nagetieren untersuchten peripheren Geweben und Organen ebenfalls Uhrengene nachgewiesen werden, darunter auch im Pinealorgan. Allerdings oszillieren diese Uhren im Gegensatz zur Uhr im SCN nicht selbständig, sondern sind auf eine exogene Signalzuführung angewiesen. Bedeutung und Funktion peripherer Uhren sind bislang noch nicht vollständig geklärt. Im Pinealorgan des Schafs konnte für die beiden Uhrengene *Per1* und *Cry1* keine Rhythmizität gefunden werden, wohingegen in post-mortalem humanem Pinealgewebe für die Uhrengene *Per1*, *Cry1*, und *Bmal1* ein diurnaler Rhythmus gezeigt wurde.

Die Untersuchung der molekularen Vorgänge der Melatoninbiosynthese im Pinealorgan des Menschen ist nur unter Verwendung von post-mortalem Material möglich. Zur Bestätigung der Validität der experimentellen Nutzung von humanem post-mortalem Gewebe sind in den letzten Jahren zahlreiche Studien durchgeführt worden. Dabei konnte gezeigt werden, dass die Degradation post-mortalen Gewebes ein geordnetes System darstellt, so dass molekularbiologische Untersuchungen tatsächlich ein Bild der prä-mortalen Situation des Organismus widerspiegeln.

Ziel dieser Arbeit war es, durch Analyse einer großen Fallzahl von Individuen ein verlässliches Abbild der prä-mortalen molekularen Situation im Pinealorgan des Menschen zu erhalten. Die Untersuchungen wurden auch auf eine weitere neuroendokrine Drüse, die Hypophyse, sowie die endogene Uhr im SCN selbst ausgedehnt. Durch die in dieser Studie durchgeführten Untersuchungen sollte so ein besseres Verständnis der molekularen Mechanismen zeitgebender Strukturen im Menschen erreicht werden, um dadurch Grundlagenwissen für eine medizinische Interaktion bei chrono-pathologischen Störungen beizutragen.

Zur Beantwortung der Aufgabenstellungen wurden zunächst humane Pinealorgane und Hypophysen vom Zentrum der Rechtsmedizin aquiriert, wo sie bei staatsanwaltschaftlich angeordneten Sektionen entnommen wurden. Die Gewebe wurden in vier tageszeitliche Gruppen (Tag – Abend – Nacht – Morgen) entsprechend dem Todeszeitpunkt der Personen eingeordnet. Mittels RT-PCR und real-time PCR, Enzymaktivitätsmessungen, ELISA, Immunoblotting und Immunofluoreszenz, sowie Co-Immunopräzipitation wurden humane Pineale und Hypophysen simultan untersucht.

Ein zunächst durchgeführter Kontrollversuch zeigte, dass die mRNAs aller untersuchten Gene sehr gleichmäßig degradieren, und damit eine vergleichende Analyse trotz unterschiedlich langer post-mortaler Liegezeiten der Personen durchgeführt werden kann. Somit war es möglich, die erhaltenen Daten von Personen mit ähnlichem Todeszeitpunkt zu einer Gruppe zusammenzufassen und statistisch auszuwerten.

Enzymatische Aktivitätsmessungen der bei der Melatoninsynthese beteiligten Enzyme AANAT und HIOMT ergaben wie erwartet eine konstitutive Aktivität des letzten Enzyms der Synthese, wohingegen für die AANAT ein signifikanter Zusammenhang zwischen Enzymaktivität und Todeszeitpunkt gefunden werden

konnte. Eine hohe Enzymaktivität ging dabei einher mit der Melatoninproduktion während der Dunkelphase, während am Tage wenn überhaupt nur eine sehr geringe Aktivität der AANAT messbar war.

Mit Hilfe eines Melatonin-ELISAs konnte aus Proteinhomogenaten die Melatoninkonzentration relativ zum gesamten Proteingehalt ermittelt werden. Das erhaltene Melatoninprofil zeigte dabei den typischen hohen Melatoningehalt ausschließlich während der Nacht, was die bereits erhobenen Daten aus menschlichem Serum bzw. Urin bestätigt, und auch direkt mit dem Profil der Aktivität der AANAT korreliert.

Nach mRNA-Extraktion aus Bruchstücken der Pineale konnte mittels RT-PCR allerdings weder für die *Aanat*- und die *Hiomt*-mRNA, noch für verschiedene Uhrengene, ein signifikanter Unterschied der Expression im Tagesgang gefunden werden.

Entgegen der rhythmischen AANAT-Aktivität konnte mittels Immunoblotting keine Veränderung des AANAT-Proteingehaltes im Tagesgang ermittelt werden, was gegen einen sofortigen Abbau des Proteins während der Hellphase des Tages spricht. Weiterhin wurde mit Hilfe der Immunfluoreszenz festgestellt, dass die AANAT sowohl in humanen Pinealozyten, als auch im Pinealorgan des Schafes, welches zu Vergleichszwecken herangezogen wurde, unabhängig von der Tageszeit sowohl in Zellfortsätzen als auch in kondensierten Strukturen im Kern, sowie im Zytoplasma der Kernumgebung vorkommt. Mit Hilfe der Immunofluoreszenz sowie Co-Immunopräzipitation konnte gezeigt werden, dass die AANAT unabhängig von der Tageszeit sowohl mit dem 14-3-3 Protein, als auch mit der HIOMT komplexiert vorliegt.

Die Ergebnisse der vorliegenden Arbeit zeigen, dass, wie bei Ungulaten und dem Primaten *Macaca mulatta*, eine post-translationale Regulation der AANAT, und damit der Melatoninbiosynthese, im humanen Pinealorgan stattfindet. Weiterhin zeigten die erhobenen Daten, dass das AANAT Protein beim Menschen unabhängig von der Tageszeit in konstanter Menge vorhanden ist, und darüber hinaus ständig im Komplex mit HIOMT und einem 14-3-3-Dimer zur Verhinderung der proteasomalen Proteolyse vorliegt. Daraus leitet sich die Hypothese ab, dass es einer weiteren post-translationalen Modifikation bedarf, um die Inhibierung der AANAT-Aktivität

während der Nacht aufzuheben. Über diese Regulationsmechanismen zur Steuerung der AANAT-Aktivität liegen beim Menschen keine Daten vor.

In der vorliegenden Arbeit wurden zum ersten Mal Uhrengenproteine in verschiedenen humanen neuralen Geweben nachgewiesen. Zur Untersuchung der Uhrengenprodukte aus Pineal- und Hypophysenhomogenaten wurde die Immunoblot-Methode angewendet. Dabei konnte für keines der untersuchten Uhrengenproteine, PER1, CRY1, CLOCK und BMAL1 eine signifikante Änderung des Proteingehaltes im Tagesgang, gefunden werden. Wie beim Schaf scheint damit auch beim Menschen keine transkriptionale Kontrolle der Uhrengene in peripheren Oszillatoren vorzuliegen. Statt dessen indizieren die hier erhobenen Daten, dass Uhrengenproteine über post-translationale Modifikationen funktionell reguliert werden.

Diese Vermutung konnte mittels Immunfluoreszenz bekräftigt werden, da die Uhrengenproteine im Tagesgang eine Translokation zwischen Zellkern und Zytoplasma zeigten, das sogenannte ‚nucleo-cytoplasmic shuttling'. Die Beobachtung, dass die Proteine PER1 und CRY1 simultan während der Nacht vom Zellkern in das Zytoplasma translozieren, unterstreicht ihre Wirkungsweise als Heterodimer. CLOCK befand sich zu jeder Tageszeit im Zellkern, jedoch wurde in Pinealozyten überraschenderweise eine Lokalisierung an der Zellmembran während der Nacht gefunden. Möglicherweise wird CLOCK in die Blutbahn sezerniert, zumal bereits Fragmente des Proteins in Serum nachgewiesen wurden. Diese Annahme wurde gestützt durch den Befund, dass CLOCK im Zytoplasma von humanen Hypophysen mit FSH (follicle-stimulating hormone) co-lokalisiert werden konnte, was auf ein Vorkommen von CLOCK in sekretorischen Vesikeln hindeutet. Da CLOCK zumindest im Tiermodell auch mit Adipositas in Verbindung gebracht wurde, scheint es daher möglich, dass das Protein neben seiner Funktion innerhalb des zirkadianen Systems noch weitere, bislang ungeklärte Aufgaben im Organismus erfüllt.

Sowohl bezüglich der AANAT als auch der Uhrengenproteine erfordern die in dieser Arbeit gefundenen Regulationsmechanismen keine *de novo* Proteinsynthese, um auf sich ändernde Umgebungsreize zu reagieren. Dadurch sind sie nicht nur zeitsparender, also schneller, sondern auch deutlich energieeffizienter als die bei Nagern beobachteten Mechanismen, die vornehmlich eine transkriptionale

Regulation aufweisen. Der evolutionäre Hintergrund dieser verschiedenen Strategien ist nicht bekannt, es ist jedoch denkbar, dass vor allem die schnelle und effiziente Reaktion auf sich verändernde Umweltbedingungen einen Selektionsvorteil für Ungulaten und Primaten bedeutet haben könnte.

Weiterhin ist es in dieser Arbeit zum ersten Mal gelungen, den Nachweis von Uhrengenproteinen im humanen SCN zu erbringen. Dazu wurde formalin-fixiertes Material mit sehr kurzer post-mortaler Liegezeit verwendet und immunhistochemisch bzw. mittels Immunofluoreszenz untersucht. Dabei konnte, im Gegensatz zu den untersuchten peripheren Geweben, im SCN des Menschen eine Oszillation der Uhrengenprodukte PER1 und CLOCK gezeigt werden.

Insgesamt liefern die in dieser Arbeit erhobenen Datensätze neue Einblicke in die Regulationsprozesse der Melatoninbiosynthese und der zirkadianen Rhythmik beim Menschen. Die vorgestellten Ergebnisse zeigen aber auch, dass es in Neuronen eine funktionelle Dynamik der Uhrengenproteine neben den herkömmlichen transkriptionalen und (post-)translationalen Mechanismen gibt.

Teile der vorliegenden Arbeit wurden bereits in wissenschaftlichen Journalen veröffentlicht.

Summary

Rhythmic changes in natural lighting conditions have ever been the most reliable environmental cue for life on earth. Therefore, anticipation of these cyclic changes constitutes a major selection advantage for any organism living at or close to the surface. Nature has therefore selected a genetically encrypted endogenous clock very early in evolution, as it provided cells and subsequently organisms with the ability to anticipate persevering periods of light (and darkness) and thus, most importantly, of food availability.

In mammals, the endogenous clock is located in the suprachiasmatic nucleus (SCN) of the anterior hypothalamus. Together with the retina, the retino-hypothalamic tract and the pineal gland, the SCN constitues the photoneuroendocrine system. The pineal organ as a driven oscillator is dependent on afferent information that is derived from the endogenous clock.

The best characterized function of the pineal gland is the nocturnally elevated synthesis of the hormone melatonin, which provides the body with the signal of the duration of the night period. The ultimate enzymatic step in melatonin synthesis is achieved by the hydroxyindole *O*-methyltransferase (HIOMT), the rate-limiting enzyme is, however, the arylalkylamine *N*-acetyltransferase (AANAT). In contrast to the transcriptional regulation of the *Aanat* gene in rodents, a post-translational shaping of the melatonin pattern has been suggested for the human pineal gland.

Despite the fact that melatonin can be determined easily in various body fluids, interpretation of measured levels of melatonin is problematic, as no other species exhibits such a diversity in lifestyle, working conditions and habitats - factors which all influence melatonin synthesis and/or secretion. The molecular elements involved in shaping rhythmic hormone synthesis can not be analyzed experimentally *in vivo* in humans. However, the use of post-mortem pineal material is a valid approach to decipher the regulation of human melatonin synthesis.

The mammalian pineal gland does not contain an endogenous clock, but instead it is depending on afferent signals from the master clock within the SCN. Rhythm generation within the mammalian SCN is achieved by so-called clock genes and their protein products. Both, the pineal gland and the pituitary gland, function as output systems of the SCN, and are therefore important mediators of time and seasonality. It is currently unclear, whether clock gene expression in the mammalian

pineal gland and other peripheral oscillators can be considered as a phylogenetic relic of its ancestral oscillator capacity, or whether they actively participate in regulating rhythmic output. An indication of function can be gained by comparing the regulation of clock gene expression with melatonin synthesis in the pineal gland, as already done in rodents and sheep.

A number of human disorders and syndromes are associated with alterations in circadian rhythms of clock genes and their protein products and/or a dysfunction in melatonin synthesis. In the human, little is known about the molecular signature of time management. Therefore, one aim of this work was to elucidate regulation of melatonin synthesis in the human pineal gland. In addition, the presence and dynamics of clock genes and their protein products were analyzed in the human pineal gland and the pituitary, and in the human SCN.

Pineal tissue, taken from regular autopsies was analyzed simultaneously for *Aanat*, *Hiomt*, and clock gene mRNA levels by RT-PCR, for AANAT activity, using ^{14}C-acetyl-coenzyme A, for HIOMT activity, using S-Adenosyl-*L*-[^{14}C]-methionine, for AANAT protein content using immunoblotting, and for melatonin content employing an ELISA. Immunoblotting and immunofluorescence followed by confocal laser scanning microscopy was used for simultaneous analyses of clock gene protein and AANAT/14-3-3 abundance and intracellular localization. Complexation of AANAT with 14-3-3 protein was determined using co-immunoprecipitation.

Results were allocated to asserted time-of-death groups (day - dusk - night - dawn). RNA degradation rates for genes of interest ran in parallel and therefore, data normalization could be established, irrespective of post-mortem delay in tissue sampling. *Aanat* and *Hiomt* mRNA, and HIOMT activity showed no diurnal rhythm. Despite the observed diurnal rhythms in activity of the AANAT and in melatonin content, mRNA levels for the clock genes *Period1*, *Cryptochrome1*, *Clock*, and *Bmal1*, and also amounts of corresponding clock gene proteins showed no differences between time-of-death groups. In contrast, a time-of-day dependent nucleo-cytoplasmic shuttling of clock gene proteins was detected.

Similarly, no significant rhythms in clock gene mRNA or protein content could be detected in the second neuroendocrine tissue analyzed, the human pituitary.

However, also here a nucleo-cytoplasmic shuttling of PER1 and CRY1 was detected. Furthermore, the presence of CLOCK in secretory vesicles was indicated.

For the first time the presence and an oscillation in abundance with time of day for clock gene proteins could be demonstrated in the human SCN, using immunofluorescence and immunohistological methods.

Presented data demonstrate that post-mortem brain tissue can be used to detect a remnant profile of pre-mortem neuronal activity. In particular, our results give strong experimental support for the idea that transcriptional mechanisms are not dominant for the generation of a rhythmic melatonin pattern in the human pineal gland. Rather, AANAT is constitutively expressed and complexed with 14-3-3 and HIOMT independent of time of day. Therefore, a novel hypothesis for dynamics in melatonin synthesis can be postulated, with a nocturnal release of AANAT activity inhibition via an as yet unknown mechanism. Moreover, with the detected nucleo-cytoplasmic shuttling of clock gene proteins in both, the human pineal gland and the pituitary, a novel twist in the molecular competence of these proteins was described for the first time.

Parts of the present work have been published in scientific journals.

1 Introduction

1.1 Biological rhythms and the photoneuroendocrine system

The 24-h day-night rhythm, resulting from the rotation of the earth around its axis, has ever been the most reliable environmental cue for life on earth. Therefore, anticipation of cyclic changes in environmental lighting conditions constitutes a major selection advantage for any organism living at or close to the surface, as behavioral characteristics (e.g. reproductiveness), metabolism (e.g. plasma cortisol level) and body functions (e.g. heart rate) have to be adjusted constantly to changing light and dark periods. Nature has therefore selected a genetically encrypted endogenous clock very early in evolution, as it provided cells and subsequently organisms with the ability to anticipate persevering periods of light (and darkness) and thus, most importantly, of food availability.

An endogenous rhythm that is dependent on periodic environmental stimuli (e.g. light) is called 'diurnal'. If this rhythm persists in the absence of 'zeitgeber', (i.e. in constant darkness) it is called 'circadian' (*circa* = about, *dies* = day).

In vertebrates, the synchronisation of the endogenous clock with the environment and the subsequent signalling of light information to the body, is achieved by a neuronal circuit, the so-called photoneuroendocrine system (PNS).

The concept of the PNS was first defined by Ernst Scharrer in 1964. As environmental light is the most potent zeitgeber from the very beginning of life, an organism`s capacity to orientate not only in space, but also in time was strongly supported and led to the development of lateral eyes for orientation and sensing light, and of an endogenous clock with intrinsic circadian rhythms in all vertebrates investigated so far. According to Scharrer`s concept, the PNS serves to perceive light information, and to convert this information into a neuroendocrine response [Scharrer 1964].

In mammals, the pineal gland is embedded in the PNS that consists of two additional interconnected elements, the retina and the suprachiasmatic nuclei of the hypothalamus (SCN; Fig. 1) [Korf *et al*., 1998]. The SCN harbors the endogenous circadian master oscillator, which is entrained via retinal input of environmental lighting conditions and generates a circadian (e.g. about 24-h) rhythm, which is subsequently distributed to the body via efferent neuronal and humoral signals [Korf

et al., 1998; Reppert & Weaver, 2002]. Thus, the SCN disseminates circadian time cues to other cells, peripheral tissues and organs for proper coordination of activity rhythms. In this context, the pineal gland serves as one 'hand of the clock'. Importantly, the SCN integrates operating experience on the photoperiodic history to mirror and precisely anticipate environmental lighting conditions [Reppert & Weaver, 2002; Antle & Silver 2005].

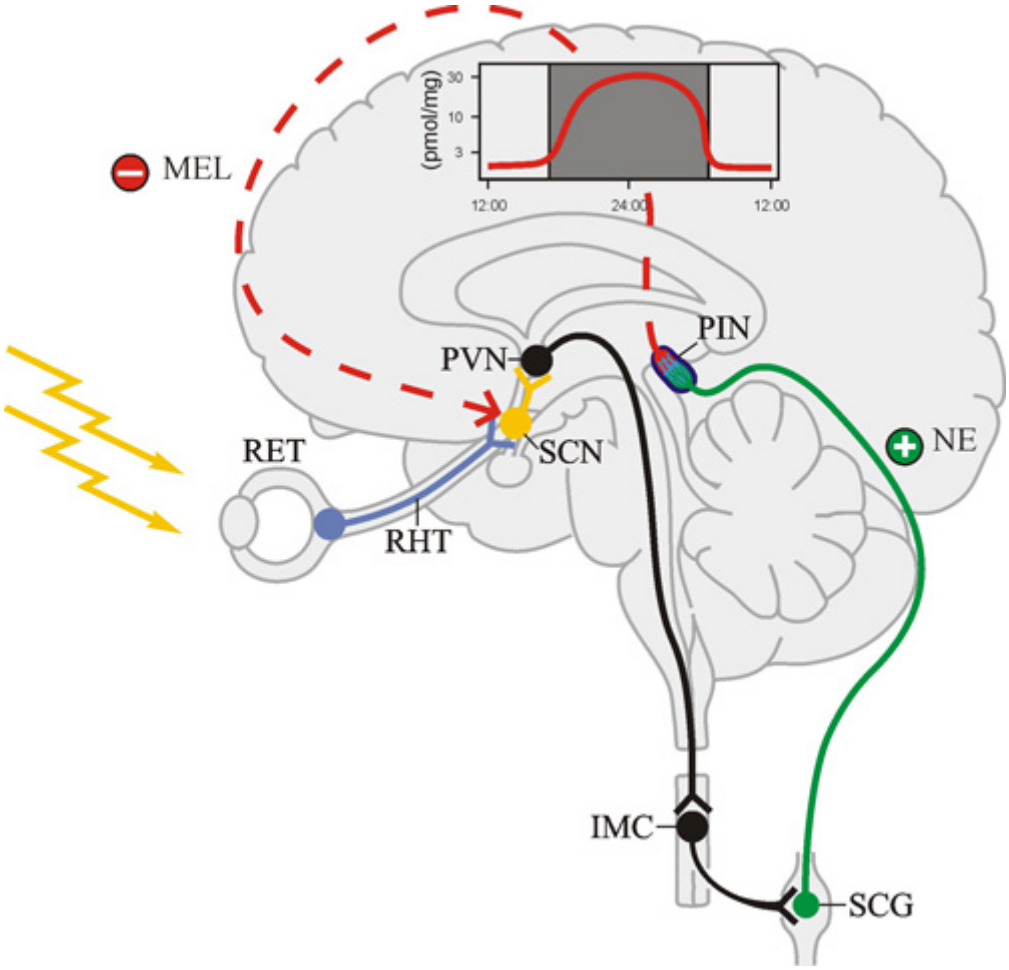

Fig. 1: Schematic drawing of the human PNS.

The graph in the inset shows the oscillation of melatonin levels in the human pineal gland with respect to clock-time. Abbreviations: IMC – intermediolateral column of the spinal cord; MEL – melatonin; NE – norepinephrine; PIN – pineal; PVN – paraventricular nuclei; RET – neuroretina; RHT – retinohypothalamic tract; SCG – superior cervical ganglia; SCN – suprachiasmatic nucleus. [adapted from Maronde & Stehle, 2007]

1.2 The pineal gland – a 'hand of the clock'

In 1963, only five years after the discovery of melatonin by Lerner [Lerner *et al.*, 1958], the first round-table-discussion on the pineal organ (*Epiphysis cerebri*, *Glandula pinealis*) was organized by Ariens Kappers. One of the major results of this discussion was the formulation of a concept, which defined the pineal organ as a photoneuroendocrine transducer, converting afferent neuronally coded photic information into an efferent hormonal signal of darkness [Kappers & Schadé, 1965].

Of utmost importance is the dissemination of circadian time cues from the SCN to other cells, peripheral tissues and organs for proper coordination of activity rhythms. One well-described example of such a coordination is the neuroendocrine transduction of rhythmic SCN output by the pineal gland [Korf *et al*., 1998]. In all vertebrates investigated so far, the pineal gland serves these time-coding needs by the rhythmic synthesis of melatonin, with nocturnally elevated levels dynamically adapting to changes in the duration of the dark period [Korf *et al*., 1998; Klein *et al*., 1997].

Even in simplest vertebrates, the pineal gland constitutes a photosensory organ with an endogenous clock. During evolution, its function switched from a photoendocrine role in lower vertebrates to a neuroendocrine in mammals. It is still not fully clear whether pinealocytes have progressively lost their photoreceptive capacities during phylogeny, or if changes in their regulatory network have not only changed cell morphology, but also function. The latter theory is the result of an alternative data interpretation and recently reported studies [Ekström & Meissl, 2003]. Yet, there are no final proofs for the one or the other developmental theory, keeping the phylogeny of the pineal organ still enigmatic.

Taken together, mammalian pinealocytes are purely SCN-driven transducers (type '*sensu stricto*'), signalling the message of darkness to the body [Maronde *et al*., 1999(a); Stehle *et al*., 2001(a,b); Ekström & Meissl, 2003; Maronde & Stehle, 2007].

1.3 The melatonin biosynthesis pathway

1.3.1 Components of the melatonin synthesis pathway

In the pineal gland of all mammals, the circadian rhythm in melatonin synthesis depends on the SCN-driven nocturnally elevated release of the neurotransmitter norepinephrine (NE) from sympathetic nerve fibers, and the subsequent activation of the cyclic adenosine monophosphate (cAMP) signalling pathway [Klein *et al*., 1997; Korf *et al*., 1998] via β_1-adrenergic receptors. Subsequently, the activity of the penultimate and rate-limiting enzyme in melatonin synthesis, the arylalkylamine *N*-acetyltransferase (AANAT), is strongly increased [Borjigin *et al*., 1995; Maronde *et al*., 1999(b)], leading to an elevated synthesis and release of the hormone melatonin, thus coding for the duration of the dark period. To protect AANAT from dephosphorylation and subsequent proteasomal degradation, the enzyme is complexed with 14-3-3 protein in the cytoplasm [Ganguly *et al*., 2001]. For complexation, phosphorylation of AANAT at the threonine at position 31 (T31) is necessary [Ganguly *et al*., 2001]. Recently, it was shown that the second phosphorylation site of the AANAT, the serine at position 205 (S205), which is located near the C-terminus, plays also a critical role in the regulation of the enzyme´s activity, and thereby melatonin production [Ganguly *et al*., 2005; Zheng *et al*., 2005].

Melatonin synthesis (Fig. 2) starts with the active uptake of the amino acid tryptophan into the gland. This precursor is then subsequently hydroxylated by the tryptophan-hydrolase and decarboxylated by the aromatic *L*-aminoacid decarboxylase to serotonin (5-hydroxytryptamine). Serotonin is *N*-acetylated by the AANAT and in the last step converted to melatonin (*N*-acetyl-5-methoxytryptamine) by the enzyme hydroxyindole-*O*-methyltransferase (HIOMT) [Klein, 1999]. At the end of the night, this signalling pathway is inactivated and melatonin synthesis shut down [Korf *et al*., 1998; Stehle *et al*., 2001(a)]. The gating of the melatonin signal is a conserved similarity between species, determined by the rhythmic activity of the AANAT. Regulation mechanisms behind the AANAT activity rhythm are, however, remarkably different between species [Stehle *et al*., 2001(b)], occuring either on the transcriptional or the (post-)translational level.

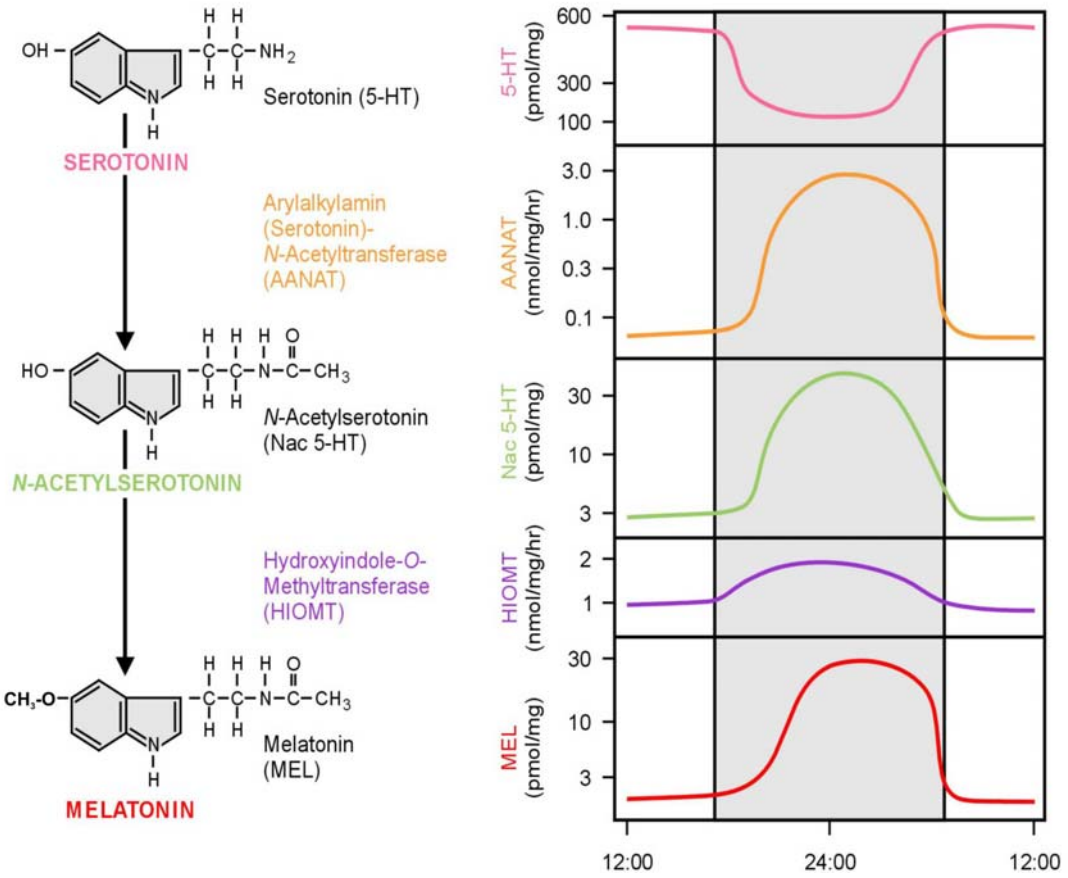

Fig. 2: Melatonin biosynthesis in pinealocytes.

On the left side synthesis steps and respective enzymes of melatonin biosynthesis are depicted, starting from serotonin. On the right side diurnal rhythms of AANAT and HIOMT activities, and of melatonin synthesis are depicted, together with substrate concentrations of serotonin and *N*-acetylserotonin. [modified after Klein, 1999]

1.3.2 Melatonin synthesis in rodents

Melatonin synthesis is best studied in rodents (mouse, rat, hamster), where its regulation occurs mainly at the transcriptional level, with pCREB (phosphorylated cAMP response element [CRE] binding protein) as the major activating and ICER (inducible cAMP early repressor) as an important inhibiting transcription factor [Stehle *et al.*, 1993; Maronde *et al.*, 1999(b); von Gall *et al.*, 2000; Ceinos *et al.*, 2004] (Fig. 3). In rodents, both the *Aanat* gene and the AANAT protein, show a characteristic circadian pattern, with high levels of transcription (> 100-fold) and translation at night [Roseboom *et al.*, 1996; Gauer *et al.*, 1999; Maronde *et al.*,

1999(a); Stehle *et al*., 2001(a)]. This transcriptional regulation is efficiently flanked by post-translational mechanisms [Gastel *et al*., 1998; Koch *et al*., 2003].

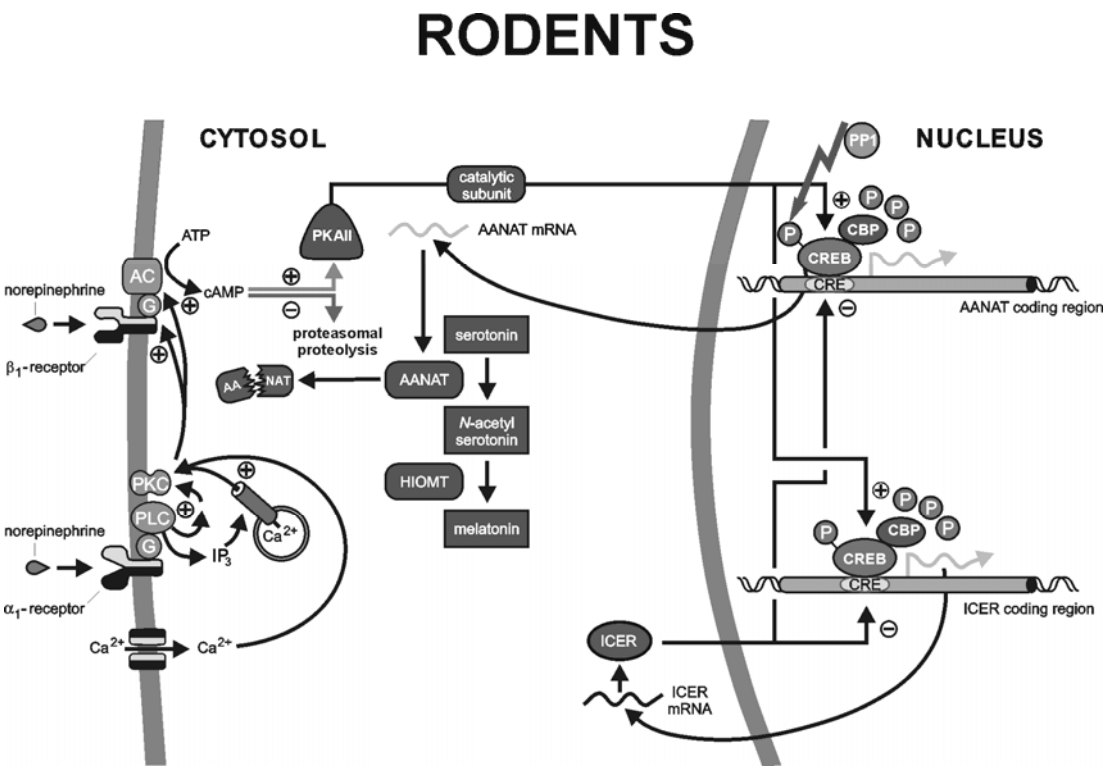

Fig. 3: Regulation of melatonin synthesis in rodents.

Abbreviations: AANAT = arylalkylamine *N*-acetyltransferase; AC = adenylate cyclase; AMP = adenosine monophosphate; ATP = adenosine trisphosphate; CBP = CREB binding protein; CRE = cyclic AMP response element; CREB = CRE binding protein; G = GTP-binding protein; HIOMT = hydroxyindole *O*-methyltransferase; ICER = inducible cyclic AMP early repressor; IP_3 = inositoltrisphosphate; P = phosphate groups; PKAII = cyclic AMP-dependent protein kinase type II; PKC = protein kinase C; PLC = phospholipase C, PP1 = protein phosphatase 1. [adapted from Stehle *et al*., 2001(b)]

1.3.3 Melatonin synthesis in non-rodent mammals

In all ungulates studied so far (sheep, cow), *Aanat* mRNA levels do not show significant differences between day and night [Coon *et al*., 1995; Johnston *et al*., 2004], resulting in a constitutive up-regulation of AANAT protein, which is thought to be rapidly degraded via proteasomal proteolysis during the day [Coon *et al*., 1995; Korf *et al*., 1998; Stehle *et al*., 2001(b)] (Fig. 4). This degradation is inhibited as

soon as the cAMP-signal-transduction-pathway is activated at night, due to the SCN-driven release of NE from sympathetic pinealopetal nerve fibers [Brownstein & Axelrod, 1974; Rüppel & Olcese, 1991]. It could be demonstrated that, at least in bovine pinealocytes, melatonin synthesis is regulated by type II cAMP-dependent protein kinase (PKAII) [Maronde *et al*., 1997]. Moreover, by transferring results from *in vitro* experiments [Schomerus *et al*., 2000; Ganguly *et al*., 2001], it was concluded that the nocturnal increase in AANAT activity and melatonin content in the ungulate pineal gland [Coon *et al*., 1995; Johnston *et al*., 2004] is due to a NE-induced inhibition of proteasomal degradation of this enzyme, probably via a highly conserved cAMP-operated PKA/14-3-3 binding switch: a cAMP-regulated PKA-catalyzed phosphorylation of AANAT at a threonine near the N-terminus promotes complex formation with 14-3-3-protein, and thereby melatonin production [Ganguly *et al*., 2001].

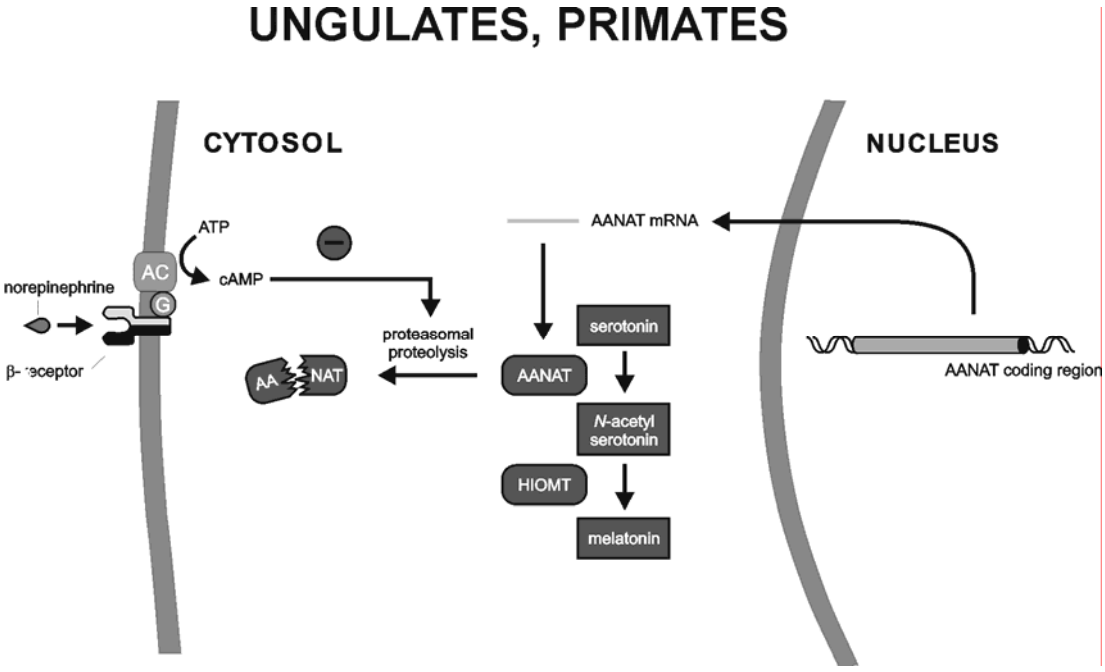

Fig. 4: Regulation of melatonin synthesis in ungulates and primates.
Abbreviations see figure 3. [adapted from Stehle *et al*., 2001(b)]

A posttranscriptional regulation mechanism could also be shown for a primate, the Rhesus monkey *Macaca mulatta* [Coon *et al*., 2002], where it was

demonstrated that *rhAanat* and *rhHiomt* mRNA do not exhibit a significant day-night-rhythm, whereas a large rhythm in both AANAT activity and AANAT protein was shown in the pineal, with about 10-fold higher values at night, as compared to day-time values. The authors conclude that post-transcriptional control of rhAANAT plays a dominant role in regulating melatonin synthesis, similar to mechanisms deciphered in ungulates. In theory, this post-transcriptional proteolysis-based regulation permits more rapid changes in melatonin production as compared to the transcriptional regulation in rodents, because no altering of gene expression is needed. This assumption is supported by the fact that melatonin values in *Macaca mulatta* cerebrospinal fluid increase without a lag period shortly after lights off [Reppert *et al*., 1979], and rapidly decrease upon light exposure at night-time [Reppert *et al*., 1981].

Whereas melatonin profiles in humans can be easily assessed using saliva, blood samples, or urine, insight into the molecular mechanism driving rhythmic melatonin synthesis in the pineal gland can currently only be achieved by using post-mortem tissue. The feasibility of such an approach was demonstrated by anecdotal reports describing a remnant profile of a melatonin rhythm in post-mortem material [Oxenkrug *et al*., 1990; Hofman *et al*., 1995] that correlates significantly to the diurnal profile obtained in healthy men [Smith *et al*., 1977; Arendt, 1995]. In addition, using autoptic human pineal tissue, residual AANAT and HIOMT enzyme activities were demonstrated in a small number of specimens [Smith *et al*., 1977], and no significant differences were found between day and night for *Aanat* and *Hiomt* mRNA levels in a control group of specimens of old age [Wu *et al*., 2003].

1.3.4 Melatonin rhythm in humans

In humans, the rhythmic melatonin production, with high levels during the night (around 100 pg/ml plasma) and low levels during the day (< 20 pg/ml plasma) [Lynch *et al*., 1975; Arendt, 1985; Arendt & Skene 2005], develops between the second and third month of life. Up to this time, maternal melatonin serves *in utero* via a maternal-fetal communication and post-natally via breast-feeding as a zeitgeber for the developing organism [Reppert *et al*., 1989; Kennaway *et al*., 1992]. Highest melatonin levels are found in prepubertal children [Waldhauser *et al*., 1988], but an

involvement of melatonin in human puberty, as expected from studies with boys with delayed puberty [Cohen *et al*., 1982], remains to be proven [Arendt, 1995]. In the elderly (> 60 years), nocturnal melatonin levels were shown to decline significantly between 20-80% in some studies [Touitou *et al*., 1984; Ferrari *et al*., 1995; Magri *et al*., 1997]. Others studies, however, showed no age-related decline in the amplitude, duration and average nocturnal melatonin surge [Kennaway *et al*., 1999; Zeitzer *et al*., 1999]. The problematic interpretation of measured levels of melatonin and its derivates in human body fluids are obvious, as no other species exhibits such a diversity in lifestyle, working conditions and habitats - factors which all influence melatonin synthesis and/or secretion. It also has been shown that some healthy subjects do not have any detectable melatonin rhythm at all [Arendt, 1985].

Studies using salivary melatonin concentrations of human subjects exposed to natural bright light summer days have shown that melatonin rhythms are adjusted to lighting conditions rapidly [Vondrasová *et al*., 1997, 1999]. The melatonin profile in blood plasma and also in saliva shows a rapid dim-light-melatonin-onset (DLMO) [Lewy *et al*., 1999], and another study with human subjects living under controlled laboratory conditions [Smith *et al*., 2004] revealed that melatonin suppression at night occurs already upon application of low light levels, in accordance to the nonlinear intensity-suppression relationship established by Zeitzer [Zeitzer *et al*., 2000]. The rhythmic profile of human melatonin concentration in saliva persists even in the absence of a light-dark cycle [Arendt, 1995]. Rhythm characteristics are highly reproducible from day to day in the same individual, with however, large inter-individual differences in absolute values [Arendt, 1995].

1.4 Clock genes

As described above, the pineal organ signals the body the message of darkness via synthesis of the hormone melatonin. Importantly, the gland does not contain an intrinsic or endogenous clock, so that it depends on afferent signals initiating or inhibiting melatonin production.

The basis for the discovery and isolation of genes responsible for circadian rhythm generation was laid by Benzer and Konopka more than 35 years ago [Konopka & Benzer, 1971], who described gene mutations in the fruitfly *Drosophila*

melanogaster leading to an altered day-night rhythm. These genes responsible for endogenous rhythmicity and timing were later on named 'clock genes'. In all mammals investigated so far, time-management is achieved by interactions of these genes, and is organized hierarchically, with a self-sustaining circadian master oscillator residing in the SCN [Lowrey *et al*., 2000; Reppert & Weaver, 2002; Hastings *et al*., 2003].

1.4.1 The transcriptional-translational feedback loop model

As a molecular prerequisite for endogenous circadian rhythm generation in the mammalian SCN, the clock genes of the *Period* (*Per*) and *Cryptochrome* (*Cry*) families, of *Bmal1* and presumably of *Clock*, and their corresponding protein products (PER, CRY, BMAL1, CLOCK) are required [Lowrey *et al*., 2000; Reppert & Weaver, 2002; Debruyne *et al*., 2006]. These clock gene proteins form transcriptionally active complexes that interact with their own genes in a feedback loop (Fig. 5), thereby providing the basis for a perpetual and cycling regulation of clock controlled genes [Reppert & Weaver, 2002; Hastings *et al*., 2003], as analyzed in detail in mouse SCN cells [Reppert & Weaver, 2002]: the positive components of the loop are the clock gene products BMAL1 and CLOCK. These proteins are translocated into the nucleus after forming heterodimers in the cytoplasm. In the nucleus, BMAL1/CLOCK-heterodimers bind to E-box elements in the promoter region of the *Per*, *Cry*, and *Rev-Erbα* genes, thus activating their transcription. REV-ERBα acts on specific response elements in the *Bmal1* promoter to repress *Bmal1* transcription. The protein products of the *Per* and *Cry* genes constitute the negative components of the loop. After phosphorylation by casein kinase 1δ/ε, PER and CRY proteins also form heterodimers as stabilizing complexes, allowing them to enter the nucleus and suppress their own gene expression via interaction with the BMAL1/CLOCK-complex. Finally, CLOCK and BMAL1 proteins are degraded via proteasomal proteolysis. Thus, the clock genes and their transcriptionally active protein products form a transcriptional-translational feedback loop, with one cycle lasting about 24 hours (*circa-dian*).

In mammals, clock gene expression is not limited to the SCN but has been detected in almost all tissues investigated [Reppert & Weaver, 2002; Hastings *et al*.,

2003], including the pineal gland [Karolczak *et al*., 2005]. It is currently unclear, whether clock gene expression in the mammalian pineal gland [Karolczak *et al*., 2004, 2005] can be considered as a phylogenetic relic of its ancestral oscillator capacity, or whether they actively participate in regulating rhythmic output [Ekström & Meissl, 2003; Maronde & Stehle, 2007]. An indication of function can be gained by comparing the regulation of clock gene expression with melatonin synthesis, as already done in rodents and sheep [Johnston *et al*., 2004; Karolczak *et al*., 2005].

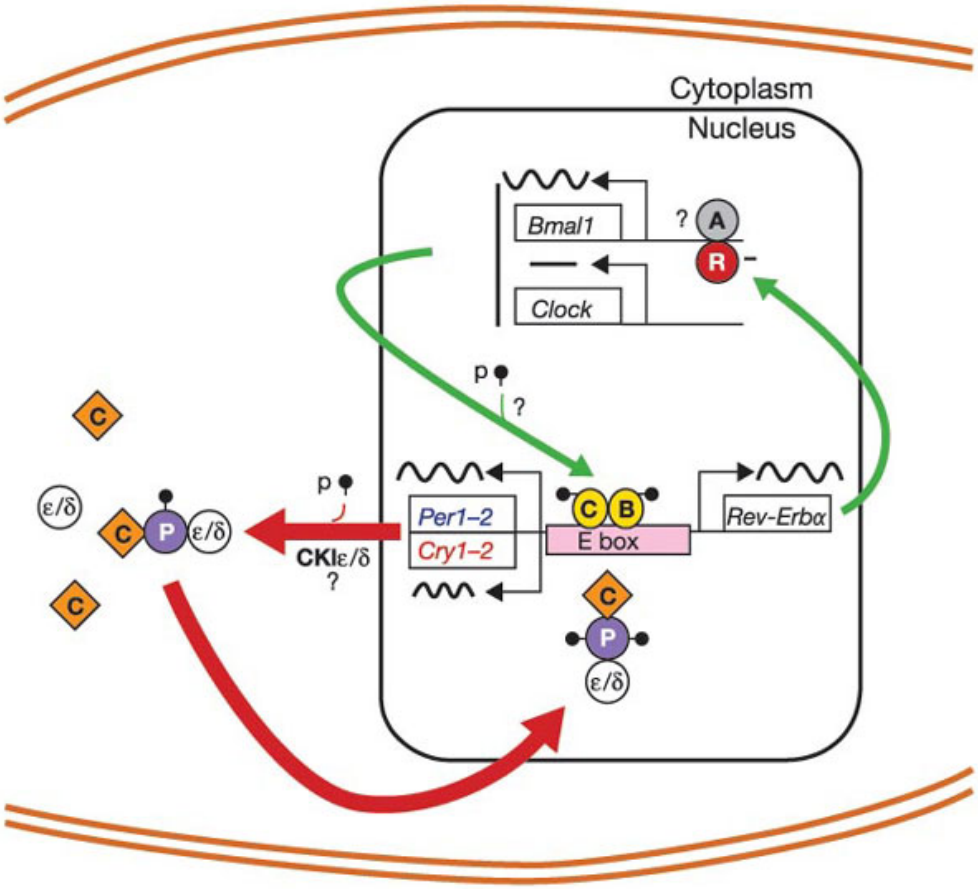

Fig. 5: Transcriptional-translational feedback loop of the mammalian circadian clockwork model in the SCN.

Detailed explanation is given in the text. Green arrows: positive feedback loop, red arrows: negative feedback loops. Abbreviations: CLOCK: C, yellow; BMAL1: B; PER: P; CRY: C, orange; casein kinase Iε/δ: ε/δ; phosphorylated: p; REV-ERBα: R; activator: A. [adapted from Reppert & Weaver, 2002]

1.4.2 Clock genes in the rodent pineal gland

In the rodent pineal gland, clock gene expression and regulation is well described, with *Per1*, *Cry1*, *Bmal1* and, to a lesser extent, *Clock* mRNA exhibiting a circadian expression pattern [Takekida *et al*., 2000; von Gall *et al*., 2001; Karolczak *et al*., 2004, 2005; Fukuhara *et al*., 2005].

Interestingly, it was found that *Per1* expression is temporally closely related to *Aanat* expression in rats [Fukuhara *et al*., 2000]. Together with the presence of CRE elements (cyclic AMP response element) in the promoter region of *Per1* [Travnickova-Bendova *et al*., 2002], it was concluded that *Per1* is regulated in the same way as the *Aanat* gene, namely via the β-adrenergic elevation of cAMP levels, leading to gene expression enhanced by the transcription factor CREB (CRE binding protein). In contrast, a cAMP-independent pathway for *Per2* regulation in the rat pineal gland was suggested, as isoproterenol, a β-adrenergic receptor agonist, had no effect on *Per2* expression, whereas *Per1* expression was rapidly induced [Takekida *et al*., 2000]. Also in the mouse pineal gland, the NE-dependent regulation of *Per1* transcription was confirmed by *in vitro* experiments [von Gall *et al*., 2001]. Furthermore, it could be shown that, in contrast to *Aanat* transcription, *Per1* transcription could be stimulated by the BMAL1/CLOCK complex in cultured rat pinealocytes [Fukuhara *et al*., 2002]. In this study, it was also found that, besides the cAMP signalling pathway, also the cGMP-MAPK pathway is involved in regulation of *Per1*, but not of *Aanat*, demonstrating important differences in the regulation of these two genes [Fukuhara *et al*., 2002].

A comprehensive study comprising not only clock gene expression, but also protein data was conducted using pineal glands of two mice strains, namely melatonin-proficient C3H and melatonin-deficient C57BL mice [Karolczak *et al*., 2004]. In this study, rhythmic day-night fluctuations in the abundance for transcripts of *mPer1-3*, *mCry1-2*, *mClock* and *mBmal1*, and for protein products PER1-3, CRY1-2, and CLOCK could be demonstrated in the mouse pineal gland. As no major differences in clock gene mRNA and protein pattern was found between the two strains analyzed, the authors conclude that an absent synthesis of melatonin does not affect the clock output that drives pineal rhythms.

1.4.3 Clock genes in the pineal gland of non-rodent mammals

In non-rodent mammalian species, data on clock genes, their protein products, and regulation mechanisms in the pineal gland are sparse and also controversial.

The first study determining clock gene expression in pineal glands of a non-rodent mammalian species, the Soay sheep [Johnston *et al*., 2004], was challenging the dogma of a transcriptional regulation of clock genes. In this study, no rhythmic expression was found for *Cry1* irrespective of photoperiod, whilst a low amplitude rhythm was observed for *Per1* only in animals that were kept under short days, i.e. pinealocytes were exposed to a prolonged sympathetic stimulus. This observation is especially remarkable, as in the sheep melatonin synthesis is driven downstream of transcription, likewise to the situation in the Rhesus monkey *Macaca mulatta* [Coon *et al*., 2002].

In humans, the presence of clock gene mRNAs and proteins have been demonstrated in several peripheral tissues and in body fluids [Bjarnason *et al*., 2001; Boivin *et al*., 2003; Takimoto *et al*., 2005; Teboul *et al*., 2005; Pardini *et al*., 2005; Cajochen *et al*., 2006]. Yet, data obtained in these studies are not consistent, even when the same subgroup of cells, like peripheral mononuclear blood cells, was investigated [Boivin *et al*., 2003; Teboul *et al*., 2005]. Concerning pineal clock gene expression in the human, a recent study [Wu *et al*., 2006] described a significant diurnal profile for the clock genes *Per1*, *Cry1* and *Bmal1*.

As pineal data obtained from Johnston and Wu are discussed controversially, it is still unclear if regulation downstream of transcription plays the dominant role in regulating rhythmic pineal output in non-rodent mammals, or if regulation occurs at the level of transcript abundance.

1.5 Human chronobiological dysfunctions

Melatonin synthesis is a reliable and easily accessible parameter to analyze the functional state of the endogenous circadian clock in the mammalian SCN, as it directly depends on neuronal input from the master clock. Human chronobiological dysfunctions often appear in conjunction with perturbations of pineal melatonin synthesis [Arendt, 1995, 2005; Klerman, 2005] and/or mutations of clock genes

[Hastings *et al*., 2003, Klerman, 2005]. Furthermore, retinopathies or disturbances of the synchronization and/or communication of the SCN with peripheral organs can finally lead to chronopathologies [Klerman 2005]. Blind people often show an altered or disrupted melatonin synthesis [Lewy *et al*., 2005].

In addition to the reported dampening of circadian rhythms and night-time melatonin amplitude with age [Arendt, 1985], recent studies described alterations of melatonin rhythms in humans with chronopathologies:

- The delayed sleep phase syndrome (DSPS) is a circadian rhythm sleep disorder with delayed sleep-onset, accompanied by difficulties in awakening. It could be shown that melatonin rhythms in patients with DSPS are delayed when compared to normal subjects [Shibui *et al*., 1999], which may be due to a single nucleotide polymorphism (SNP) revealed in the *Aanat* gene [Hohjoh *et al*., 2003]. Some years ago, also SNPs in the *Period* gene were implicated with sleep abnormalities, like the delayed or advanced sleep phase syndrome [Toh *et al*., 2001; Archer *et al*., 2003].

- Patients with Alzheimer Disease suffer from a disturbed sleep-wake rhythm, which is correlated with decreased melatonin levels at night and a disrupted circadian melatonin rhythm, which is similar to what is observed in elderly or blind people. Interestingly, it was reported that the day-night rhythm of β_1-adrenergic receptor mRNA in the pineal gland is absent already in preclinical Alzheimer Disease stages (Braak stages I-II), suggesting that this dysregulation may be the basis for the lack of day-night rhythms in melatonin synthesis [Wu *et al*., 2003]. Taken together with the finding that melatonin increases survival and inhibits amyloid pathology in an Alzheimer mouse model [Matsubara *et al*., 2003], Wu *et al*. [2003] support the idea of a therapeutic supplementation of melatonin in case of decreased night-time melatonin levels to slow down Alzheimer Disease development.

- The Smith-Magenis syndrome (SMS) is another example for circadian rhythm abnormalities of melatonin. Patients suffering from SMS exhibit neurobehavioral abnormalities and significant sleep disturbances. A study of Potocki and co-workers [Potocki *et al*., 2000] shows that SMS patients have an inverted circadian rhythm of melatonin secretion, with high serum melatonin levels during the day and low levels during the night. Most SMS patients are haploinsufficient for subunit 3 of the COP9 signalosome (*COPS3*), which is closely related to the proteasome regulatory complex involved in the control of AANAT metabolism in

mammals [Wei *et al*., 1998]. A direct role for *COPS3* in SMS remains to be established.

- Disruption of the normal sleep-wake-pattern, as seen during night or shift work, was reported to be associated with an increased cancer risk [Schernhammer *et al*, 2004].

For years, melatonin has been widely used as a chronobiotic agent. Its applications range from treatment of minor sleep problems due to jet-lag, night or shift work [Arendt, 2005] to a medication in seasonal depressive disorder (SAD, 'winter depression') [Lewy *et al*., 2006], or even to entrainment of totally blind people [Lewy *et al*., 2005].

1.6 Subject and goals of this study

Rhythms in the mammalian pineal organ depend on afferent information that is derived from the endogenous clock, residing in the hypothalamic SCN. The best characterized function of the pineal gland is the nocturnally elevated synthesis of the hormone melatonin, which provides the body with the signal of the duration of the night period. In contrast to the transcriptional regulation of the *Aanat* gene in rodents, a post-translational shaping of the melatonin pattern was suggested in the human pineal gland. Despite the fact that melatonin can be determined easily in various body fluids, the molecular elements involved in shaping rhythmic hormone synthesis can not be analyzed experimentally in the living organism. Thus, the use of post-mortem pineal material is indispensable.

Within the mammalian SCN, the generation of circadian rhythmicity is achieved by clock genes and their protein products in mammals. The role of clock genes in peripheral tissues is still elusive. In the rodent pineal gland, clock genes are regulated on the transcriptional level, similar to the regulation of the *Aanat* gene. In non-rodent mammals, interactions and regulation mechanisms of clock genes are far from being understood, and the question of a transcriptional or a (post-)translational regulation of these transcription factors is still a matter of debate.

The first aim of this study was the validation and establishment of the use of human post-mortem material as a valid experimental approach to decipher regulation mechanisms of circadian rhythms. As for a future use of melatonin in preventive or

curative interference with the human circadian system, a complete understanding of the generation of the rhythmic hormonal signal in the pineal gland is mandatory. Therefore, a variety of components of the melatonin synthesis pathway were analyzed in detail in human post-mortem pineal glands.

Furthermore, understanding of the regulation of rhythm generation within a neuroendocrine human tissue is of fundamental importance for the medical treatment of chrono-pathologies. Thus, another aim of this study was to validate the detection of clock genes and their protein products, and to get insight into their dynamics in the pineal gland. In addition, after validation and establishment of methods, analyses were to be expanded onto another neuroendocrine gland, the pituitary, which is also known to be a potent mediator of time and seasonality [Wittkowski *et al*., 1999]. It is of utmost importance to understand circadian rhythm generation in the master clock, the human SCN. By now, there is no data on the presence or even regulation of clock genes and their protein products in this endogenous oscillator. Therefore, clock gene proteins were to be analyzed in the human SCN.

2 Methods

2.1 Tissue sampling

2.1.1 Human tissue

All experiments were conducted in accordance with The Declaration of Helsinki, and experiments were formally approved by the local ethics commission of the University Clinics, Frankfurt/Main, Germany. Autopsies were conducted as a consequence of an obligatory assignment by federal prosecutor and German law. Prior to autopsy, the human bodies were kept at 4-8°C after transfer to the Institute of Forensic Medicine. During mandatory autopsies, the scull was opened and adhesive meninges (dura mater, arachnoid membrane) were removed. The brain was cut horizontally (Flechsig cut), the pineal stalk was dissected, the pineal gland removed, fractionalized into several pieces and stored individually at -80°C until further use.

Tissues from 250 specimens were collected. Only a subgroup of those specimens could be used for analyses of diurnal parameters. Criteria for excluding specimens from further analyses were brain atrophy, exposure of the body to heat, severe damage to brain tissue, documented dementia or other mental/affective illnesses, long agony or hospitalization prior to death, transmeridian flights during the last week alive, or an unclear time of death. A detailed list of the specimens analyzed is given in table 1, chapter 7.1.

Time of death was appointed, according to the routinely post-mortem inspection, as documented in the death certificate. Altogether, 74 pineal glands (male: n = 49; female: n = 25) were processed for RNA and protein analyses. Three additional samples were used exclusively for an RNA degradation control experiment (see below). Post-mortem interval (time between death and pineal excision, PMI) ranged between 9 and 147 hours (mean: 47 h $\pm$ 3 h). The age of the analyzed subjects ranged between 10 and 96 years (mean: 47 y $\pm$ 2 y; age distribution: < 20 y: n = 1; 21-30 y: n = 9; 31-40 y: n = 20; 41-50 y: n = 13; 51-60 y: n = 16; 61-70 y: n = 5; 71-80 y: n = 7; 81-90 y: n = 2; > 90 y: n = 1), and did not vary significantly between males and females (male [n = 49]: mean 47 y $\pm$ 2 y; female [n = 25]: mean 49 y $\pm$ 4 y). Causes of death were heart diseases (n = 22), intoxication (n = 18), bleeding to death (n = 10), traffic accidents (n = 5), purler (n = 3),

strangulation (n = 2), pneumonia (n = 2), hanging (n = 2), multiorgan failure (n = 2), drowning (n = 2), brain death (n = 1), decapitation (n = 1), aspiration (n = 1) hypoxia (n = 1), circulatory collapse (n = 1), and undetermined (n = 1) (for details, see table 1, chapter 7.1).

Pineal glands were allocated to four groups, according to the appointed time of death, with a day group (1000 h to 1630 h; n = 11), a dusk-group (1630 h to 2200 h; n = 18), a night–group (2200 h to 0730 h; n = 22), and a dawn–group (0730 h to 1000 h; n = 10). Bin widths of the four time groups were chosen on the basis of epidemiologic coincidence with melatonin onset and offset [Arendt, 1995], and a season-independent gating of the day-time interval.

As an internal control, an analysis of dynamics in mRNA-degradation was performed, using three additional complete human pineal glands, selected from different time groups. These samples were kept at 4°C upon autopsy, to study degradation processes under controlled experimental conditions.

Besides the pineal gland, also the pituitary gland and the hypothalamus were collected and stored individually at -80°C. In addition, formalin-fixed human hypothalami were obtained from Prof. Den Dunnen, University Groningen, Netherlands (age between 39 and 59; PMI between 5 and 12 hours).

Pituitaries of the same specimens that were analyzed for melatonin content (see below) were processed for clock gene analysis. The glands were cut on dry ice in half in the sagital plane. One half was used for preparation of cryostat sections, the second half was used for RNA and protein analyses. Thereby, 30µm sections were cut on a cryostate, and were alternately collected in two different tubes for RNA isolation or tissue homogenization, respectively, ensuring a similar distribution of tissue to facilitate comparison of results. Samples were allocated to the four time-of-death groups as described above.

2.1.2 Animal tissue

Sheep pineal heads were obtained at a local slaughterhouse and immediately transferred to the Institue of Anatomy on ice. Within two hours after death (0600 h in June), the skull was opened and the pineal gland removed and stored immediately at -80°C until further use.

Dehydrated sheep pineal sections, mounted on glass slides, from animals that were kept under short photoperiod (SD 8:16), or killed after first long day treatment (LD 16:8) [Johnston *et al*., 2004] were kindly supplied by D. Hazlerigg, University of Aberdeen, Scotland.

Rat pineal glands that were either unstimulated or stimulated for 6 h with NE were kindly provided by Dr. Marco Koch, Institute of Anatomy II, JWG-University Frankfurt.

2.2 RNA isolation, reverse transcription, and polymerase chain reaction

2.2.1 RNA isolation and transcription

Total RNA from human pineal fractions or pituitary sections was isolated using the Absolutely RNA miniprep kit (Stratagene) according to the manufacturer´s instructions. RNA concentration was assessed spectrophotometrically.

A random-primed reverse transcription (RT) was performed for 1 h at 37°C, with 1 µg of total RNA, 1.5 µl 10x hexanucleotide mixture (Roche), 200 U Moloney Murine Leukemia Virus (M-MLV) reverse transcriptase (Promega), 5 µl M-MLV RT reaction buffer, 1 µl dNTPs (10 mM, 2.5 mM each) in a final volume of 25 µl. Obtained cDNA was stored at -20°C.

2.2.2 Standard PCR and real-time PCR

2.2.2.1 Standard PCR

Polymerase chain reaction (PCR) amplification was performed with a *Taq* DNA polymerase kit (Invitrogen). Briefly, 1 µl of the RT reaction was mixed with 2.5 µl 10x PCR-buffer, 0.75 µl $MgCl_2$ (50 mM), 0.5 µl dNTPs (10 mM, 2.5 mM each), 1 µl of each primer (10 mM), and 0.25 µl *Taq*-polymerase in a final volume of 25 µl.

Primers for human *Aanat* and *Gapdh* were designed using the AbiPrism primer design software (Applied Biosystems); primers for human *Hiomt* were kindly provided by M. Bernard, Poitiers [Bernard *et al*., 1995]; primers used for human clock genes were described previously [Wu *et al*., 2006], all primer sequences are

given in table 2, chapter 7.2. For each primer pair, PCR amplification was performed with at least two different cDNA samples. Optimal annealing temperature (T_a) and cycle numbers were determined by comparing amplification specificity and efficiency of different annealing temperatures and cycle numbers.

Amplification conditions were as follows: first amplification round at 94°C for 5 min, T_a for 1 min, 72°C for 2 min; subsequent amplification rounds: 94°C for 45 s, T_a for 1 min, 72°C for 2 min. Number of cycles and T_a were optimized for each primer pair (*Aanat*: 32 cycles, T_a = 61°C; *Hiomt*: 35 cycles, T_a = 65°C; *Per1*: 33 cycles, T_a = 57°C; *Cry1*: 33 cycles, T_a = 54°C; *Clock*: 36 cycles, T_a = 59°C; *Bmal1*: 32 cycles, T_a = 61°C; *Gapdh*: 26 cycles, T_a = 61°C).

PCR-products were visualized upon size separation through electrophoresis on high-resolution agarose gels (3.5%). For comparative reasons between different gels, samples from all time-of-death-groups were loaded randomly on a given gel. PCR-products were quantified using an image analysis system (ChemiDoc XRS, BioRad) and a DNA mass standard (EZ Load Precision Molecular Mass Standard, BioRad). This mass standard contains different amounts of DNA per fragment (from 10 to 100 ng) and can therefore be used to generate a calibration curve. Band intensities of target gene and *Gapdh* PCR products, as amplified from each pineal cDNA, were digitized and the calibration curve was applied (Quantity One, BioRad), and for comparative reasons expressed as the percentage of the maximal value for a given gel. Values of band intensities of each target gene were normalized against corresponding values of the house-keeping gene *Gapdh*.

2.2.2.2 Real-time PCR

To verify pineal data from RT-PCR analyses, real-time PCR was performed on an ABI Prism 7000 Sequence Detection System (Applied Biosystems) with selected samples (n = 3 per time-of-death-group), using the SYBR Green PCR kit (Applied Biosystems), according to the manufacturer´s instructions. PCR was carried out with 1µl cDNA in a final volume of 25 µl in a 96-well plate, with the same primers as used in the standard PCR analyses, except for *Aanat* and *Hiomt*, where primers were used as previously described [Wu *et al*., 2003]. Samples were measured in triplicate and the values obtained were averaged. Data analysis was performed

using the 2(-delta delta C(T)) method, which was validated according to a protocol provided by the manufacturer [Livak & Schmittgen, 2001].

cDNA obtained from human pituitaries was analyzed on a LightCycler 1.5 (Roche) using the FastStart DNA SYBR Green PCR kit (Roche), according to the manufacuturer´s instructions. PCR was carried out with 1µl cDNA in a final volume of 20µl per glass capillary, with the same clock gene primers as described above; for normalization the house-keeping gene *Elongation Factor 1α* (*EF 1α*) was used (see table 2, chapter 7.2) [Wu *et al*., 2006]. Samples were measured in triplicate and obtained values averaged. For all genes analyzed, cDNA from one and the same sample was used as a positive control throughout all experiments. All data obtained in one experiment were normalized against the value of the positive control to allow comparison of different experiments. Data analysis was performed using the second derivative maximum method (Roche).

2.3 Protein analyses

2.3.1 Preparing pineal and pituitary homogenates

For immunoblotting as well as for determination of AANAT activity and melatonin content, tissue homogenates of pineal fractions or pituitary sections were sonicated in 0.1 M ammonium acetate buffer (pH 6.8), containing protease (Protease Inhibitor Cocktail Tablets, Roche) and phosphatase (Phosphatase Inhibitor Cocktail Set II, Calbiochem) inhibitors, and centrifuged at 14.000 rpm for 15 min at 4°C. Pineal homogenates for HIOMT activity assay were prepared using 0.1 M phosphate buffer (pH 7.9). Supernatants were removed and protein concentrations were determined using a Protein Assay Kit (Pierce), with BSA as a standard, according to the manufacturer´s instructions. Supernatants were stored at -80°C.

For dephosphorylation experiments (see 2.3.4) homogenates were prepared in ammonium acetate buffer as described above, though without addition of phosphatase inhibitors.

2.3.2 AANAT and HIOMT enzyme activity

AANAT activity was reliably determined using a slightly modified protocol as described [Schomerus *et al*., 2002]. Freshly prepared pineal homogenates (20 µl per sample) were incubated at 37°C in an ammonium acetate buffer (pH 6.8), containing tryptamine (1 mM; Fluka) and ^{14}C-acetyl coenzyme A (10 mM, specific activity: 60 Ci/mol; Perkin Elmer).

For HIOMT activity, freshly prepared homogenates (20 µl per sample) were incubated at 37°C in phosphate buffer (pH 7.9), containing *N*-acetyl-serotonin (1.3 mM, Sigma-Aldrich) and adenosyl-L-methionine, S-[methyl-^{14}C] (0.06 mM, specific activity: 55 Ci/mol; Perkin Elmer).

The organic phase was washed twice with ammonium acetate buffer (0.1 M, pH 6.8; AANAT) or sodium borate buffer (20 mM, pH 10; HIOMT), chloroform extracted and dried.

For both, AANAT and HIOMT activity, incorporated radioactivity was measured for each subject in duplicate, averaged, and normalized to protein content.

2.3.3 Immunoblotting (Western Blot analysis)

For Western blot analysis, homogenates of pineal or pituitary fractions were boiled in SDS/PAGE sample buffer and subsequently subjected to denaturing gel-electrophoresis [Laemmli, 1970] (30 µg protein per lane). Thereby, samples from all time-of-death groups were randomly mixed for comparative reasons. Gels were blotted onto a nitrocellulose membrane, and successful transfer was checked by staining the membranes with Ponceau Red to visualize proteins unselectively. Membranes were washed three times in TBS-Tween (0.1 % v/v) for 10 minutes, blocked for 1 hour at room temperature using Rotiblock (Roth), or bovine serum albumine (PAA Laboratories) and incubated overnight at 4°C with primary antibodies (see table 3, chapter 7.3).

Membranes were washed (3 x 10 minutes each) in TBS-Tween (0.1 % v/v) and incubated with the respective secondary antibodies (see table 4, chapter 7.3) in Rotiblock for 1 hour at room temperature.

Chemiluminescence was enhanced using SuperSignal West Pico Chemiluminescent Substrate (Pierce). For detection of chemiluminescence an image analysis system (ChemiDoc XRS, BioRad) was used. Band intensities of the proteins of interest and β-actin, acquired from each protein extract, were analyzed and digitized using the Quantity One software (BioRad), and for comparative reasons expressed as the percentage of the maximal value for a given membrane. Values for AANAT, PER1, CRY1, CLOCK and BMAL1 bands were normalized against corresponding values for bands of the house-keeping protein β-actin.

Specificity of bands was verified by their disappearance upon pre-incubation of primary antibodies with the commercially available immunizing peptides (concentrations according to the manufactures' instructions) prior to incubating the membrane. The immunizing peptide for the AANAT antibody was not commercially available and was therefore synthesized by a University service (Institute of Organic Chemistry and Chemical Biology, JWG-University Frankfurt), according to the sequence given in the datasheet.

2.3.4 Dephosphorylation of AANAT protein

Pineal protein homogenates kept in ammonium acetate buffer (pH 6.8) without phosphatase inhibitors were used for treatment with phosphatase (human/sheep: 30 µg protein). Homogenates were mixed with calf intestinal alkaline phosphatase (CIP; 30 Units/sample; New England Biolabs) in NEB buffer 3 and incubated at 37°C for 30 minutes. To stop the reaction, an equal volume of 2x SDS/PAGE sample buffer was added and samples were prepared for Western Blot analysis (see chapter 2.3.3).

For the dephosphorylation experiment under denaturing conditions, SDS was added to the homogenates mixed with NEB buffer to a final concentration of 1 % and incubated at room temperature for 20 minutes. Directly before adding CIP, NP 40 was added to the mixture to a final concentration of 1 % to stabilize the enzyme. The following procedure of incubation and preparation for Western blotting was as described (see above, and chapter 2.3.3).

2.3.5 Immunofluorescence

A subgroup of human pineal glands (n = 15, for details see table 1, chapter 7.1), that was shown to be representative with respect to clock gene protein content over diurnal time, was used for immunofluorescence and confocal laser scanning microscopy analyses. Cryostat cut sections (5 µm) of pineal glands were stored at -20°C until use. Sections were dried for 20 minutes at room temperature and fixed by immersion with 4 % paraformaldehyde (PFA) in phosphate-buffered saline (PBS; 0.01 M, pH 7.4).

PFA-fixed dehydrated cryostat cut sections of sheep pineal glands were re-hydrated in aqueous solutions with decreasing alcohol concentrations, and equilibrated in water for at least 20 minutes before further processing.

Sections were blocked for 45 minutes using either normal goat serum (NGS, dilution 1:100; Sigma) or normal donkey serum (NDS, dilution 1:200; Sigma) in phosphate buffer (0.01 M, pH 7.4). The same primary antibodies were used as in Western blotting (see table 3, chapter 7.3). In addition, a Nuclear Pore Complex Proteins (NPCP) monoclonal antibody (clone MAb414) covalently coupled to Alexa Fluor 488 (see table 3, chapter 7.3) was used in double-labeling experiments for an effective discrimination between nuclear and cytoplasmic localization of the target proteins. Sections were incubated overnight in a humidified chamber with a mix of the respective primary antibodies directed against AANAT or clock gene products and NPCP in phosphate buffer containing NGS or NDS.

For co-localization of AANAT with HIOMT, or 14-3-3 protein, the respective primary antibodies were used in double-labeling experiments on human pineal sections.

Sections were washed (3 times, 10 minutes each) in PBS (0.01 M, pH 7.4) and incubated for 1 hour with the secondary antibody (see table 4, chapter 7.3) in phosphate buffer (0.01 M, pH 7.4). To block autofluorescence, sections were incubated in Sudan Black (0.1 % w/v in 70 % ethanol; Chroma) for 10 minutes. Sections were mounted using DakoCytomation Fluorescent Mounting Medium (DakoCytomation) and kept in the dark at 4°C until use.

Specificity of immunoreactivity was verified by its disappearance upon pre-incubation of primary antibodies with the immunizing peptides (concentrations according to the manufactures' instructions) prior to incubating the pineal sections.

Intracellular localization of target proteins was determined using a confocal laser scanning microscope (LSM510, Zeiss). For visualization of protein staining, monochromatic light at 543/488 nm with a dichroic beam splitter (FT 543/488) and an emission bandpass filter of 585-615/505-530 nm was used. To visualize subcellular details in confocal images, the electronic zoom of LSM system was used as described [Dehghani *et al*., 2003].

Intracellular localization of the clock gene proteins PER1, CRY1, CLOCK and BMAL1 in pinealocytes was qualitatively determined double-blind in 3 randomly chosen sections per pineal gland (n = 15). At 400-fold magnification an immunoreaction was appointed as nuclear, cytoplasmic, or as present in both compartments. The immunoreaction was appointed as absent, when the amount of immunoreactive glandular cells for clock gene proteins was less than 3 % of all cells. The appointment made for a given pineal gland with respect to clock gene protein distribution (nuclear, cytoplamic) was independent of the absolute number of (i) immunopositive cells per section, and of (ii) the observed intracellular localization.

A subgroup of the pituitaries analyzed by immunoblotting was used for immunofluorescence to determine intracellular localization of clock gene proteins (n = 10). Furthermore, for co-localization of CLOCK with follicle-stimulating hormone (FSH), double-labeling experiments were performed. Samples were chosen on the basis of corresponding melatonin values of the specimens: only specimens with high night-time and low day-time melatonin values were included in the study to possibly detect dynamics in the intracellular localization of proteins. Immunofluorescence was performed as described above.

Cryostat-cut sections of human formalin-fixed hypothalami were used for immunofluorescence analyses of clock gene proteins.

2.3.6 Immunohistochemistry

It was demonstrated earlier that the human SCN can be reliably localized employing an anti-calbindin antibody as a marker [Koutcherov *et al*., 2003]. Therefore, cryostat cut sections of human hypothalami were stained with an anti-calbindin antibody for determining the SCN area. Subsequently, immunohistochemistry was performed on SCN-containing sections for demonstrating expression of clock gene proteins in the human SCN.

Sections were dried for 30 min at room temperature before washing in 0.01 M PBS for 10 min. Activity of endogenous peroxidase was blocked by incubation of the sections in 1 % H_2O_2 for 10 minutes in the dark. Sections were blocked with either NGS or NDS and incubated with primary antibodies as described above (see. 2.3.5 and table 3, chapter 7.3). After incubation with the respective secondary antibodies (table 4, chapter 7.3), sections were incubated for 1 h with ExtrAvidin-peroxidase (1:100; Sigma). DAB-solution (Merck) was freshly prepared in 0.05 M Tris buffer, and reaction was started by adding H_2O_2 to the solution. Sections were incubated 3 to 6 minutes in DAB solution in the dark before dehydrating and mounting with Entellan (Merck).

2.3.7 Co-immunoprecipitation

Human pineal homogenates (60 µg protein per experiment) were used for co-immunoprecipitation of AANAT and 14-3-3 protein. Homogenates were diluted in 0.5 ml ammonium acetate buffer and pre-incubated with the respective primary antibodies (1.5x concentration as used for immunoblotting, see table 3, chapter 7.3) for 1 h at room temperature under agitation. Resuspended protein A/G agarose (20 µl) was added and the mixture was incubated overnight at 4°C under agitation. Protein A/G agarose is a mixture of protein A- and protein G-agarose, and therefore can specifically bind to a broader variety of immunoglobulins. Thus, protein A/G agarose could bind to all antibodies used for precipitation. Agarose-protein-antibody-complexes were precipitated by centrifugation for 1 min at 3.000 rpm. After resuspension of the pellet, the protein complexes were washed twice in 0.5 ml cold ammonium acetate buffer. Subsequently 20 µl 2x SDS-sample buffer was added and

gel electrophoresis and immunoblotting was performed as described above (see chapter 2.3.3). Samples that had been precipitated with the anti-14-3-3 antibody were probed with the anti-AANAT, and the anti-HIOMT antibodies. As a control experiment, the samples that had been precipitated with the anti-AANAT antibody were probed with the anti-14-3-3 and the anti-HIOMT antibodies.

2.3.8 Melatonin enzyme-linked immuno-sorbent assay (ELISA)

Melatonin content in pineal tissue was determined in duplicate for each sample and with two dilutions (1:50 and 1:500) with an ELISA kit (IBL). Homogenized samples were diluted in ammonium acetate buffer (pH 6.8) and melatonin was extracted according to the manufacturer's protocol, using reversed-phase C18-columns. Signals were analyzed densitometrically with an ELISA reader (Multiscan RC, LabSystems). Melatonin content was calculated against standard values provided by the manufacturer and normalized to protein content.

2.4 Statistical analyses

The hypotheses of normality and homogeneity of the variance were tested using the Kolmogorov-Smirnov-test and Levene tests, respectively. The Pearson's chi-squared test (χ^2) was used to compare the gender distribution among the four groups. Statistical differences of the measurements of clock gene mRNA and proteins, as well as age and PMI between time-of-death groups were analyzed using a one-way ANOVA, followed by post hoc Bonferroni test. Statistical differences between two groups were analyzed using unpaired *t*-tests (two-tailed). The Kruskal and Wallis H-test was applied to determine whether the time of death of the subjects (allocated to the four time-of-death-groups) was associated to AANAT, or HIOMT activity, or to melatonin content, respectively. Significant associations were further characterized by means of a nonparametric trend analysis. The criterion of significance was $P < 0.05$, with analyses performed using SPSS Software (Release 13; SPSS Inc., Chicago, USA).

3 Results

3.1 Pineal analyses

3.1.1 Statistical pretests

All obtained data were allocated to the four time-of-death groups (night, dawn, day, dusk). Gender was equally distributed among the four time-of-death groups in both protein- and RNA-samples (RNA: $\chi^2 = 3.2$, df = 3, $P = 0.4$; protein: $\chi^2 = 3.8$, df = 3, $P = 0.3$). All continuous variables (age, and PMI) had a normal distribution within the four time-of-death groups and did not show significant differences between the groups (all P-values > 0.05).

3.1.2 Degradation experiment

Total RNA was extracted from all samples kept at 4°C, and was subjected to reverse transcription according to the protocol given in chapter 2.2.1. PCR amplification was applied on the cDNA yield, revealing a clear decline with time in all mRNA levels investigated (Fig. 6).

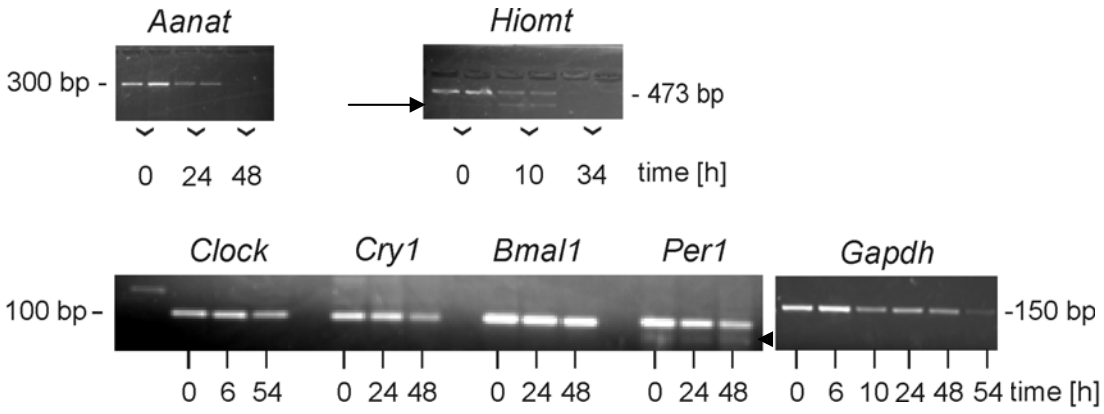

Fig. 6: RNA degradation over time in human pineal tissue.

Amplification products of RT-PCR analyses, achieved with specific primers for *Aanat*, *Hiomt*, *Per1*, *Cry1*, *Clock*, *Bmal1*, and *Gapdh*, visualized on high resolution agarose gels. Band sizes are indicated. To study mRNA degradation over time, tissue samples were maintained for indicated time intervals at 4°C. Note the general loss of signal intensities with time, and the appearance of degradation products for *Hiomt* (indicated by arrow), and possibly for *Per1* (indicated by arrowhead).

For the *Hiomt* amplification product, sized 473 bp, also a smaller degradation product can be seen on the gel already after 10 h, similar to *Per1* (Fig. 6).

Slopes of regression lines for *Aanat* (y = -1.5648x + 90.328), *Hiomt* (y = -1.0604x + 70.04), *Per1* (y = -0.8355x + 99.99), *Cry1* (y = -1.0559x + 103.24), *Clock* (y = -0.9937x + 90.988), *Bmal1* (y = -0.9859x + 101.75), and the house-keeping gene *Gapdh* (y = -1.3874x + 95.302) were remarkably similar (Fig. 7).

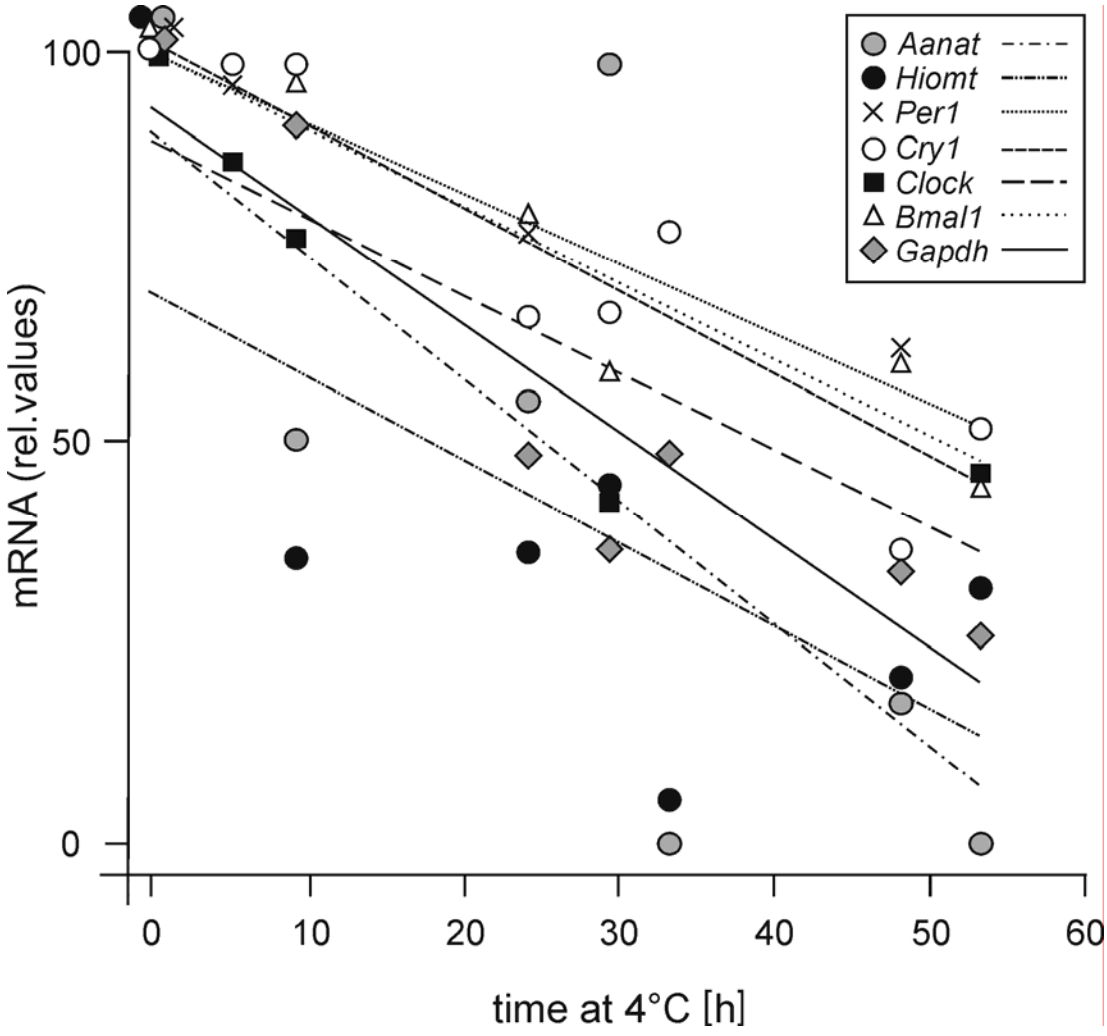

Fig. 7: Regression analysis of RNA degradation.

Semiquantitative densitometric analyses of signals for individual samples, as shown in Fig. 6, with a linear regression curve fitted to obtained values. Note the almost parallel decline in the signal intensities of investigated mRNAs, representing the decay of overall template availability for amplification with time.

Extending regression lines indicates a total absence of intact RNA at the latest after 100 h under these artificial conditions. This decline in RNA content is largely accelerated as compared to the situation in the corpse, where intact RNA could still be recovered at a PMI of 141 h.

With this degradation experiment, it could be confirmed that degradation of human autoptic pineal material can be considered an ordered process with similar degradation rates for different mRNAs, as reported earlier in other brain tissue [Yasojima *et al*., 2001; Hynd *et al*., 2003; Preece *et al*., 2003].

3.1.3 Melatonin biosynthesis parameters

3.1.3.1 *Aanat* and *Hiomt* mRNA levels

Intact mRNA was extracted from 55 pineal glands processed. Thereby, it could be confirmed that reverse transcription of isolated RNA with random hexamers is the method of choice, because transcription using oligo-dT primers failed to provide useable cDNA (not shown), as demonstrated earlier [Yasojima *et al*., 2001; Hynd *et al*., 2003].

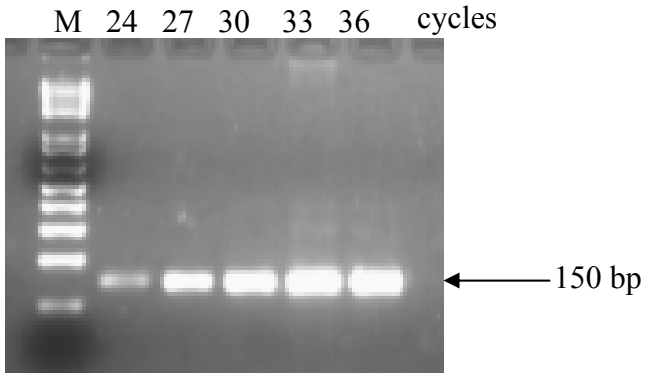

Fig. 8: Determining the optimal cycle number for *Gapdh* amplification (150 bp, indicated by arrow).

A strong correlation between the number of cycles and the *Gapdh* signal intensity can be seen. The plateau phase of amplification is reached at latest after 33 cycles. 27 amplification cycles were considered optimal to match the logarithmic phase of amplification. M = DNA marker.

All primers were optimized concerning T_a and number of cycles. Thereby, especially the optimal cycle number is important as it ensures that, at the end of the PCR, amplification of the template is still in its logarithmic phase. An example of such an optimization experiment is given in Fig. 8.

PCR amplification products for *Aanat* and *Hiomt* showed bands of the expected size (see Fig. 6). Employment of high-resolution agarose for gel electrophoresis induced both, exact separation and a sharp definition of bands (Fig. 9).

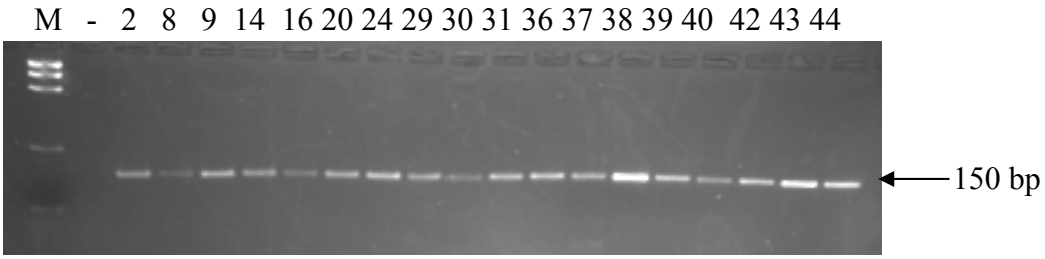

Fig. 9: PCR amplification products for *Gapdh*, separated on a high-resolution agarose gel (3.5%).

Lane 1: molecular mass marker; lane 2: negative control; lanes 3 – 20: PCR amplification products (150 bp, indicated by arrow) obtained with *Gapdh* primers in human pineal cDNA samples. Sample numbers are indicated (see table 1, chapter 7.1).

Mean RNA amounts, as assessed by RT-PCR for the targeted genes *Aanat* and *Hiomt*, did not show significant differences between the four time-of-death groups, when normalized against the house-keeping gene *Gapdh* (*Aanat*: $P = 0.49$; *Hiomt*: $P = 0.81$; Fig. 10).

To confirm these results, real-time PCR analyses were performed for all genes investigated, using randomly selected samples from each time-of-death group (n = 3 per group). After normalization of the target genes against the house-keeping gene *Gapdh*, statistical analysis affirmed data obtained by standard PCR methods (*Aanat*: $P = 0.10$; *Hiomt*: $P = 0.14$).

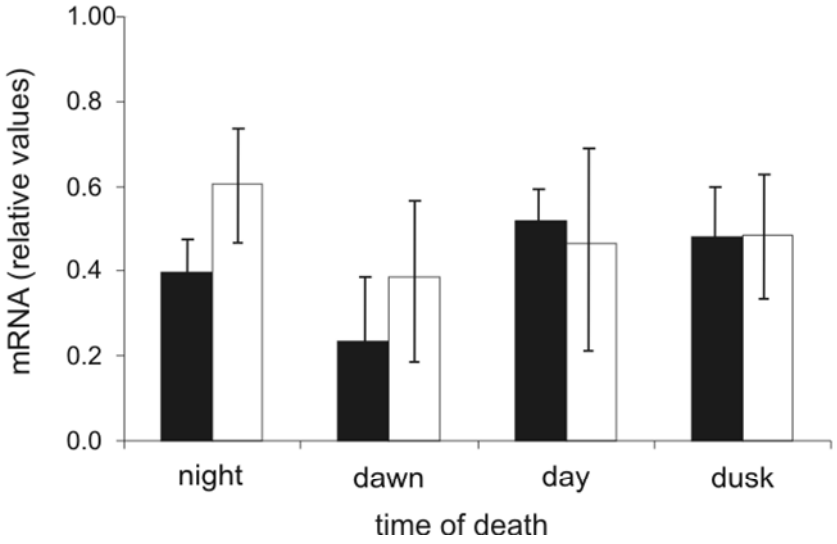

Fig. 10: Diurnal analyses of relative *Aanat* (black bars) and *Hiomt* (open bars) mRNA levels in human pineal tissue.

Standardized RT-PCR analyses were applied to RNA, extracted from human pineal tissue (n = 55). Obtained signals for *Aanat* and *Hiomt* amplification products were normalized against corresponding *Gapdh* values. Results were allocated to the four groups (night: n = 21, dawn: n = 8, day: n = 11, dusk: n = 15) according to time of death of each individual subject. Depicted are the means ± SEM of the relative mRNA values. No significant correlation was found between mean values for *Aanat* and *Hiomt* mRNA and time of death.

3.1.3.2 Protein analyses

3.1.3.2.1 Enzyme activity assays

It was shown earlier that HIOMT activity (halving time: about 24h [Bernard *et al*., 1993]) is far more stable than AANAT activity (halving time: about 3 min [Klein & Weller, 1972]). Values for HIOMT activity measured in this study range from 0 to 1800 fmol/h/µg protein, whereas AANAT activity values were much lower, ranging from 0 to 100 fmol/h/µg protein. Thus, HIOMT activity is by far the most reliable parameter to characterize the remnant biochemical integrity of pineal tissue. Therefore, those subjects were excluded from statistical analysis, which showed no, or very low levels of HIOMT activity (< 100 fmol/h/µg protein; n = 10). Indeed, subsequent analyses showed no or very low levels of AA-NAT activity and

melatonin content exactly in these samples, irrespective of time of death of the subjects.

AANAT activity measurements in human pineal glands

AANAT activity was measured in 61 human pineals, out of which 10 samples with no or very low activity were excluded from further analysis, as they showed also very low or absent levels of HIOMT activity (see above).

Although the number of samples investigated in the dusk (n = 13) and in the night group (n = 20) outreach by far the sample number in the dawn (n = 8) and in the day group (n = 10), pineals with undetectable AANAT activity were notably higher in number in the latter groups (dawn/day: n = 12 *vs.* dusk/night: n = 7). High values of AANAT activity (> 26 fmol/h/µg protein content; n = 13) were only present in the dusk and night group (Fig. 11).

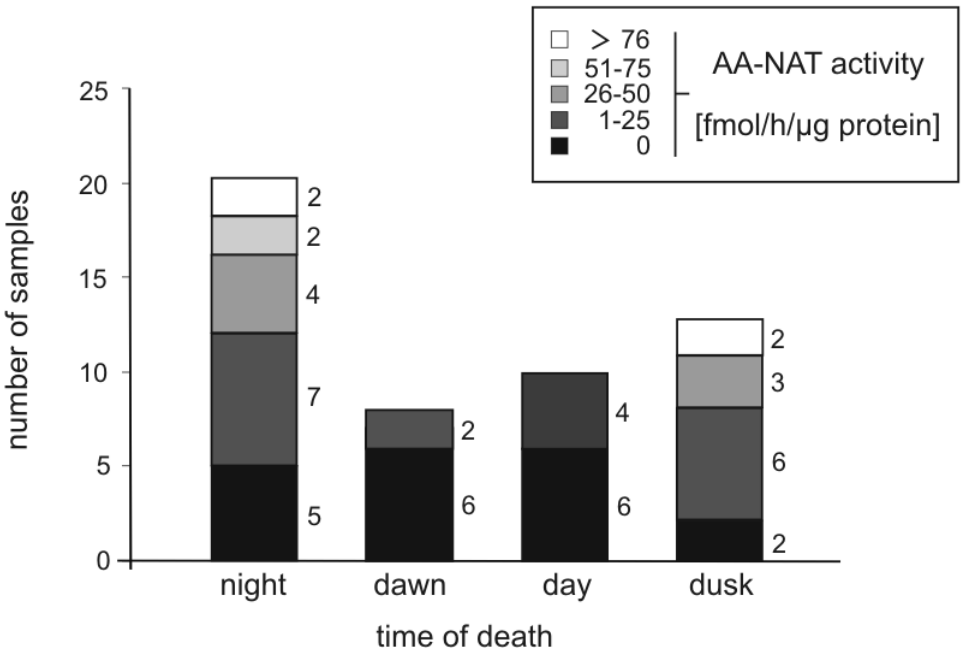

Fig. 11: Diurnal analysis of AANAT activity in autoptic pineal tissue.

Distribution of AANAT activity values within the four groups (night, dawn, day, dusk), allocated to five ranges in enzyme activity. Note the exclusive appearance of high and highest AANAT activity (> 26 fmol/h/µg protein) in the dusk and night groups. Number of samples that were allocated to the different range groups according to the measured AANAT activity is indicated at the right of each column.

AANAT activity values were significantly correlated to time of death ($H_{corr} = 9.0330$; $P < 0.05$). Subsequent nonparametric trend analysis revealed furthermore a significant quadratic trend for the correlation between AANAT activity and time of death ($H_{quad} = 7.4965$; $P < 0.01$; Fig. 12).

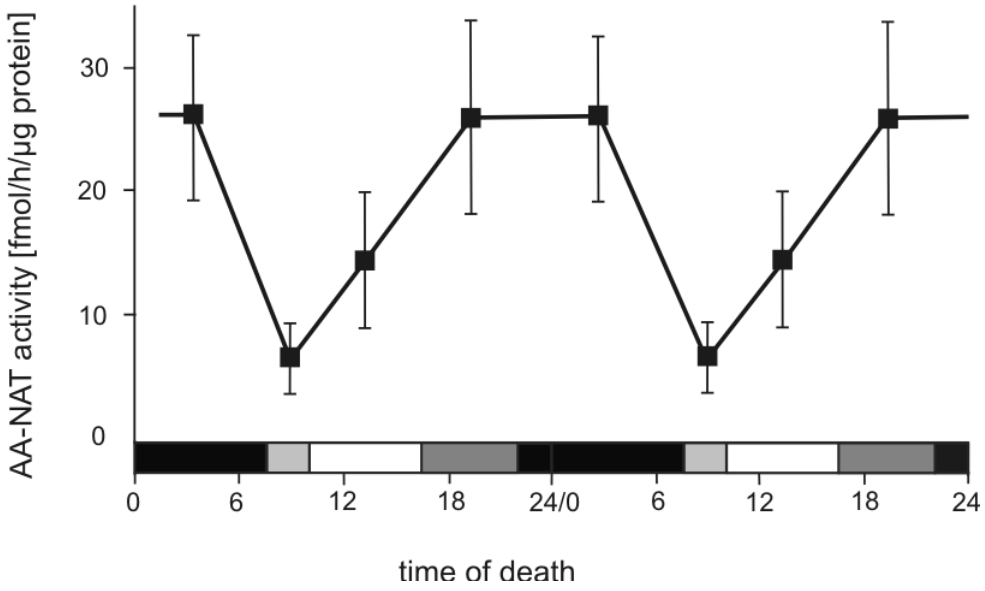

Fig. 12: Diurnal analysis of AANAT activity in autoptic pineal tissue.

Double-plot of the diurnal pattern of AANAT activity, depicted as mean AANAT enzyme values (± SEM) for each of the four time-of-death groups (night: black, 2200 h to 0730 h; dawn: grey, 0730 h to 1000 h; day: white, 1000 h to 1630 h; dusk: dark grey, 1630 h to 2200 h). A significant quadratic correlation was found between mean values for AANAT activity and time of death.

HIOMT activity measurements in human pineal glands

Due to a restriction in tissue availability HIOMT activity could not be analyzed in 18 out of 61 pineal glands analyzed for AANAT (see above). However, in these 18 samples all other parameters were determined.

Measured HIOMT values were uniformly distributed with respect to time of death (Fig. 13). Further statistical analysis revealed no significant correlations between time of death and measured activity values (Fig. 14).

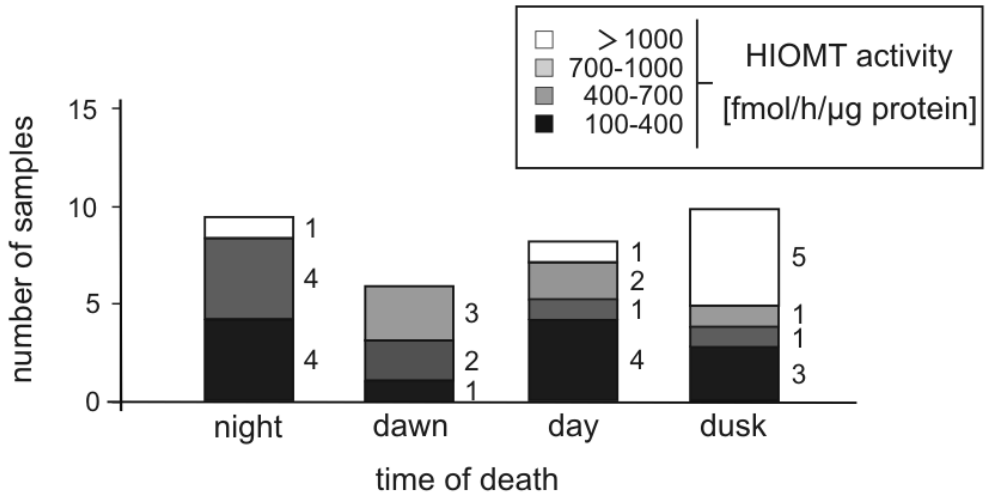

Fig. 13: Diurnal analysis of HIOMT activity in autoptic pineal tissue.

Distribution of HIOMT activity values within the four time-of-death groups, allocated to four ranges in enzyme activity. Number of samples that were allocated to the different range groups according to the measured HIOMT activity is indicated at the right of each column.

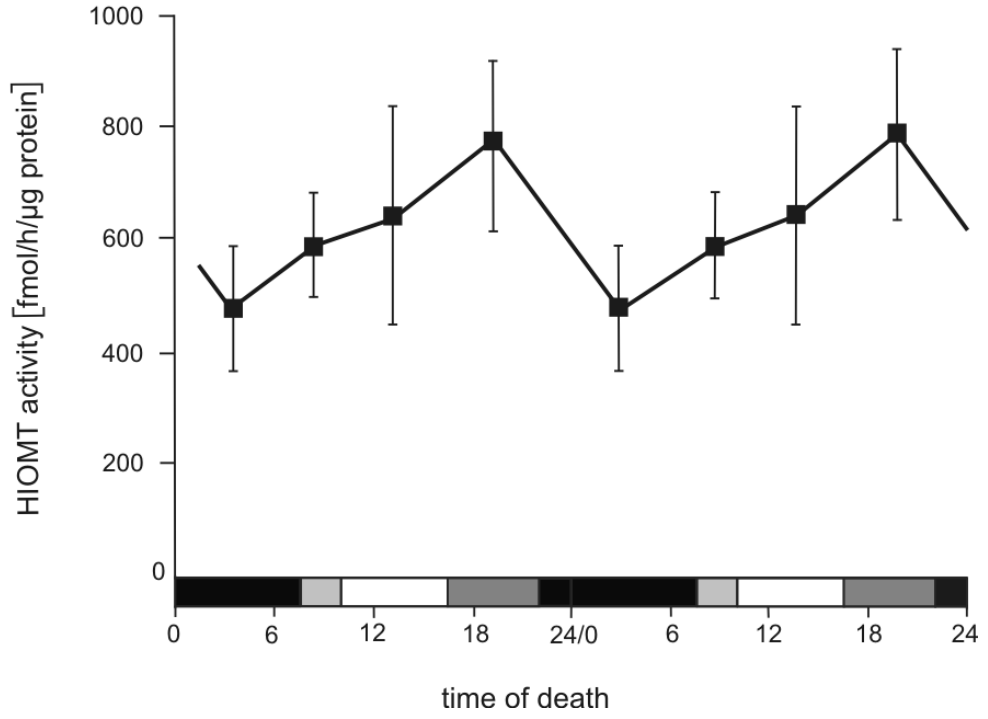

Fig. 14: Diurnal analysis of HIOMT activity in autoptic pineal tissue.

Double-plot of the diurnal pattern of HIOMT activity, depicted as mean HIOMT enzyme values (+/- SEM) for each of the four time-of-death groups (night: black, 2200 h to 0730 h; dawn: grey, 0730 h to 1000 h; day: white, 1000 h to 1630 h; dusk: dark grey, 1630 h to 2200 h). No significant correlation was found between mean values for HIOMT activity and time of death.

3.1.3.2.2 Immunoblot analyses of AANAT protein content

The anti-AANAT antibody used in this study was characterized in detail earlier [Ganguly *et al*., 2001, 2005]. It was described to bind specifically the phosphorylated N-terminal PKA site of rat, ovine and human AANAT.

Immunoblot signals for AANAT showed bands of the expected size (Fig. 15).

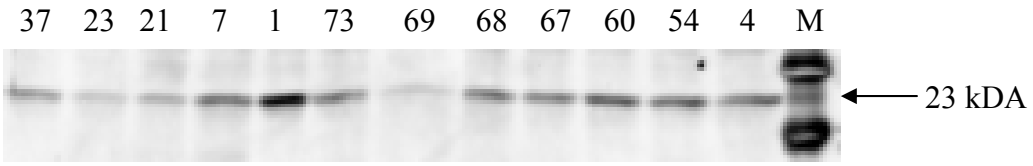

Fig. 15: Representative immunoblot of human pineal homogenates.

The membrane was probed for AANAT protein using an anti-phospho-AANAT antibody. Size of the bands obtained from human pineal protein homogenates is indicated by an arrow. Sample numbers are indicated (see table 1, chapter 7.1); M = protein marker.

When signal intensities were normalized against β-actin, AANAT protein content showed no significant differences between the four time-of-death groups ($P = 0.95$; Fig. 16).

To confirm these results, specimens with low night-time melatonin and low HIOMT activity values were deliberately excluded (n = 9) and statistical analysis was repeated. Again, no significant differences in the amount of AANAT protein over diurnal time bins were found ($P = 0.87$).

To test the phospho-specificity of the antibody, a dephosphorylation experiment was performed using rat pineals (unstimulated or stimulated for 6 h with NE), human and sheep pineal homogenates (Fig. 17).

Dephosphorylation was succesful in rat pineal homogenates: a strong decline in signal intensity between phosphatase-untreated and phosphatase-treated NE-stimulated rat pineal glands could be observed (Fig. 17, lanes 3, 4). Unstimulated rat pineal glands (both CIP-treated and CIP-untreated), which were used as negative controls, showed bands of a similar intensity as the band observed for NE-stimulated and CIP-treated rat pineal gland (Fig. 17, lanes 1, 2, 4). However, the antibody detected AANAT bands in human and sheep pineal homogenates independent of

CIP-treatment, with no change in signal intensity of the AANAT bands (Fig. 17, lanes 5 – 8). These results confirm the phospho-specificity of the AANAT antibody only for rat, but not for human and sheep, as reported earlier [Ganguly *et al*., 2001].

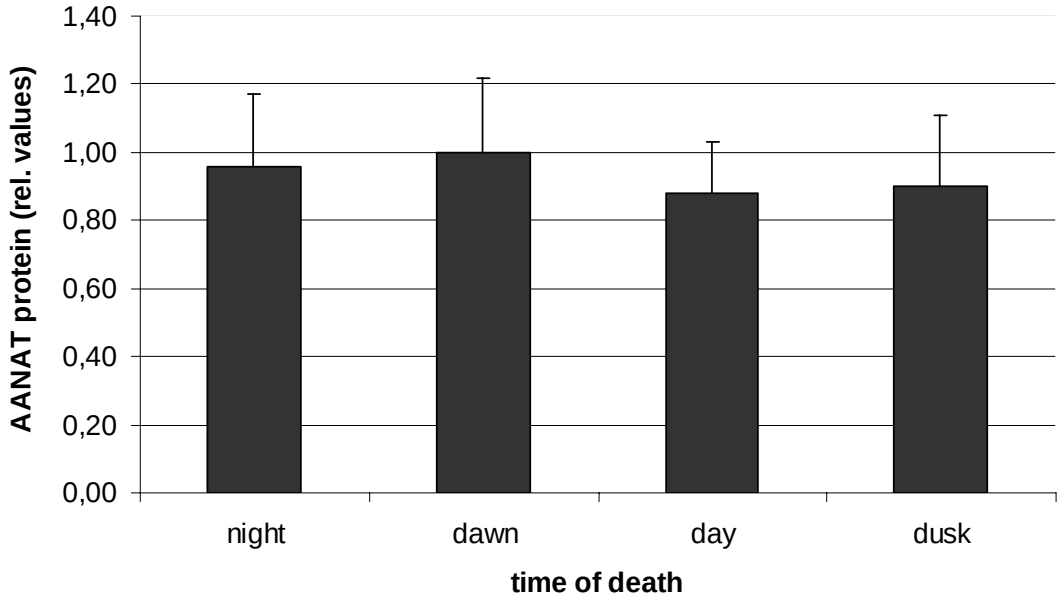

Fig. 16: Analyses of relative AANAT protein levels in human pineal tissue.

Depicted are the mean relative values (+ SEM) of AANAT protein content for the four time groups (night, dawn, day, dusk; n = 60), according to time of death. Signals obtained for AANAT and β-actin were digitized and for comparative reasons values were expressed as percent of maximum for a given membrane. AANAT protein values were normalized against corresponding β-actin values.

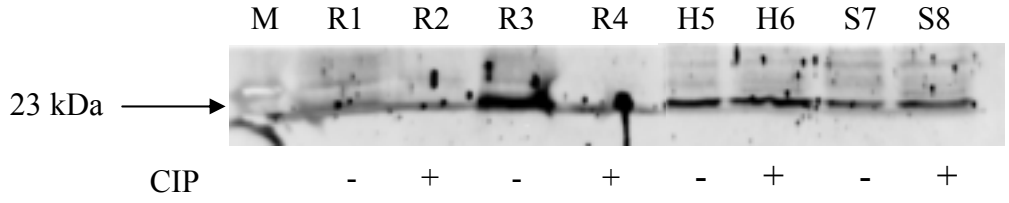

Fig. 17: AANAT dephosphorylation experiment.

Pineal homogenates were subjected to phosphatase treatment followed by immunoblotting. Dephosphorylation was successfull in rat pineal gland, as can be seen from the different band intensites in lanes 3 and 4. However, CIP-treatment had no effect on band intensities of AANAT in human or sheep pineal glands. M = molecular weight marker; lanes 1-4: rat pineal homogenates (R), lanes 1-2: unstimulated, lanes 3-4: 6 h NE, lanes 5-6: human night pineal homogenates (H), lanes 7-8: sheep pineal homogenates (S). Band size is indicated by arrow.

It has been shown that dephosphorylation at T31 is strongly inhibited when AANAT is complexed with 14-3-3 protein [Ganguly *et al*., 2001]. Therefore, the dephosphorylation experiment was repeated under denaturing conditions employing SDS (Fig. 18).

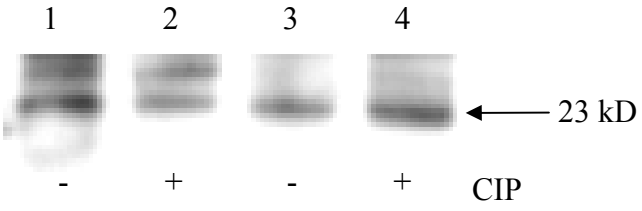

Fig. 18: Dephosphorylation experiment under denaturing conditions.

Pineal homogenates of humans (lanes 1, 2) and sheep (lanes 3, 4) were incubated in a 1% SDS-solution and subsequently subjected to CIP-treatment. No differences in signal intensities could be detected. Band size is indicated by arrow.

Despite the mild denaturing conditions, dephosphorylation of the complex was not successful. Yet, it was not possible to use a higher SDS concentration in order to break the tight association of the protein complex, as stronger denaturing conditions would also inhibit CIP-activity.

3.1.3.2.3 Intracellular localization of AANAT protein

Intracellular localization of AANAT protein did not change throughout the 24h-cycle in human and sheep pineal glands. AANAT was found in the cytoplasm close to or at the nuclear membrane, within the nucleus in small condensed structures, and also extensively in cellular processes in the human glands (Fig. 19).

Exactly the same distribution as described above for the human pineal glands was also found on sections of sheep pineal tissue (Fig. 20): an intense staining of AANAT protein within the network of cellular processes could be observed, together with a staining in compartments of the cell nucleus and the peri-nuclear region. This pattern of AANAT staining on sheep pineal sections also did not change during the 24h-cycle.

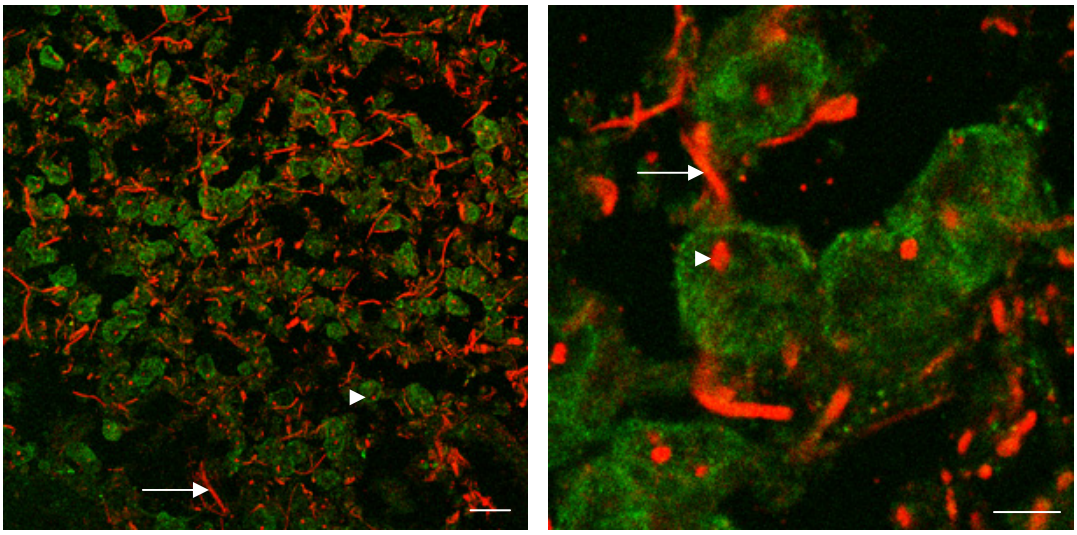

Fig. 19: Representative immunofluorescence images obtained from double-staining of AANAT (red) and NPCP (green) on human pineal sections.

Note the intense staining of AANAT protein in cellular processes (arrows) and condensed structures in the cell nucleus (arrowheads). Left scale bar: 20 µm, right scale bar: 5 µm.

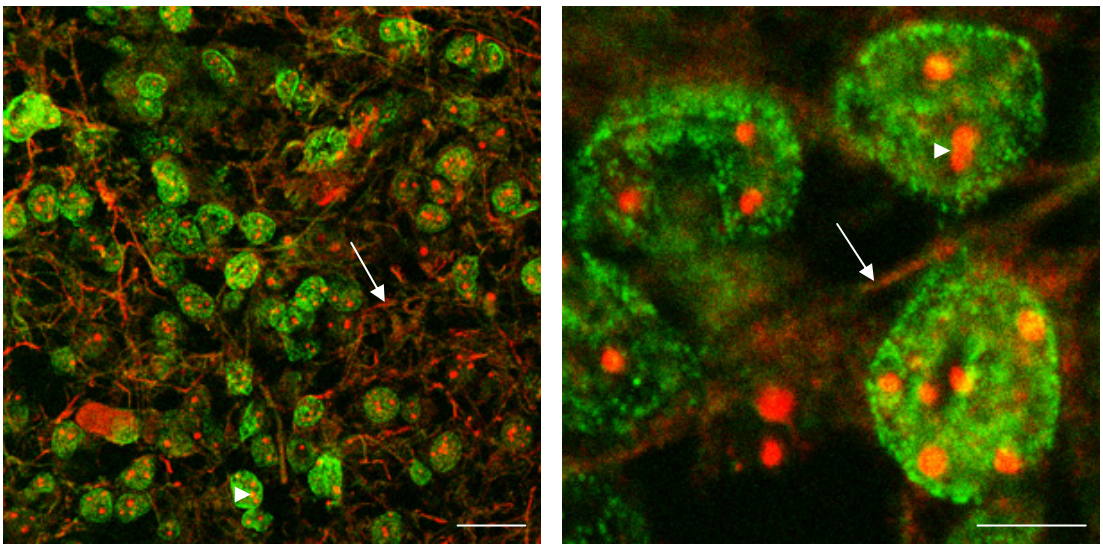

Fig. 20: Representative immunofluorescence images obtained from double-staining of AANAT (red) and NPCP (green) on sheep pineal sections.

Note the intense staining of AANAT protein in cellular processes (arrows) and condensed structures in the cell nucleus (arrowheads), similar as observed for the human pineal gland (Fig. 19). Left scale bar: 20 µm, right scale bar: 5 µm.

3.1.3.2.4 Co-localization of AANAT and 14-3-3 protein

Double-immunolabeling of AANAT and 14-3-3 protein on sections of human pineal tissue revealed a co-localization of both proteins in cellular processes, independent of time of day. As expected, a strong staining of 14-3-3 protein was also found in the cytoplasm (Fig. 21).

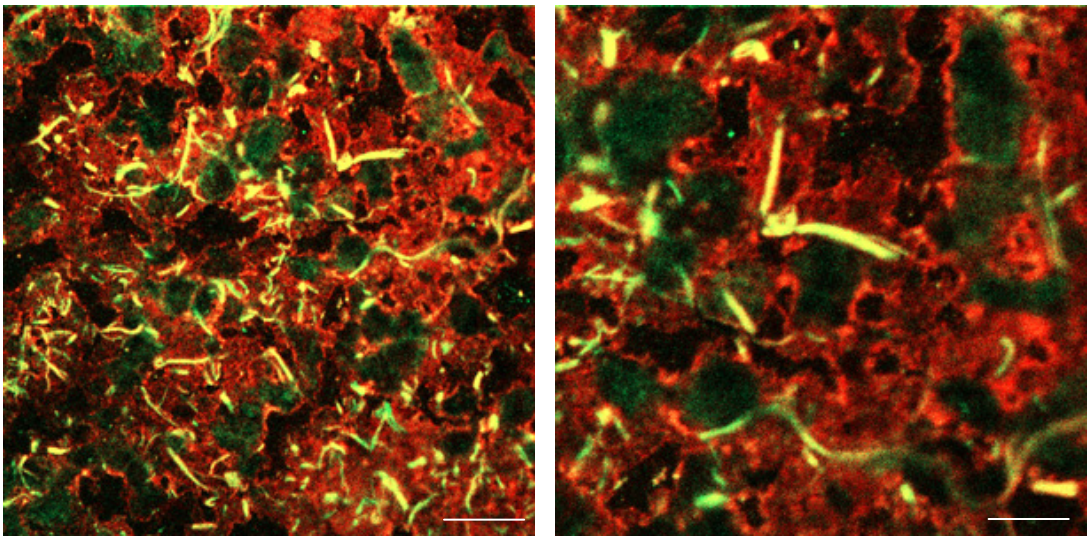

Fig. 21: Representative immunofluorescence images obtained from double-staining of AANAT (green) and 14-3-3 protein (red) on human pineal sections.
Note the simultaneous presence of AANAT protein and 14-3-3 protein in cellular processes (yellow staining). 14-3-3 protein is also present in the cytoplasm of pinealocytes. Left scale bar: 20 µm, right scale bar: 10 µm.

3.1.3.2.5 Co-localization of AANAT and HIOMT

Double-immunolabeling of AANAT and HIOMT on human pineal sections revealed a co-localization of both proteins in cellular processes, independent of time of day. Notably, HIOMT was not found to be co-localized with AANAT within the cell nucleus (Fig. 22).

It has to be stated that the HIOMT antibody has not been fully validated yet. The commercially available immunizing peptide is covalently coupled to a glutathione S-transferase-tag, which has to be cleaved with a specific protease and

separated from the peptide before conducting blocking experiments. These experiments are currently in progress.

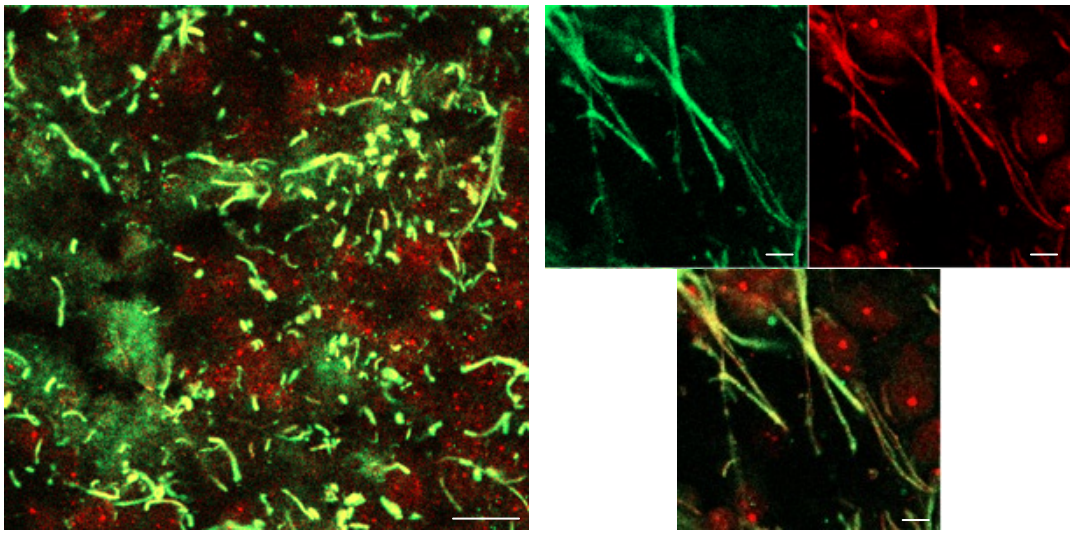

Fig. 22: Representative immunofluorescence images obtained from double-staining of AANAT (red) and HIOMT (green) on human pineal sections.

Note the simultaneous presence of AANAT protein and HIOMT in cellular processes (yellow staining). Note that HIOMT is not colocalized with AANAT in the cell nucleus of pinealocytes (upper panel: HIOMT and AANAT staining separately, lower panel: merge). Left scale bar: 20 µm, right scale bar: 5 µm.

3.1.3.2.6 Co-immunoprecipitation of AANAT and 14-3-3 protein

Co-immunoprecipitation experiments revealed the presence of AANAT/14-3-3 complexes in both day and night human pineal homogenates. Homogenates were incubated with the anti-AANAT antibody, precipitated and subjected to immunoblotting employing the anti-14-3-3 antibody (Fig. 23), and *vice versa* (Fig. 24). Thereby, the yield of complex was lower when precipitating with the anti-AANAT antibody than when precipitating with the anti-14-3-3 antibody.

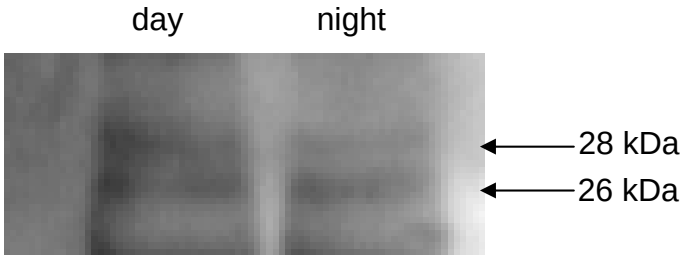

Fig. 23: Co-immunoprecipitation of AANAT and 14-3-3.

Day and night human pineal homogenates were precipitated using the anti-AANAT antibody and probed with the anti-14-3-3 antibody, which recognizes the two lower molecular weight subunits of protein 14-3-3 (band sizes are indicated).

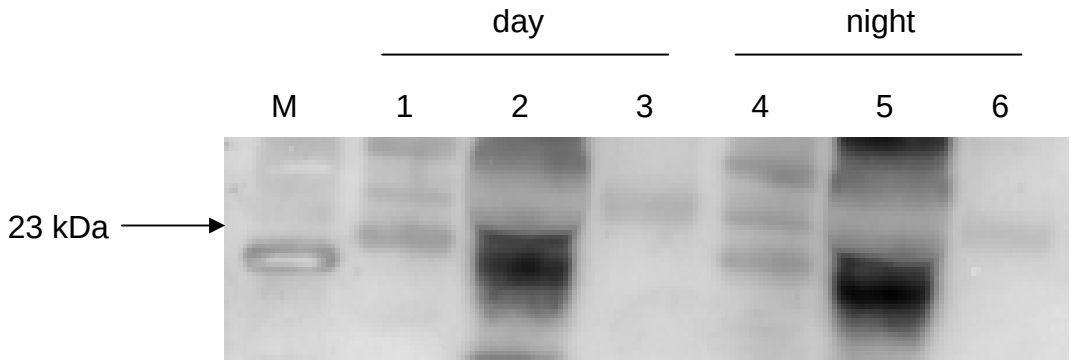

Fig. 24: Co-immunoprecipitation of 14-3-3 and AANAT.

Day and night human pineal homogenates were precipitated using the anti-14-3-3 antibody and probed with the anti-AANAT antibody. M = molecular weight marker; lanes 1, 4: pure homogenate; lanes 2, 5: precipitate; lanes 3, 6: supernatant. Band size is indicated.

To determine whether HIOMT is also complexed with AANAT and 14-3-3 protein, the respective Western Blots were also probed with an anti-HIOMT antibody. As already stated in chapter 3.1.3.2.5, validation experiments for the anti-HIOMT antibody are currently in progress.

Expected molecular weight of HIOMT protein is 36 kDa. In pure pineal homogenates (lanes 1, 4 in Fig. 25), the antibody also detects proteins in a molecular range of 38 to 45 kDa, which are declared by the manufacturer as HIOMT ubiquitinylation products. In precipitates obtained from human day and night pineal homogenates, only bands of the correct molecular weight were detected (lanes 2, 5 in

Fig. 25). In the supernatants (lanes 3, 6 in Fig. 25) no HIOMT signal could be detected. These data indicate that HIOMT may also be part of the AANAT/14-3-3-protein complex in the human pineal gland.

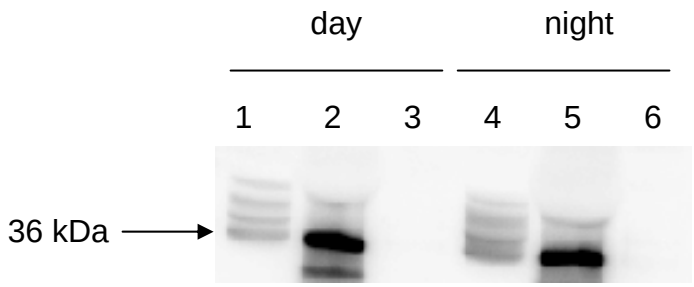

Fig. 25: Immunoblot showing the precipitates of human pineal glands probed with an anti-HIOMT antibody.

HIOMT bands of the correct size (36 kDa as indicated) can be seen in the precipitates of both, day and night samples, whereas in pure homogenates also higher molecular weight bands are detected. No HIOMT immunoreaction can be found in the supernatants. Lanes 1, 4: pure homogenate; lanes 2, 5: precipitate; lanes 3, 6: supernatant.

3.1.3.2.7 Melatonin content and correlation to time of death

Melatonin was measured in the same 61 human pineal samples, as analyzed for AANAT activity. In those 10 samples with very low or undetectable HIOMT activity (see above), no or very low amounts of melatonin could be detected and samples were excluded from further analyses. Highest melatonin levels (> 1000 pg/mg protein) were found only in the night-time group. Notably, out of the 30 subjects with undetectable, or very low values (0-100 pg/mg protein), the smallest subset (n = 6) was present in the group with the highest number of samples, the night group (n = 20) (Fig. 26).

Time of death was highly significantly correlated with melatonin content (H_{corr} = 10.7135; $P < 0.025$). Further nonparametric trend analysis revealed a significant quadratic trend for this correlation (H_{quad} = 4.0650; $P < 0.05$; Fig. 27).

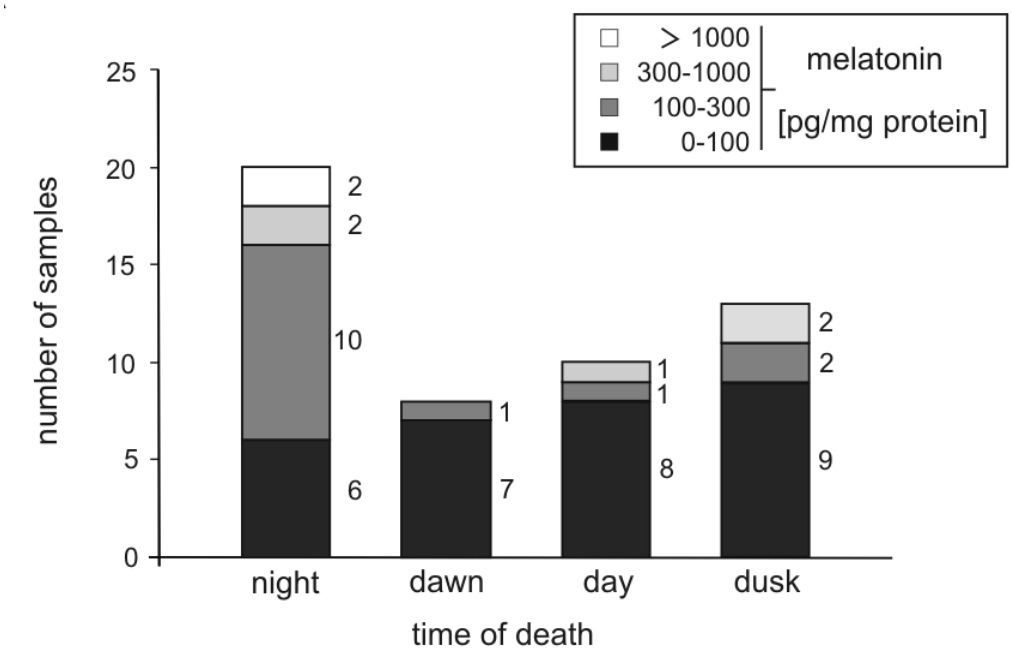

Fig. 26: Diurnal analyses of melatonin content in autoptic pineal tissue.

Distribution of melatonin values within the four groups (night, dawn, day, dusk), allocated to four ranges in hormone values. Note that, although the night group is the largest of all time-of-death groups (n = 20), the sample number with low to undetectable melatonin levels is the smallest (n = 6) in this group, and that highest melatonin values appear exclusively in this time-of-death group. Number of samples that were allocated to the different range groups according to the measured melatonin content is indicated at the right side of each column.

When melatonin concentrations were measured without preceding extraction of the hormone from protein homogenates, no reliable results were obtained, as measured melatonin values were always higher in the higher dilutions of the same sample. Therefore, extraction of melatonin from pineal homogenates using reversed-phase C18-columns provided by the manufacturer was indispensable. The reason for this effect is unclear, but is probably related to cross-reactions and interferences of the pure pineal homogenates with the chemicals used in the kit.

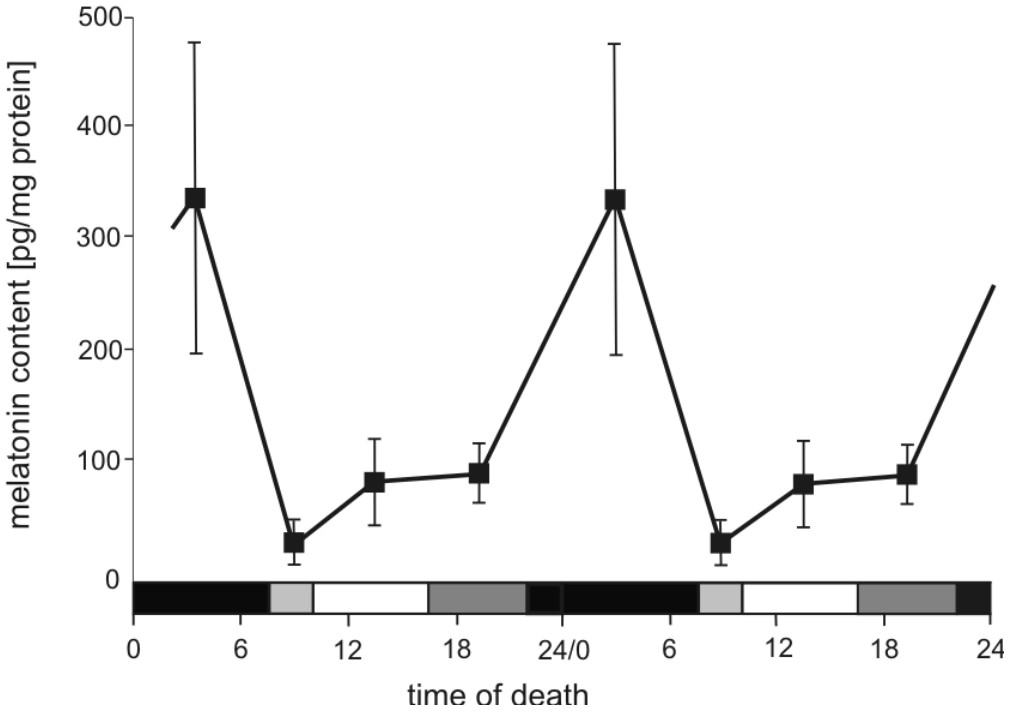

Fig. 27: Diurnal analyses of melatonin content in autoptic pineal tissue.

Double-plot of the diurnal pattern of measured melatonin levels, depicted as mean hormone values (± SEM) for each of the four time-of-death groups (night: black, 2200 h to 0730 h; dawn: grey, 0730 h to 1000 h; day: white, 1000 h to 1630 h; dusk: dark grey, 1630 h to 2200 h). A significant quadratic correlation was found between mean values for melatonin content and time of death.

3.1.4 Clock genes and their protein products

3.1.4.1 Presence of clock gene mRNA and proteins in human pineal tissue

Intact mRNA was extracted from 55 human pineal glands. PCR amplification products for all clock genes investigated showed bands of the expected size, when separated on high-resolution agarose gels (see Fig. 28).

Protein homogenates from 71 human pineal glands were analyzed by Western blotting. Immunoblot signals for PER1, CRY1, CLOCK, BMAL1 and actin showed bands of the expected size (Fig. 29).

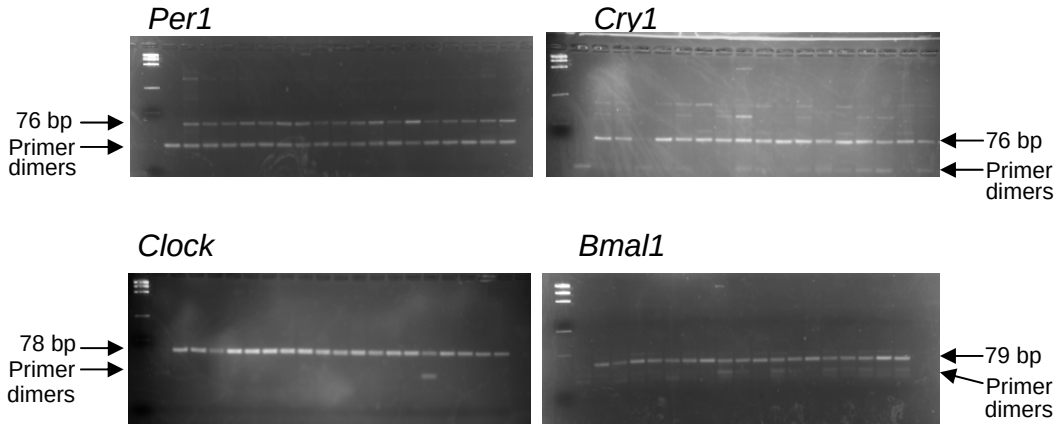

Fig. 28: Representative high-resolution agarose gels for *Per1*, *Cry1*, *Clock*, and *Bmal1* PCR amplification products, obtained from human pineal cDNA.

For comparative reasons, randomly chosen samples from each time-of-death group were separated on each gel. Band sizes and bands of primer dimers for each amplification product are indicated by arrows. Only for *Cry1*, unspecific signals of weak intensity, which are larger than the correct amplification product, can be seen on the gel.

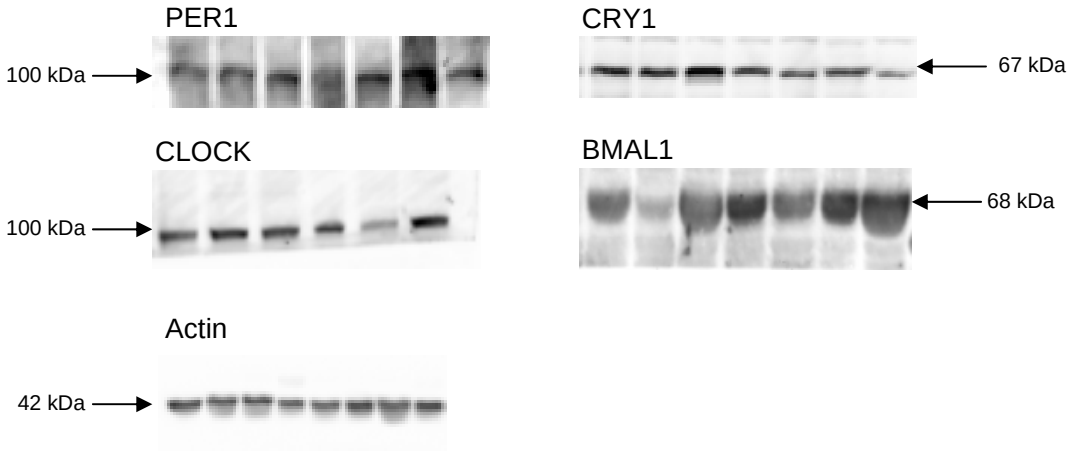

Fig. 29: Representative immunoblots for PER1, CRY1, CLOCK, BMAL1 and actin, obtained from human pineal homogenates.

For comparative reasons, randomly selected samples from each time-of-death group were separated on each membrane. Band sizes are indicated by arrows.

3.1.4.2 Analysis of clock gene mRNA and proteins in human pineal tissue

Mean RNA amounts as assessed by RT-PCR for the targeted genes *Per1*, *Cry1*, *Clock,* and *Bmal1* did not show significant differences between the four time-of-death groups, when normalized against the house-keeping gene *Gapdh* (*Per1*: $P = 0.98$; *Cry1*: $P = 0.16$; *Clock*: $P = 0.99$; *Bmal1*: $P = 0.49$; Fig. 30). To confirm these results, real-time PCR analyses were performed for all genes investigated, using randomly selected samples from each time-of-death group (n = 3 per group). After normalization of the target genes against the house-keeping gene *Gapdh*, statistical analysis affirmed data obtained by standard PCR methods (all *P*-values > 0.1).

RNA analyses for clock gene mRNA content over diurnal time were repeated after specimens had been separated into a short-PMI-group (9-30 hours), a long-PMI-group (> 50 hours), as well as into specific age groups (20-40 years and 60-90 years). In an additional analysis, specimens with low night-time melatonin values were excluded. In neither of these subgroups significant differences in the amount of clock gene mRNA over diurnal time bins were found. In the short-PMI-group all *P*-values were > 0.99, in the long-PMI-group *P*-values for *Per1* and *Bmal1* were > 0.99, the *P*-value for *Clock* was 0.44, and the *P*-value for *Cry1* was 0.82. *P*-values obtained for the young-age group ranged between 0.40 for *Cry1* and 0.85 for *Clock*. *P*-values obtained for the old-age group ranged between 0.60 for *Clock* and 0.82 for *Per1*. *P*-values obtained after exclusion of samples with low melatonin values at night ranged between 0.34 for *Cry1* and 0.88 for *Clock*.

When immunoblot signal intensities were normalized against β-actin none of the clock gene proteins investigated showed significant differences between the four time-of-death groups (PER: $P = 0.43$; CRY1: $P = 0.60$; CLOCK: $P = 0.75$; BMAL1: $P = 0.32$; Fig. 30).

Also when specimens with low night-time melatonin values were deliberately excluded, no significant differences in the amount of clock proteins over diurnal time bins were found (PER1: $P = 0.28$; CRY1: $P = 0.61$; CLOCK: $P = 0.39$; BMAL1: $P = 0.61$).

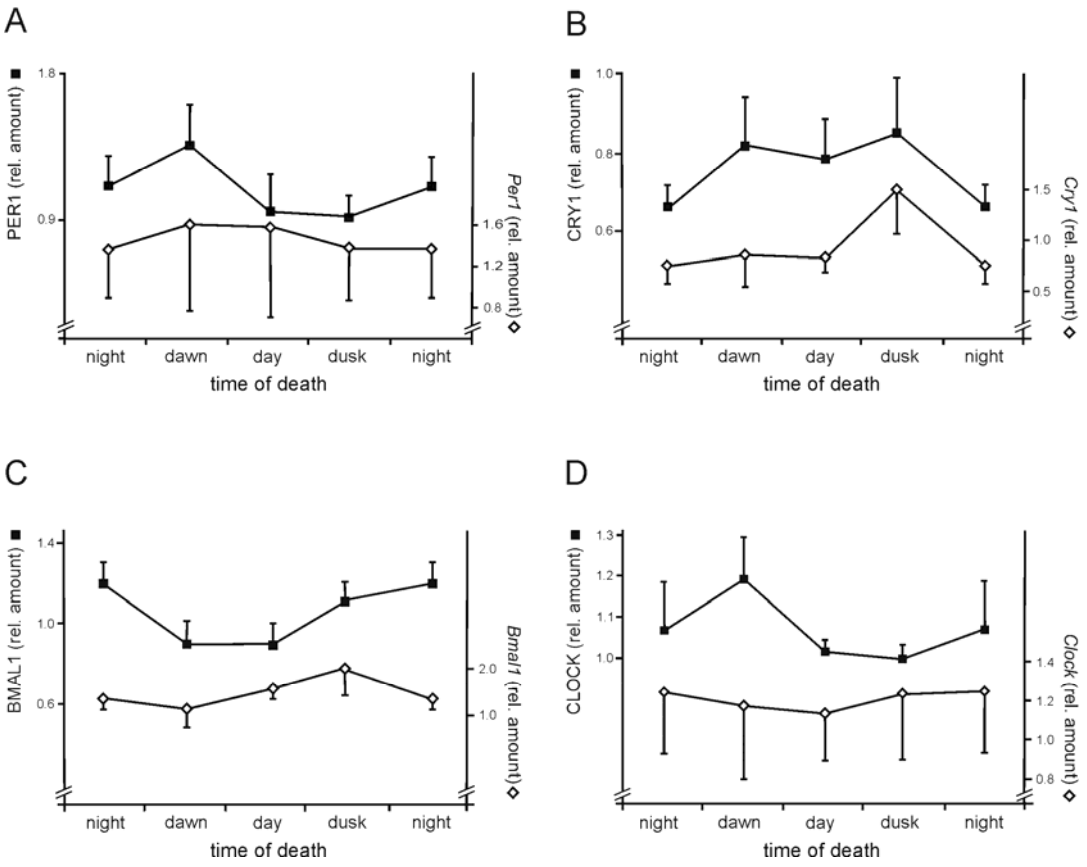

Fig. 30: Analyses of clock gene mRNA abundance and clock gene protein levels in human pineal tissue.

Mean relative values (± SEM) for clock gene mRNAs (open symbols, scaling on the right) and proteins (closed symbols, scaling on the left) analyzed in human pineal tissue, for the four time groups (night, dawn, day, dusk), according to time of death. mRNA: Signals obtained for *Per1*, *Cry1*, *Clock*, and *Bmal1* amplification products were expressed as percent of maximum for a given gel for comparative reasons. Clock gene values are normalized against corresponding *Gapdh* values. Protein: Signals obtained for PER1, CRY1, CLOCK, and BMAL1 were expressed as percent of maximum for a given membrane for comparative reasons. Clock protein values were normalized against corresponding β-actin values (n = 71 for PER1, CRY1 and CLOCK; n = 55 for BMAL1).

3.1.4.3 Nucleo-cytoplasmic shuttling of clock gene proteins

In contrast to the uniform immunoblot signals over diurnal time for all clock gene proteins investigated using whole cell lysates (Fig. 30), the sub-cellular distribution of clock gene proteins the PER1, CRY1, and CLOCK changed remarkably with time (Fig. 31). Different cells in the same section exhibited variations in the intensity of their immunoreactivity as well as in their distribution.

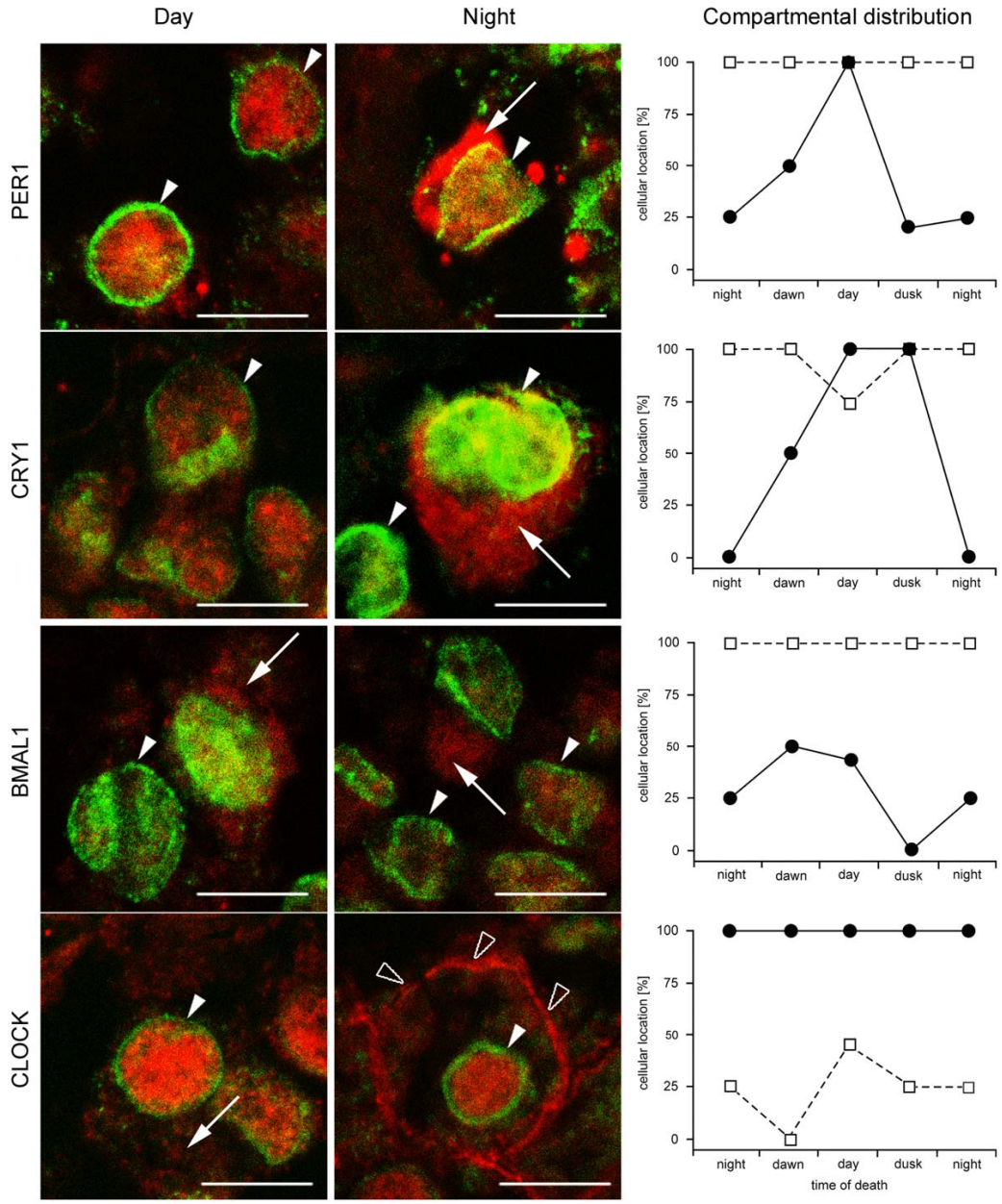

Fig. 31: Sub-cellular localization of clock gene proteins in human pinealocytes.

Left columns (Day, Night) show representative confocal laser scanning microscopic images of clock gene products (red) and nuclear pore complex proteins (green). *Arrows*: cytoplasm; *arrow heads*: nucleus; *open arrow heads*: membrane-associated immunoreaction. Scale bar: 5µm.

Right column (relative amount) shows superimposed graphs depicting the proportion of clock gene products in relation to time of death and to the sub-cellular compartments for both, nucleus (●) and cytoplasm (□). Note that a given clock protein can be present in both compartments at the same time in a given pinealocyte. Note also the synchronous sub-cellular translocation of PER1 and CRY1 from the nucleus to the cytoplasm with respect to time of day.

While PER1 was always present in the cytoplasm, levels in the nuclear compartment showed profound diurnal variations, with maximal values reached during day-time (Fig. 31).

Likewise to PER1, the CRY1 immunoreaction was at all time-points present in the cytoplasm, whereas the nuclear abundance changed markedly, with low levels during night and elevated levels during day and dusk (Fig. 31).

The BMAL1 immunoreaction was present in the cytoplasm at all time points investigated. In some instances a BMAL1 staining was evident in cytoplasmic processes in varying intensities. The BMAL1 signal was seen in the nucleus during late night/early morning and during day-time, but not during dusk (Fig. 31).

CLOCK protein was localized in the nucleus at all time-points investigated, while the cytoplasmic signal varied, with elevated levels evident during day-time. Intriguingly, a translocation of the CLOCK protein to the cell membrane was observed during night-time only (Fig. 31). This localization at the membrane becomes especially evident when lower magnification is used to visualize a united cell structure (Fig. 32).

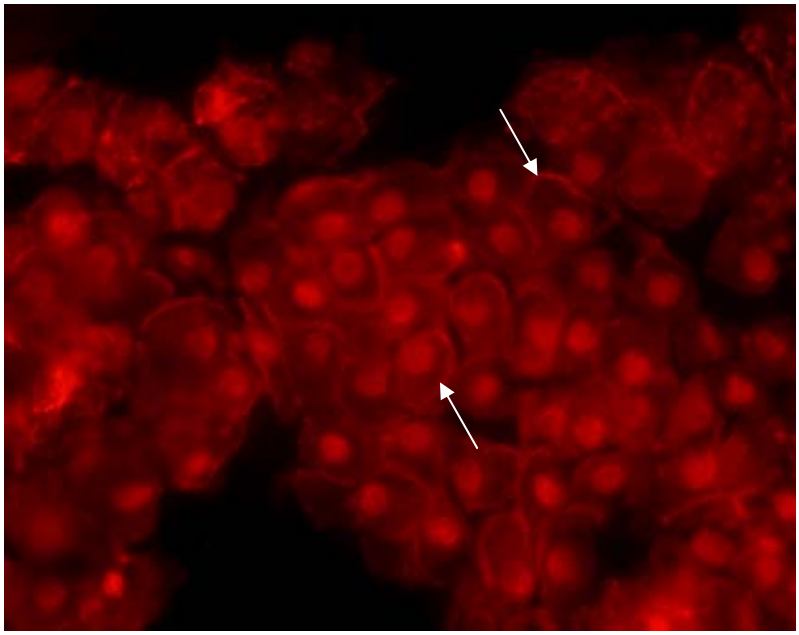

Fig. 32: CLOCK protein localization at the cell membrane.

CLOCK was localized in the cell nucleus and at the cell membrane (indicated by arrows), as visualized in a united cell structure of a night-time sample in human pinealocytes. 400-fold magnification.

3.2 Pituitary analyses

3.2.1 Statistical pretests

All data were allocated to the four time-of-death groups (night, dawn, day, dusk). Gender was equally distributed among the four time-of-death groups ($\chi^2 = 3.4$, df = 3, $P > 0.3$). All continuous variables (age, and PMI) had a normal distribution within the four time-of-death groups and did not show significant differences between the groups (all *P*-values > 0.05).

Only those pituitary glands were used for this study, where melatonin content and AANAT activity were determined from corresponding pineal glands, with respective values reflecting a reliable and intact circadian rhythmicity of this subgroup of specimens. Thus, a set of human pituitaries was chosen, where the pre-mortem situation of the specimens was characterized by melatonin synthesis parameters, thereby allowing compiling samples into distinct time-of-death groups, as described for the human pineal glands.

3.2.2 Analysis of clock gene mRNA levels

Mean RNA amounts as assessed by real-time PCR for the targeted genes *Per1*, *Cry1*, *Clock,* and *Bmal1* did not show significant differences between the four time-of-death groups, when normalized against the house-keeping gene *EF 1α* (*Per1*: $P = 0.65$; *Cry1*: $P = 0.68$; *Clock*: $P = 0.49$; *Bmal1*: $P = 0.99$; n = 52; Fig. 33).

Notably, mean values obtained for *Per1* expression were only about 20 % as compared to values obtained for *Cry1*, while levels obtained for *Clock* and *Bmal1* were similar when compared to each other for all time-of-death groups (Fig. 33).

RNA analyses for clock gene mRNA content over diurnal time were repeated after specimens had been separated into a short-PMI-group (9-30 hours), a long-PMI-group (> 50 hours), as well as into specific age groups (20-40 years and 60-90 years). In an additional analysis, specimens with low night-time melatonin values were excluded. In neither of these subgroups significant differences in the amount of clock gene mRNA over diurnal time bins were found: *P*-values in the short-PMI-group were $P = 0.14$ for *Per1*, $P = 0.90$ for *Cry1*, $P = 0.21$ for *Clock*, and $P = 0.90$ for *Bmal1*; *P*-values in the long-PMI-group were $P = 0.47$ for *Per1*, P = 0.58 for

Cry1, $P = 0.30$ for *Clock*, and $P = 0.18$ for *Bmal1*. *P*-values obtained for the young-age group were $P = 0.56$ for *Per1*, $P = 0.95$ for *Cry1*, $P = 0.43$ for *Clock*, and $P = 0.71$ for *Bmal1*. *P*-values obtained for the old-age group were $P = 0.70$ for *Per1*, $P = 0.19$ for *Cry1*, $P = 0.56$ for *Clock*, and $P = 0.46$ for *Bmal1*. *P*-values obtained after exclusion of samples with low melatonin values at night were $P = 0.55$ for *Per1*, $P = 0.99$ for *Cry1*, $P = 0.15$ for *Clock*, and $P = 0.57$ for *Bmal1*.

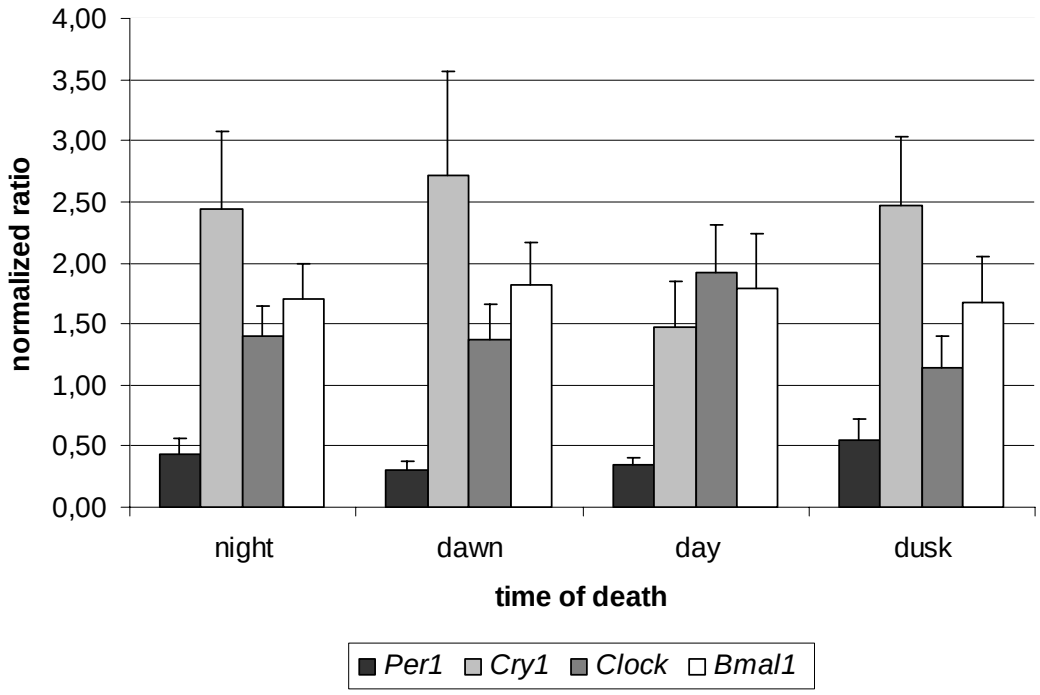

Fig. 33: Analyses of relative clock gene mRNA levels in human pituitary tissue.
Given are the mean relative values (+ SEM) of clock gene mRNAs *Per1*, *Cry1*, *Clock*, and *Bmal1*, for the four time groups (night, dawn, day, dusk), according to time of death. Values obtained for *Per1*, *Cry1*, *Clock*, and *Bmal1* amplification products were normalized against corresponding *EF 1α* values.

3.2.3 Protein analyses

3.2.3.1 Analysis of clock gene protein levels

Relative clock gene protein levels of human pituitary tissue (n = 52) were analyzed by immunoblotting. When immunoblot signal intensities were normalized against β-actin, none of the clock gene proteins investigated showed significant

differences between the four time-of-death groups (PER: $P = 0.47$; CRY1: $P = 0.82$; CLOCK: $P = 0.07$; Fig. 34). Due to serious quality problems with the new batch of the anti-BMAL1 antibody, no reliable results could be obtained for BMAL1 levels as yet.

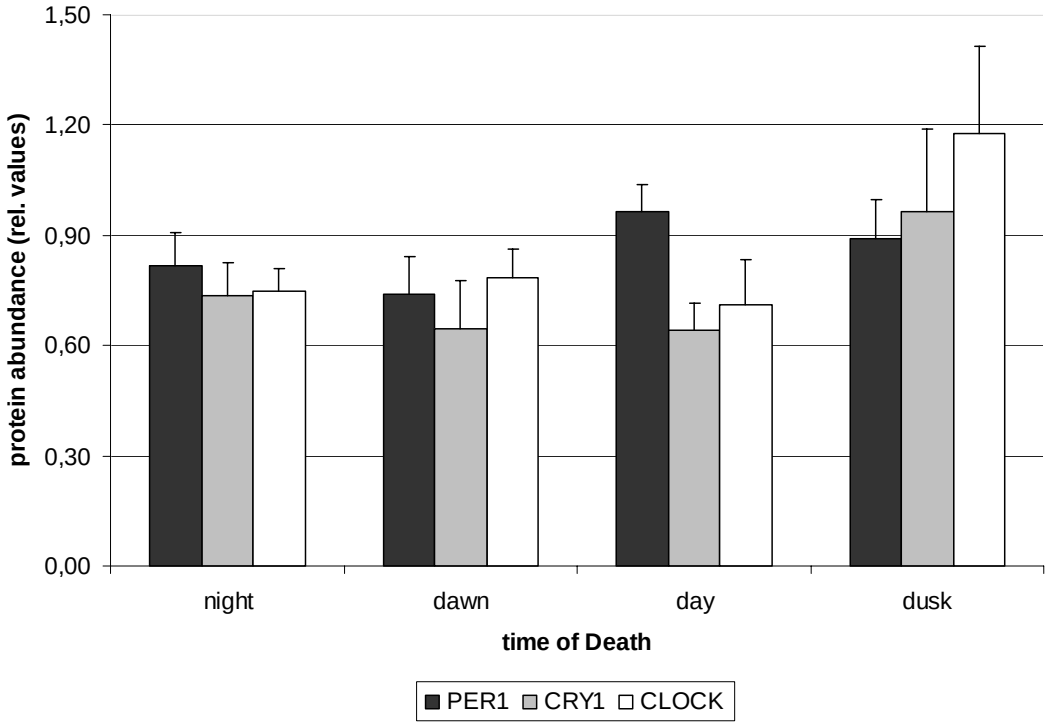

Fig. 34: Analyses of relative clock gene protein levels in human pituitary tissue.
Given are mean relative values (+ SEM) of clock gene proteins for the four time groups (night, dawn, day, dusk), according to time of death. Signals obtained for PER1, CRY1, and CLOCK were digitized and for comparative reasons values were expressed as percent of maximum for a given membrane. Clock protein values were normalized against corresponding β-actin values.

Analyses for clock gene protein content over diurnal time were repeated after specimens had been separated into a short-PMI-group (9-30 hours), a long-PMI-group (> 50 hours), as well as into specific age groups (20-40 years and 60-90 years). In an additional analysis, specimens with low night-time melatonin values were excluded. In neither of these subgroups significant differences in the amount of clock gene proteins over diurnal time bins were found. In the short-PMI-group *P*-values were $P = 0.21$ for PER1, $P = 0.66$ for CRY1, and $P = 0.57$ for CLOCK. In the long-PMI-group *P*-values were $P = 0.10$ for PER1, $P = 0.78$ for CRY1, and $P = 0.73$ for

CLOCK. *P*-values obtained for the young-age group were $P = 0.96$ for PER1, $P = 0.98$ for CRY1, and $P = 0.86$ for CLOCK. *P*-values obtained for the old-age group were $P = 0.25$ for PER1, $P = 0.35$ for CRY1, and $P = 0.49$ for CLOCK. *P*-values obtained after exclusion of samples with low melatonin values at night were $P = 0.59$ for PER1, $P = 0.60$ for CRY1, and $P = 0.10$ for CLOCK.

3.2.3.2 Intracellular localization of clock gene proteins

Preliminary experiments revealed that, in contrast to the uniform immunoblot signals over diurnal time for all clock gene proteins investigated using whole cell lysates (Fig. 34), the sub-cellular distribution of the clock gene proteins PER1 and CRY1 varied with time. As already stated above for immunoblotting, no reliable results could be obtained for BMAL1, due to serious quality problems with the new batch of the anti-BMAL1 antibody.

While PER1 was always present in the cytoplasm, levels in the nuclear compartment showed diurnal variations, with elevated levels reached during day-time (Fig. 35).

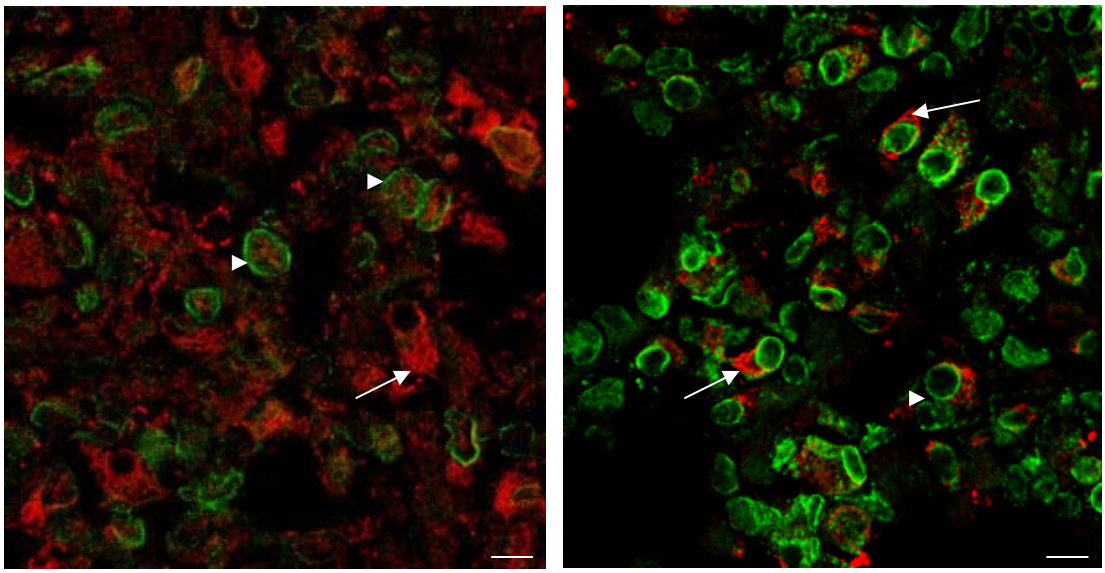

Fig. 35: Intracellular localization of PER1 in human pituitary tissue.

Double-staining of PER1 (red), and NPCP (green) on sections obtained from human pituitary tissue. The nuclear membrane is stained with NPCP. Note the lack of PER1 staining of the cell nucleus during night-time. *Left*: day, *right*: night. *Arrows*: cytoplasm; *arrowheads*: nucleus. Scale bar: 10 µm.

Likewise to PER1, the CRY1 immunoreaction was at all time-points present in the cytoplasm, whereas the nuclear abundance changed markedly, with low levels during night and elevated levels during day (Fig. 36). These observations indicate the presence of a nucleo-cytoplasmic shuttling of the clock gene proteins PER1 and CRY1, similar to the data obtained for clock gene proteins in the human pineal gland (see chapter 3.1.4.2.2).

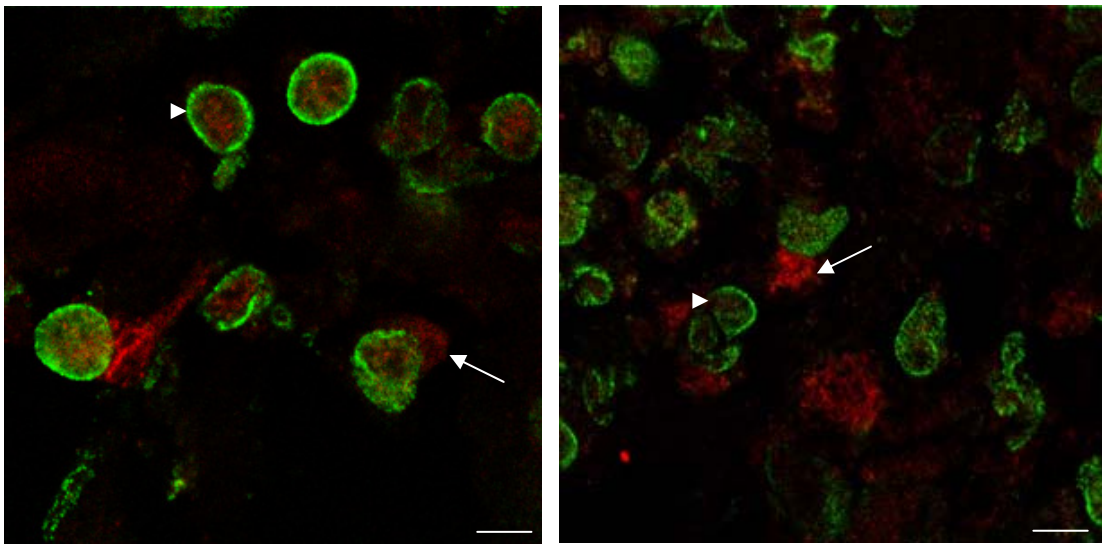

Fig. 36: Intracellular localization of CRY1 in human pituitary tissue.
Double-staining of CRY1 (red) and NPCP (green) on sections obtained from pituitary tissue. Note the very weak staining of the cell nucleus during night-time (*right*) compared to day-time (*left*). *Arrows*: cytoplasm; *arrowheads*: nucleus. Scale bar: 5 µm.

CLOCK protein was localized in the nucleus independent of time of day. In addition, CLOCK immunoreactivity was found in small vesicle-like cytoplasmic structures (Fig. 37). In order to find out if these structures are possible secretory vesicles of the adenohypophysis, immunofluorescence experiments using an antibody against follicle-stimulating hormone (FSH) were conducted.

Initial studies revealed that CLOCK immunoreactivity in cytoplasmic structures are present in FSH-positive pituitary cells, indicating that CLOCK protein is localized in secretory vesicles (Fig. 38).

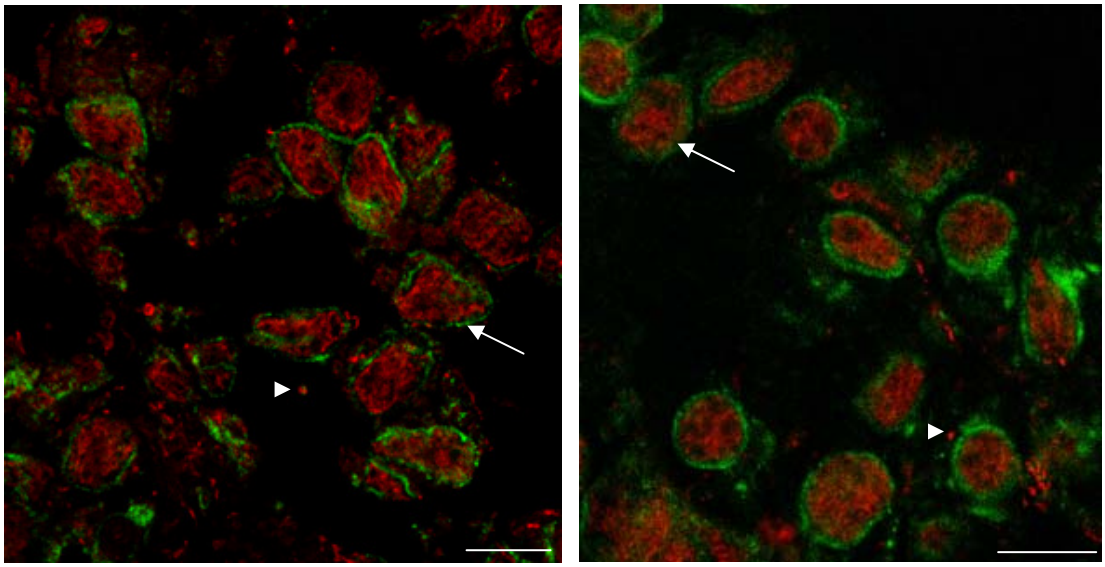

Fig. 37: Intracellular localization of CLOCK in human pituitary tissue.

Double-staining of CLOCK (red) and NPCP (green) on sections obtained from human pituitary tissue. An intense staining of the nucleus can be found independent of time of day. Small vesicle-like cytoplasmic structures also show CLOCK immunoreactivity. *Left*: day, *right*: night. *Arrows*: nucleus; *arrowheads*: vesicle-like structures. Scale bar: 10 µm.

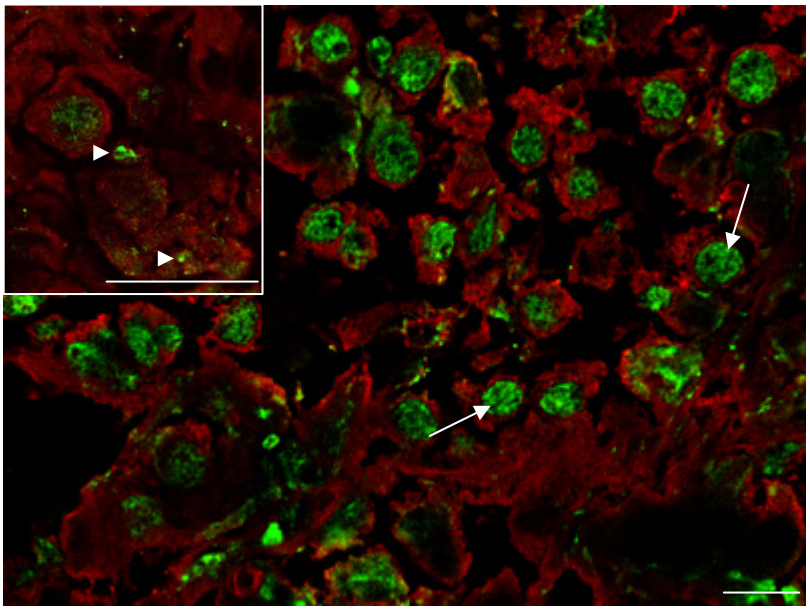

Fig. 38: Intracellular localization of CLOCK and FSH in human pituitary tissue.

Double-staining of CLOCK (green) and FSH (red) on sections obtained from human pituitary tissue. FSH is localized in the cytoplasm and surrounds the cell nucleus. Despite an intense staining of CLOCK in the cell nucleus, CLOCK can be found in FSH-enclosed mall vesicles in the cytoplasm (see inset). *Arrows*: nucleus; *arrowheads*: vesicle-like structures. Scale bar: 10 µm.

3.3 SCN analyses

Hypothalami obtained from the Institute of Forensic Medicine, Frankfurt, could not be used for cryostate sectioning and subsequent immunohistochemical or immunofluorescence analyses due to an advanced autolysis of the tissue. Therefore, formalin-fixed hypothalami were obtained from W. Den Dunnen, University Groningen, and processed for subsequent analyses.

3.3.1 Localization of the human SCN

The approximate location of the SCN region could be identified by eye inspection during the preparation of coronal cryostate sections (Fig. 39). Reliable landmarks for the presence of the SCN are the anterior commissure, together with the optic chiasm and the third ventricle (Fig. 39).

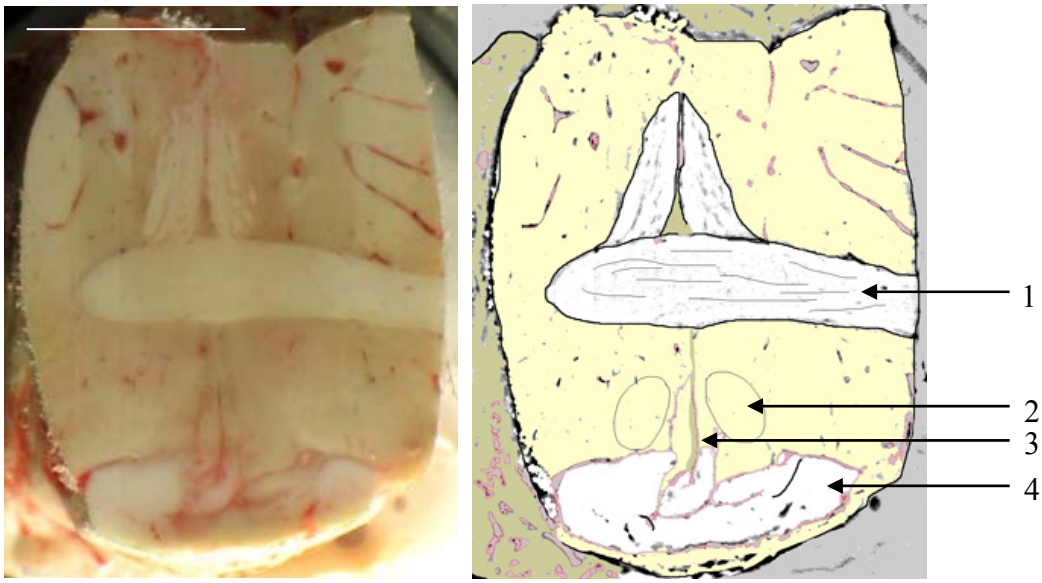

Fig. 39: Localization of the human SCN.

Left: Picture of a coronal section, as obtained from a human hypothalamus during cryostate sectioning. Scale bar: 1 cm.

Right: Drawing of the picture on the left. 1 = anterior commissure; 2 = area of the SCN (bilateral); 3 = third ventricle; 4 = optic chiasm.

Staining of calbindin was used to reliably determine the SCN region, as described earlier [Koutcherov *et al.*, 2003]. Fig. 40 shows a DAB-staining of the human SCN, which was probed with an anti-calbindin antibody for

immunohistochemical analysis. SCN cells can be found on both sides of the third ventricle, directly adjacent to the optic chiasm.

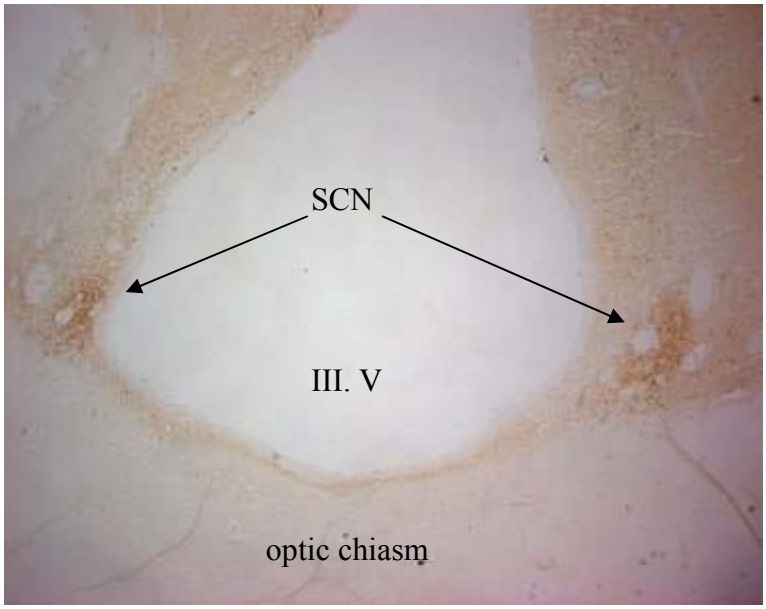

Fig. 40: Localization of the human SCN using an anti-calbindin antibody.
The SCN-region can be found on both sides of the third ventricle (III. V), directly adjacent to the optic chiasm at the bottom of the picture. 10-fold magnification.

3.3.2 Demonstration of clock gene proteins within the human SCN

As time of death of the specimens analyzed until now ranged only between 2100 h and 0700 h (exact time-points: 2100, 2215, 0200, 0445, 0700), analogous to late evening and early morning, no diurnal analysis of clock gene proteins could be conducted as yet.

A co-localization of calbindin and PER1 could be demonstrated using double-labeling experiments on sections of human SCN tissue (Fig. 41). Only the anti-PER1 antibody could be used for double-labeling experiments, as the antibodies against calbindin, CLOCK and CRY1 are hosted in the same species.

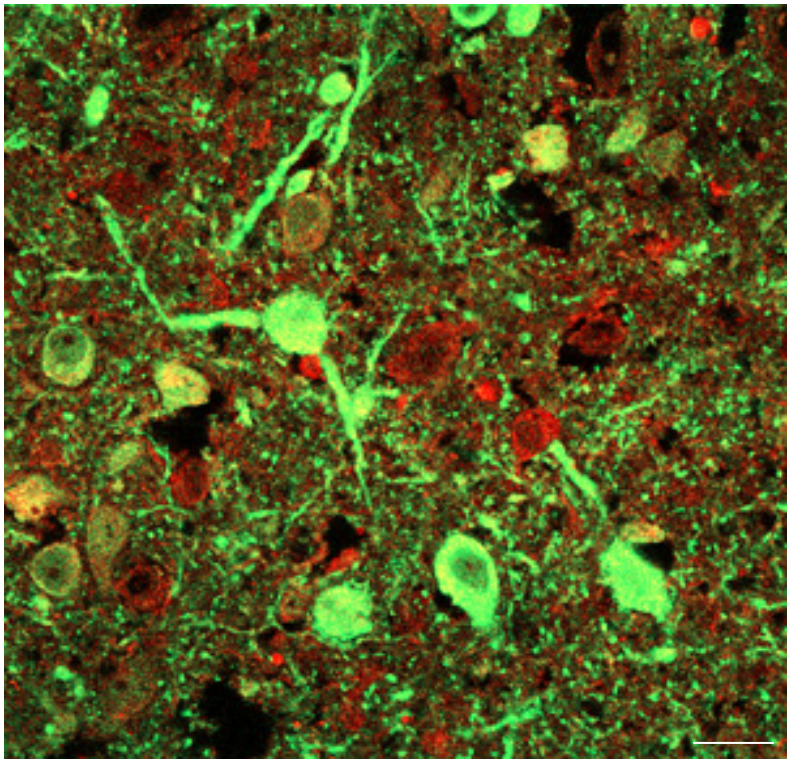

Fig. 41: Co-localization of calbindin and PER1 in the human SCN.

Double-staining of the human SCN-area with an anti-calbindin (green) and an anti-PER1 (red) antibody. For a sub-population of cells, a co-localization of both proteins can be observed (yellow staining). Scale bar: 20 µm.

DAB-staining employing antibodies against clock gene products resulted in a high background staining and/or unspecific staining of SCN-adjacent regions. With the here used anti-CRY1 antibody, no staining at all could be detected.

Yet, preliminary data obtained from few time points (see above) indicate that at least the clock gene products PER1 and CLOCK may exhibit differences in abundance between day and night (Fig. 42).

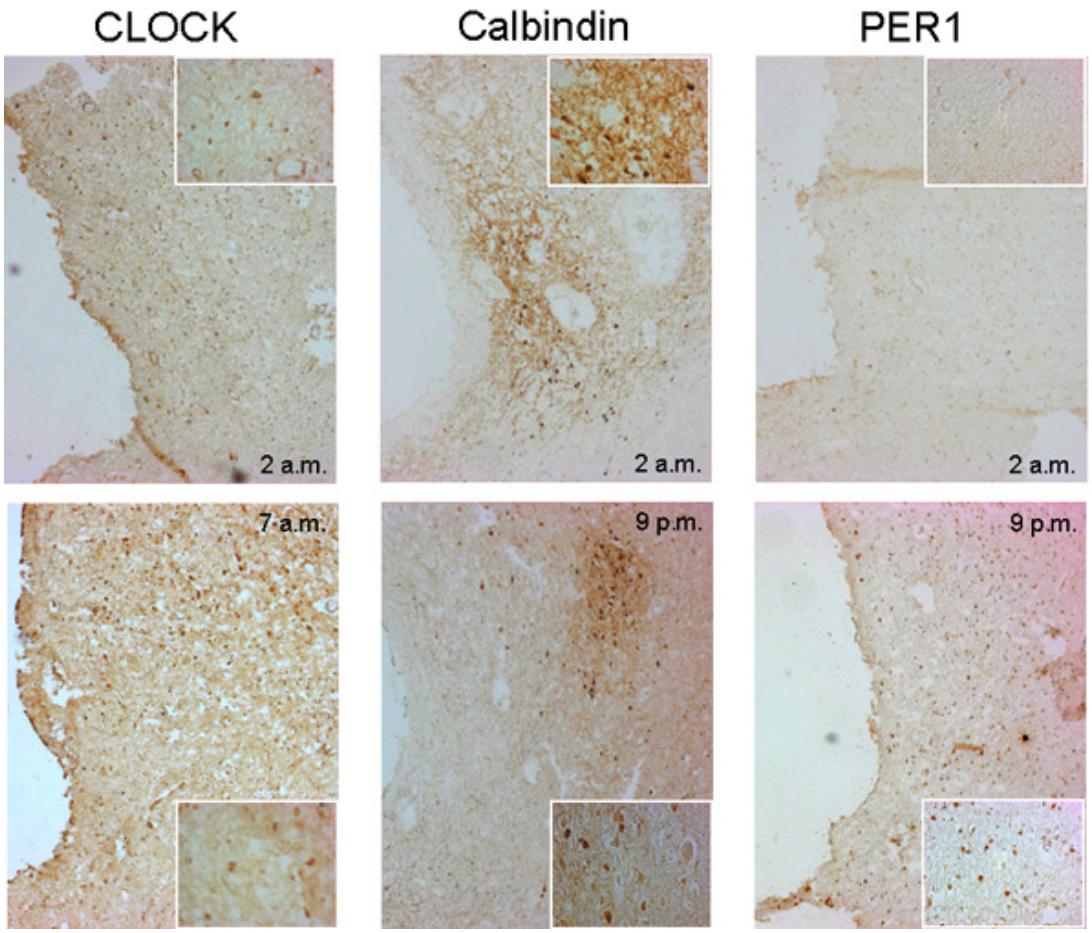

Fig. 42: Calbindin and clock gene proteins in the human SCN

DAB-staining of sections containing human SCN-regions, after probing with anti-calbindin, anti-CLOCK, or anti-PER1 antibodies. Large pictures: 25-fold magnification; insets: 200x magnification. Time of death of the specimens is indicated. Orientation: the third ventricle is located on the left of each picture, the optic chiasm is located at the bottom.

4 Discussion

4.1 Analyzing human post-mortem tissue - a valid experimental approach

In humans, the molecular mechanisms underlying dynamics in neuronal intracellular signalling events can only be analyzed using post-mortem material. Yet, the reliability of mRNA data derived from human post-mortem tissue is still a matter of debate. Uncontrolled living conditions, age, sex, and tissue pH-values are factors cited to influence RNA levels [Schramm *et al*., 1999; Hynd *et al*., 2003]. Quantitative RNA analyses in post-mortem material are hampered by the fact that there may occur a widespread and random degradation of mRNA following death, resulting in a disordered system with no relevance to the *in vivo* situation.

In this study, the validity of using post-mortem human brain tissue in order to achieve a replica of the pre-mortem situation despite a progressive tissue degradation is strengthened by the finding that mRNA decay experiments for all here investigated genes show an almost parallel decline in transcript abundance over time in the human pineal gland. These data indicate that degradation in post-mortem pineal tissue can also be treated as an ordered system. Furthermore, simultaneously out of the same subjects rhythmic and non-rhythmic parameters could be determined (rhythmic components: AANAT activity, melatonin content, clock gene protein nucleo-cytoplasmic shuttling; non-rhythmic components: *Aanat*, *Hiomt* and clock gene mRNA and protein content, HIOMT activity, AANAT protein levels, AANAT/14-3-3/HIOMT-protein complex intracellular localization), supporting the validity of the experimental approach in this study.

In addition, it could be confirmed that RNA analyses in post-mortem brain tissue by RT with random hexamers instead of oligo-dT primers is the method of choice. It was shown earlier that this method remains rather unaffected by changes of RNA structure, e.g. via loss of the poly-A tail [Yasojima *et al*., 2001; Hynd *et al*., 2003]. The validity of the experimental approach of this study was further verified by multiple statistical analyses of data obtained for mRNA and protein content, thereby eliminating possible influences of confounding factors, like age and PMI, on obtained results, confirming numerous studies that have focused on this topic during the last years (see below).

Using TaqMan™ real-time RT-PCR, it could be shown that the pool of post-mortem mRNA in human brain is essentially an ordered system, despite the ongoing degradation and the above-mentioned confounding factors. Although highly variable absolute levels of mRNA between human subjects were reported (> 1000-fold) in post-mortem brain material, strong correlations were found between mRNA transcript levels in a single brain [Preece *et al*., 2003]. In another study using post-mortem brains from schizophrenics, alcoholics and control individuals, the overall stability of mRNA for up to 72 hours was demonstrated, with no significant differences for relative/normalized mRNA levels with respect to age, gender, diagnosis, or post-mortem interval [Schramm *et al*., 1999]. Yasojima *et al*. found little deterioration in total RNA or in any of the mRNAs in post-mortem human brain tissue for up to 96 hours, yet there was gradual deterioration post-thawing of the frozen material [Yasojima *et al*., 2001]. The authors conclude that there is no indication of rapid post-mortem degeneration of RNA and that reliable mRNA values may be obtained from post-mortem brain even with long autolysis times provided the tissue has been kept in the cold [Yasojima *et al*., 2001]. A similar conclusion was drawn by Bauer *et al*., showing that overall RNA degradation in post-mortem human brain tissue is a slow process and significant differences which might be used for determination of the post-mortem interval do not occur prior to three or four days after death [Bauer *et al*., 2003].

It should be mentioned that the design of primers used for RNA detection is of importance, because the rapid loss of the polyA tail does not necessarily lead to the loss of the message, as shown for glyceraldehyde-3-phosphate dehydrogenase specific and random hexamer primed reactions [Johnston *et al*., 1997]. Although the spectrophotometric measurement (OD_{260}; OD_{260}/OD_{280}) for determination of RNA quality and quantity is widely used, it should be taken into account that this method does not permit assessment of the structural integrity of the isolated RNA; also detection of abundant and intact ribosomal RNA does not signify intact mRNA in general in a sample [Hynd *et al*., 2003].

4.2 Melatonin synthesis in the human pineal gland

In this study, *Aanat* and *Hiomt* mRNA levels, AANAT protein content, AANAT and HIOMT activity, AANAT, HIOMT and 14-3-3 protein complexation and intracellular localization, and melatonin content from human post-mortem pineal tissue were analyzed simultaneously in the same subjects. Results depict for the first time a clear diurnal rhythm in AANAT activity and melatonin content, despite constant values for *Aanat* and *Hiomt* mRNA, and for HIOMT activity. Surprisingly, also AANAT protein content did not fluctuate with time, but was instead found to be complexed with 14-3-3 protein and probably HIOMT in previously unnoticed cellular processes of pinealocytes. Thus, results demonstrate that post-translational mechanisms and/or compartimentation seem to be central for the generation of the circadian melatonin profile in the human pineal gland.

As expected, night-time melatonin levels were significantly correlated with time of death of specimens, despite the long time stretch of the chosen night interval (2200 h – 0730 h), with borders corresponding to the onset and offset of hormone secretion in temperate zones [Arendt, 1995]. Night-time melatonin values in the post-mortem material showed large inter-individual differences, matching several earlier case studies [Smith *et al*, 1977; Arendt, 1995; Smith *et al*., 2004]. In addition, our findings explain the rapid dim-light-melatonin-onset (DLMO) in humans [Lewy, 1999], as no change in gene expression is required for up-regulation of melatonin synthesis. Thus, human melatonin synthesis can easily react upon changes of environmental lighting conditions.

Based on the molecular integrity of mRNA in post-mortem pineal tissue, it can be concluded that the absence of diurnal variations in the here described elevated *Aanat* and *Hiomt* mRNA levels over time is indeed a remnant silhouette of the *in vivo* situation, as AANAT activity showed a highly rhythmic pattern, with elevated levels preceding the observed increase in pineal melatonin content at night. These findings give strong evidence for a regulation of human melatonin synthesis, independent of a rhythmic transcription, a fact which was discussed already earlier: in the ovine pineal gland, the night-to-day ratio of *Aanat* mRNA was reported to be less than 2 [Coon *et al*., 1995]. This finding was confirmed later on in the Soay sheep [Johnston *et al*., 2004]. Similarly, variations in *Aanat* mRNA levels between day and

night were reported to be negligible in the Rhesus monkey *Macaca mulatta* [Coon *et al*., 2002]. Also in the primate human, no significant rhythms in *Aanat* and *Hiomt* mRNA levels were detected [Wu *et al*., 2003]. Evidence for a diurnal post-transcriptional regulation of the human AANAT were also suggested on the basis of *in vitro* biochemical analyses of this enzyme, using the human *Aanat* clone [Coon *et al*., 1995, 2001], as elevated AANAT protein levels were shown to be independent of *Aanat* transcription, and activators of the cAMP pathway were shown to increase AANAT activity without markedly increasing the amount of AANAT protein. The authors propose that this previously unrecognized switching mechanism between inactive and activated AANAT enzyme activity could function to control melatonin synthesis without a change in AANAT protein levels.

Data presented here show that despite an undetectable rhythm in *Aanat* and *Hiomt* mRNA values over the four death-time groups, AANAT activity is profoundly elevated in the dusk and night period, as compared to dawn- and day-time. Thus, for the first time a diurnal rhythm in AANAT activity in the human pineal gland could be demonstrated.

It should be noticed that elevated values for AANAT activity during dusk- and night-time in the post-mortem pineal material are about 1000-times lower than those reported for the primate *Macaca mulatta* [Coon *et al*., 2002]. This finding can be explained by ongoing degradation/loss of enzymatic integrity of the AANAT protein, likely due to a halving time of this enzyme in rat of about 3 min [Klein & Weller, 1972]. Yet, the validity of the AANAT rhythm is strengthened by the fact that the ultimate enzyme in melatonin synthesis, the HIOMT, does not show any fluctuation over time, despite its higher stability, as compared to AANAT [Bernard *et al*., 1993].

The general diurnal silhouette of AANAT activity, as assessed from post-mortem pineal glands in the present study, shows an almost perfect parallel dynamics to observed melatonin levels, indicating the close relationship of both parameters. However, the elevated AANAT activity during dusk does not correspond with a simultaneous elevation in melatonin content. It is currently unclear whether this finding may suggest a more important role of the ultimate enzyme in melatonin synthesis, the HIOMT, for rate-limiting rhythmic hormone production, as demonstrated recently in the rodent pineal gland: the photoperiodic changes in the

amplitude of the melatonin peak of the Siberian hamster were shown not to be correlated to corresponding changes in AANAT activity, but rather HIOMT was found to exhibit a twofold increase in activity in winter (short photoperiod) [Ribelayga *et al*., 2000]. Further studies revealed that potentiation of AANAT activity via adrenergic stimulation did not result in a potentiation of melatonin production, suggesting a regulation downstream of AANAT in the metabolic pathway [Ceinos *et al*., 2004]. It was proposed that the large photoperiodic variation of HIOMT activity is due to a long-term β-adrenergic stimulation, at least in photoperiodic species [Ceinos *et al*., 2004]. Yet, also in a non-photoperiodic species, the rat, AANAT was found not to be the rate-limiting enzyme of melatonin synthesis [Liu & Borjigin, 2005]. In this study, rats with a critical mutation in the AANAT protein, namely a substitution of the histidine at position 28 with a tyrosine, resulting in a dramatically reduced AANAT activity, were found to produce the same amount of melatonin as wildtype controls, and that the continuous increase in *N*-acetylserotonin did not result in a proportional increase in melatonin levels.

In this study, analyses concerning AANAT protein levels, as well as AANAT, HIOMT, and 14-3-3 protein intracellular localization and complex formation were conducted for the first time in human post-mortem tissue. Here presented data question the established hypothesis of a proteasomal degradation of AANAT protein during day-time. According to this hypothesis, AANAT protein is made constantly, but degraded very rapidly [Klein *et al*., 1997; Gastel *et al*., 1998; Schomerus *et al*., 2000]. Only the night-time NE-signalling leads to phosphorylation at T31, thereby initiating complex formation with 14-3-3 protein, and concurrent enzyme activity, meaning that complexation of AANAT is sufficient to switch on the enzyme´s activity. Thus, proteasomal proteolysis of AANAT is inhibited by a shielding of the constitutively synthesized enzyme from active dephosphorylation and subsequent degradation by forming a stable AANAT/14-3-3 protein complex [Ganguly *et al*., 2001; Klein *et al*., 2003].

From the economic point of view, this hypothesis is questionable, as protein synthesis and subsequent degradation is accompanied by energy consuming processes. Furthermore, there is no advantage of having AANAT protein ready for activity during the day, which could explain this energy input. Thus, it is highly uneconomic for any kind of cell to produce and subsequently destroy a specific

protein for at least 12 out of 24 hours a day. As cells have to work energy-efficient in order to survive, it is worth to reconsider the existing hypothesis.

The unexpected finding that AANAT protein was constitutively present in human pineal homogenates, without any significant differences between the four time-of-death groups, provided first evidence against the existing hypothesis of a proteasomal degradation of the enzyme during day-time.

The anti-AANAT antibody used in this study was described to be specific for phosphorylated T31-AANAT in rat, sheep, and human [Ganguly *et al*., 2001]. Yet, the antibody detected AANAT bands of equal size and signal intensities in human and sheep pineal homogenates, notably independent of phosphatase treatment. In contrast, in NE-stimulated rat pineal glands that were treated with phosphatase, intensity of the AANAT band was comparable to that of the negative control, whereas in the untreated, NE-stimulated rat pineal homogenate a strong AANAT band was detectable. These results confirm the phospho-specificity of the antibody only for rat, whereas for human and sheep there remain at least two options: 1) the antibody detects both, the phosphorylated and the unphosphorylated form of the protein, and 2) the antibody detects only phosphorylated AANAT and dephosphorylation was not successful. It seams reasonable that the second option is applicable, as it was shown earlier that the resistance of AANAT protein to phosphatase treatment is due to a shielding of T31 from dephosphorylation in an AANAT/14-3-3 protein complex [Ganguly *et al*., 2001].

To analyze complex formation of AANAT and 14-3-3 in human pinealocytes, AANAT was co-immunoprecipitated with 14-3-3 protein. As the anti-AANAT antibody binding region is directly involved in complexation and therefore shielded [Ganguly *et al*., 2001], the yield of precipitated complex was lower when precipitating with the anti-AANAT antibody than with the anti-14-3-3 antibody. Still, it was demonstrated here that the stabilizing complex is constitutively present, independent of time of day. Thus, it may be concluded that T31 is permanently phosphorylated, thereby confirming the phospho-specificity of the anti-AANAT antibody.

Surprisingly, further immunoblotting experiments with the membranes obtained from co-immunoprecipitation revealed that also HIOMT protein is part of the AANAT/14-3-3-protein complex independent of time of day. These results

indicate that, instead of a duplex, consisting of AANAT and 14-3-3, a triplex formation with HIOMT protein as the third binding partner is present in human pinealocytes.

These findings were strengthened by the fact that AANAT, HIOMT and 14-3-3 protein were always jointly detectable in cellular processes of human pinealocytes. Notably, in these processes, no clock gene protein was found to be present, indicating their importance as a metabolic cellular compartment for melatonin synthesis. Analyses of sheep pineal sections confirmed that also in this species, with a regulation of melatonin synthesis similar to the human, AANAT is localized in these cellular processes.

The cellular processes accomodating the AANAT/HIOMT/14-3-3 protein complex has by now not been described in any species investigated. Yet, it is worth speculating that these processes may belong to a recently discovered sub-cellular structure, the so-called tunneling nanotubes [Gerdes *et al*., 2007]. These nanotubular structures mediate membrane continuity between mammalian cells and were found to be formed *de novo* between animal cells in culture, leading to the generation of complex cellular networks that facilitate the inter-cellular transfer of organelles, as well as of membrane components, and most importantly, of cytoplasmic molecules [Gerdes *et al*., 2007]. It remains to be shown that tunneling nanotubes fulfill important functions in the physiological processes of multicellular organisms. From results obtained in this study, it may be speculated that the melatonin production machinery is localized in nanotubes of pinealocytes. It may be envisioned that pinealocytes exchange small molecules via nanotubes involved in melatonin synthesis, like serotonin or NE, to achieve melatonin synthesis also in those cells, which are not directly reached by the sympathetic innervation.

Taken together, the insights into regulation of melatonin production obtained in this study shed new light on regulation of the key enzyme in melatonin synthesis, but likewise raise the question of the activation of AANAT activity, which could not be answered in the present study. A possible explanation for the night-time activity of the enzyme is a cAMP-gated phosphorylation of the second and so far sparsely investigated phosphorylation site of AANAT protein near the C-terminus, S205. Recently, it could be demonstrated that light exposure at night decreases both, phosphorylation at T31 and at S205, indicating a regulatory role of both sites

[Ganguly *et al*., 2005]. Furthermore, it could be shown that substitution of S205 with a stable phosphomimetic amino acid enhances binding to 14-3-3 and also the cellular stability of AANAT, and thus, strengthens the view that phosphorylation at S205 plays a critical role in regulating AANAT activity, and thereby in melatonin production [Zheng *et al*., 2005].

Here presented data strongly support the view that a post-translational regulation of the AANAT protein - in contrast to its demonstrated transcriptional regulation in rodents - is the dominant mechanism to generate rhythmic melatonin synthesis in the human pineal gland, and thus, may be common to all primates, and possibly also to ungulates. According to data obtained in this study, a schematic drawing of the regulatory differences in melatonin synthesis for rodents and the primate human is given in Fig. 43.

The new aspects of melatonin synthesis in the human and another higher mammal, the sheep, may be relevant for a future use of melatonin in preventive or curative interferences with the human circadian system. Together with the results obtained in this study, it could be demonstrated that the differences between rodents and non-rodent species concerning regulation of melatonin production are extensive. Therefore, to achieve a complete understanding of the generation of the rhythmic hormonal signal in the human pineal gland, analyses in rodent species cannot be generalized or concerned valid for all mammals.

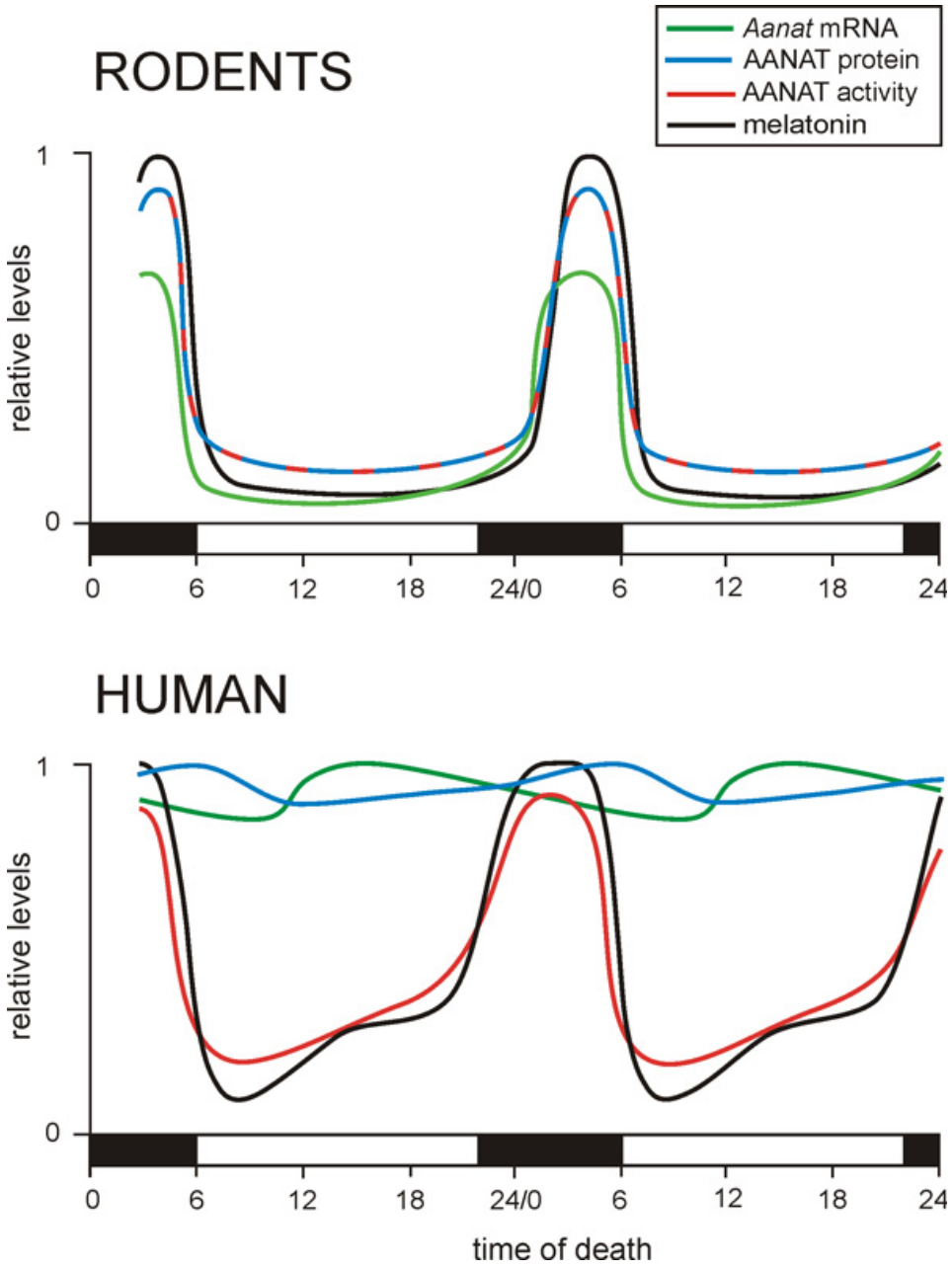

Fig. 43: Schematic drawing demonstrating differences in regulation of melatonin synthesis in rodents and humans, exemplified with selected parameters.

4.3 Clock genes in human post-mortem tissue

A complete understanding of the regulation of rhythm generation within a neuroendocrine human tissue is of fundamental importance for the medical treatment of chrono-pathologies. Disturbances of the synchronization and/or communication of

the SCN with peripheral organs are often associated with chronobiological dysfunctions [Klerman 2005]. Furthermore, SNPs in the *Period* gene were linked to sleep abnormalities, like the delayed or advanced sleep phase syndrome [Toh *et al*., 2001; Archer et al., 2003]. There is growing evidence that clock gene SNPs may also be correlated with tumor suppression, or metabolic syndroms, like adipositas [Turek *et al*., 2005]. In addition, clock gene polymorphisms could be related to alcohol and drug abuse [Spanagel *et al*., 2005]. Thus, another aim of this study was to analyze clock genes and their protein products in the human pineal and pituitary gland, in order to learn more about their regulatory mechanisms and protein interactions with time of day.

This first report on clock gene expression in a human brain tissue shows that *Per1*, *Cry1*, *Bmal1*, and *Clock* do not show a rhythmic pattern in mRNA abundance with time of day in the pineal gland. This lack of dynamics was observed despite a significant diurnal rhythm in melatonin content and AANAT activity within the same tissue samples (see above). Furthermore, also in the pituitary no significant rhythms in clock gene expression were found, and transactivating clock gene proteins are constitutively present in pinealocytes and pituitary cells during day and night. These results support the idea that regulation of gene expression by circadian transcription factors plays only a subordinate role as activity determinant in human neuroendocrine tissues.

However, the detected diurnal oscillation in the sub-cellular localization of clock gene proteins PER1, CRY1, and CLOCK in human pinealocytes raises the idea that a nucleo-cytoplasmic protein shuttling may mark a novel twist for a time-dependent function of these transcription factors to affect cellular signalling. This idea is strengthened by the finding that in initial experiments also in human pituitary cells a nucleo-cytoplasmic shuttling of the clock gene proteins PER1 and CRY1 could be observed. Currently, it can only be speculated on the driving forces behind these clock protein translocations, but evidence is accumulating that the kinetics equilibrium in translocation of clock gene proteins can be changed quickly following post-translational modifications, like phosphorylation. According to an existing model, the cellular PER pool is composed of nuclear, transcriptionally active (phosphorylated) molecules, and of cytoplasmic, transcriptionally inactive (unphosphorylated) molecules, which can enter the nucleus rapidly upon

phosphorylation [Tamanini *et al*., 2005]. Furthermore, it has already been shown for the regulation of melatonin synthesis, that modifications via protein phosphorylation are controlled by rhythmic activity of the sympathetic innervation in the human pineal gland [Gastel *et al*., 1998; Stehle *et al*., 2001(a)].

In the rodent pineal gland, clock gene expression and regulation is well described, with *Per1*, *Cry1*, *Bmal1* and, to a lesser extent, *Clock* mRNA exhibiting a circadian pattern in expression levels [Takekida *et al*., 1999; von Gall *et al*., 2001; Karolczak *et al*., 2004, 2005; Fukuhara *et al*., 2005]. Up-regulation of *Per1* seems to be established in parallel to *Aanat* on the transcriptional level via an increased activity of the sympathetic innervation and a cAMP-mediated gene expression in the pineal gland [Takekida *et al*., 1999; Coon *et al*., 2000; von Gall *et al*., 2001].

In non-rodent species, only the sheep pineal gland has been looked at for regulation of melatonin synthesis in relation to clock gene expression [Johnston *et al*., 2004]. In the sheep, kept under standard photoperiod, neither *Aanat* nor *Cry1* gene expression varied with time of day [Johnston *et al*., 2004]. It was only when animals were kept under long nights, i.e. pinealocytes were exposed to a prolonged sympathetic stimulus, that *Per1* expression showed a small variation over diurnal time [Johnston *et al*., 2004]. This observation is especially remarkable, as in the sheep melatonin synthesis is driven downstream of transcription, likewise to the situation in the Rhesus monkey *Macaca mulatta* [Coon *et al*., 2002], and in another primate, the human, as demonstrated in this study. Therefore, Johnston and co-workers hypothesize that, together with a regulation of melatonin synthesis downstream of transcription in ungulates, there seems to be a general reduction of circadian transcriptional control in non-rodent mammals, indicating that a marked evolutionary divergence in regulation mechanisms between rodents versus ungulates and primates has occurred.

In contrast to this hypothesis, a recent study concerning clock gene expression in the human pineal gland [Wu *et al*., 2006] described a significant diurnal profile for the clock genes *Per1*, *Cry1* and *Bmal1*, but not for *Clock*, indicating a regulation of the circadian clock on the transcriptional level, as shown for rodents. Yet, the rhythms reported in this study [Wu et al., 2006] are not impressive, and the statistical analyses that were used for interpretation of gene expression data are questionable. Data obtained in the present study strongly support

the view of Johnston [2004], as no differences in clock gene mRNA over diurnal time was found, neither for the human pineal gland nor for the pituitary gland.

In order to further validate these results, various age-matched subgroups, including a group with similar characteristics, as the control group in the paper by Wu and co-workers [Wu *et al*., 2006] were selected and statistically analyzed. In addition, subgroups of specimens with relatively short and long PMI, as well as specimens with explicitly low day-time and high night-time melatonin values, were deliberately selected and statistically analyzed. For all subgroups of both the pineal and the pituitary gland, no indication for rhythmic levels in clock gene mRNA or protein could be detected. Therefore, data raised in this study strongly indicate that clock gene expression in the human pineal and pituitary gland lacks a rhythmic transcription, likewise as observed for primate *Aanat* and *Hiomt* mRNA [Coon *et al*., 2002; Wu *et al*., 2003].

It has to be noted, however, that there exist additional clock genes of importance for endogenous oscillations not analyzed in the present study (*Per2*, *Per3*, *Cry2, Dec1*, *Dec2*) [Takekida *et al*., 2000; Lowrey *et al*., 2000; Reppert & Weaver, 2002; Hastings *et al*., 2003; Karolczak *et al*., 2004, 2005], which possibly may exhibit variations in their diurnal expression pattern in human neuroendocrine glands.

In both neuroendocrine glands analyzed in this study, clock genes and their protein products were found to be constitutively present during day and night. However, it can be concluded from comparing data obtained for clock gene expression in the pituitary, that *Per1* is by far the lowest expressed gene analyzed. Despite this, PER1 levels were similar to all other clock gene proteins determined. Thus, differences in clock gene expression do not seem to influence transcript abundance, further indicating that regulation of rhythm generation in peripheral tissues occurs downstream of transcription in humans.

Notably, in the absence of clock gene mRNA and protein fluctuations in the human pineal gland, a time-of-day-dependent translocation of PER1, CRY1, CLOCK, and to a moderate extent also of BMAL1, was discovered in human pinealocytes. A similar result was obtained for the human pituitary gland, where a parallel nucleo-cytoplasmic shuttling of the clock gene proteins PER1 and CRY1

could be observed, without any significant rhythms in clock gene expression or transcript abundance.

This phenomenon of nucleo-cytoplasmic shuttling has been described earlier for several clock gene proteins in transiently transfected cells and mouse fibroblasts [Yagita *et al*., 2002; Tamaru *et al*., 2003; Kwon *et al*., 2006]. An increased number of mammalian clock proteins (PER, CRY, BMAL1, REV-ERBα) have been shown to contain one or more nuclear localization signal sequences (NLS), which nicely reflects their predominant localization in the nucleus and function within transcriptional regulation [Tamanini *et al*., 2005]. Apart from NLS sequences, nuclear proteins may also contain sequence motifs that allow active transport of the protein back to the cytoplasm, the so-called nuclear export signals (NES), allowing a nucleo-cytoplasmic shuttling of the protein [Tamanini *et al*., 2005]. Thus, the presence of NLS as well as NES sequences in one and the same protein renders this protein capable to shuttle between nucleus and cytoplasm. It was shown in mouse fibroblasts that this shuttling is not limited to one cycle, but that the protein can shuttle continuously between nucleus and cytoplasm without the need of *de novo* protein synthesis [Yagita *et al*., 2002; Tamanini *et al*., 2005]. The here observed nucleo-cytoplasmic shuttling of clock gene proteins affects their cellular functioning, as these proteins act as transcription factors and thus, can only be active when localized in the cell nucleus. After transportation back into the cytoplasm, which is probably regulated by interactions with other proteins [Tamanini *et al*., 2005], clock gene proteins may be degraded or kept inactive until the next cycle, depending on post-translational modifications (e.g. dephosphorylation – inactivation, ubiquitylation – degradation) of specific sequences within or in proximity to the NLS and NES sequences [Tamanini *et al*., 2005].

The finding that PER1 and CRY1 undergo nearly synchronous circadian patterns in nuclear abundance in human pinealocytes and pituitary cells confirms the general understanding of a simultaneous nucleo-cytoplasmic shuttling, as these two transcription factors act as a heterodimer [Field *et al*., 2000; Reppert & Weaver, 2002].

CLOCK was localized in the nucleus of pinealocytes and pituitary cells at all times, which is consistent with the finding that CLOCK binds constitutively to E-box elements within a nuclear transcriptional complex in a BMAL1-dependent fashion

[Kondratov *et al*., 2003; Yoo *et al*., 2005]. The unexpected night-time localization of CLOCK at the cell membrane of human pinealocytes awaits further elucidation. At the moment, it can only be speculated about the functional meaning of this occurrence and potential other roles of CLOCK protein despite its function as a transcription factor within the circadian system. Interestingly a CLOCK-derived peptide fragment is listed in the human plasma proteome database (www.plasma-proteomedatabase.org), indicating that CLOCK, or CLOCK-derived fragments are secreted into blood circulation by unknown mechanisms. The finding that CLOCK is present in pituitary secretory vesicles, as demonstrated in this study, supports this idea and gives first experimental insight into a completely new aspect of clock protein function despite the well-described transcription factor activities.

Here presented findings provide the first evidence that in the human pineal gland evolutionary morphodynamics and selective pressure have not only converted this organ from a light-sensitive endogenous oscillator to an SCN-dependent slave oscillator [Korf *et al*., 1998; Ekström & Meissl, 2003; Maronde & Stehle, 2007], but have also impaired the dominance of rhythmic transcription, as confirmed by data obtained from human pituitary analyses. From the evolutionary standpoint a rhythm generation on the basis of transcription may be too time-consuming in diurnally active ungulates and primates. A nucleo-cytoplasmic shuttling of pre-existing clock proteins may allow a necessary faster response to changing environmental conditions. Such a scenario is backed by the known mechanisms that regulate melatonin synthesis in different mammalian species: switching from a transcriptional level of regulation in the rodent pineal gland to a post-translational level in non-rodent mammals also allows a faster response to changing environmental stimuli, as no protein synthesis is required [Stehle *et al*., 2001(a)].

Besides analyses conducted in the human pineal gland [Wu *et al*., 2006], the presence of clock gene mRNAs and proteins has been demonstrated in several human peripheral tissues and in body fluids [Bjarnason *et al*., 2001; Boivin *et al*., 2003; Takimoto *et al*., 2005; Teboul *et al*., 2005; Pardini *et al*., 2005; Cajochen *et al*., 2006]. However, by now, there exist no data on the presence or even on the regulation of clock genes and their protein products in the human circadian master clock, the SCN.

In this study, the presence of the clock genes PER1 and CLOCK in the human SCN was demonstrated for the first time. Analyses using human post-mortem hypothalami turned out to be much more difficult than analyses using human post-mortem neuroendocrine glands. A possible reason may be that both glands are more homogenously structured, and more importantly, are encapsulated by connecting tissue, which shields them from the impact of oxygen and thus, from autolysis. It was possible to conduct successfully immunohistological or immunofluoresence analyses only, when using hypothalami that were prepared and formalin-fixed within few hours after death of the specimens,.

Although only a few specimens could be analyzed in this study as yet, it could be demonstrated that PER1 and CLOCK proteins in the human SCN show different levels of abundance with time of day. This result is in contrast to the constitutive presence of both proteins in the human pineal and pituitary gland. Thus, it can be speculated that, although the expression of clock genes and their protein products does not fluctuate in human peripheral neuroendocrine tissues, generation of circadian rhythmicity in the master clock relies on the transcriptional-translational feedback loop, as described in the rodent SCN [Reppert & Weaver, 2002].

5 Conclusion and outlook

5.1 The role of transcription and translation – an inter-species comparison

The pineal organ of rodents (rat, mouse) has for a long time served as a model system to study signal transduction and molecular mechanisms in neuroendocrine and neuronal tissues of mammals in general. Of special interest was the characterization of cellular and molecular mechanisms involved in melatonin synthesis, driven by the NE-cAMP-signalling cascade in pinealocytes.

Only recently, it became clear that there are fundamental differences in regulatory mechanisms controlling melatonin production between different mammalian species. Thereby, the transcriptional regulation of the *Aanat* gene as found in rodents was questioned by novel findings in non-rodent species, namely sheep [Johnston *et al*., 2004], cow [Schomerus *et al*., 2000] and monkey [Coon *et al*., 2002], with the introduction of a (post-)translational regulation of the AANAT protein. These findings questioned the dogma of a uniform regulation of melatonin synthesis valid for all mammalian species [Klein *et al*., 1997].

This species-dependent regulation is now widely accepted, and for the first time a post-translationally regulated melatonin synthesis could be demonstrated in the human in the present study. In addition, the existing hypothesis of a proteasomal degradation of AANAT protein during day-time has to be questioned by the results obtained in this study. The here introduced novel hypothesis indicates that AANAT is constitutively present and complexed with 14-3-3 and, most probably, also with HIOMT in a large protein-complex localized in cellular processes of pinealocytes. Induction of AANAT activity at night is possibly achieved via phosphorylation at its C-terminus [Ganguly *et al*., 2005; Zheng *et al*., 2005].

Besides its function as a neuroendocrine transducer, the rodent pineal gland has been studied extensively regarding clock gene expression. Here, this organ was exemplified as a model system for generation of circadian rhythmicity in a mammalian peripheral tissue. With the evolution of the vertebrate pineal gland, clock gene proteins drifted from functioning as active elements of an endogenous circadian oscillator, shaping melatonin synthesis, towards regulated genes with often so far unknown meaning [Ekström & Meissl, 2003; Maronde & Stehle, 2007].

However, when looking at patterns in clock gene expression in the pineal organ of different mammalian species, there are surprising parallels with the regulation of melatonin synthesis: clock genes show a circadian expression pattern in mRNA [Takekida *et al*., 1999; von Gall *et al*., 2001; Karolczak *et al*., 2004, 2005; Fukuhara *et al*., 2005] when the rhythm in melatonin synthesis is centered around *Aanat* transcription, as is the case in rodents [Klein *et al*., 1997; Korf *et al*., 1998; Gastel *et al*., 1998; Stehle *et al*., 2001(a); Karolczak *et al*., 2005; Maronde & Stehle, 2007]. When clock genes are constitutively transcribed as in sheep [Johnston *et al*., 2004] and in primates [this study], rhythmic melatonin synthesis relies on post-translational modifications of the AANAT (sheep [Johnston *et al*., 2004], Rhesus monkey [Coon *et al*., 2002], human [Wu *et al*., 2003]). Thus, on the basis of this coincidence in regulation, a preserved involvement of clock genes and their protein products throughout evolution of vertebrate pinealocytes with the circadian melatonin synthesis is likely.

Reasons for these changes in regulatory mechanisms are unclear at the moment. From the evolutionary point of view, a rhythm generation on the basis of transcription may be too time-consuming in diurnally active ungulates and primates. A rapid onset of melatonin production at the beginning of the night due to pre-existing *Aanat* mRNA and AANAT protein, as well as a nucleo-cytoplasmic shuttling of pre-existing clock proteins, as demonstrated in the present study, may allow a necessary faster response to changing environmental conditions.

Furthermore, the dominant role of a post-translational regulation of circadian rhythm generation could be extended to another neuroendocrine tissue, the human pituitary gland. As demonstrated for the pineal gland, mRNA and protein levels of clock genes were constitutively high, but instead a nucleo-cytoplasmic shuttling of PER1 and CRY1 with time of day could be observed, indicating a general role of this phenomenon in human peripheral tissues.

5.2 Perspectives

In the present study, a post-translational regulation of melatonin synthesis via its key enzyme, the AANAT, could be established for the first time in the primate human. The existing hypothesis of a proteasomal degradation of the AANAT during the day was challenged and replaced by the hypothesis that AANAT is constitutively present and complexed with 14-3-3, and probably also with HIOMT. This protein complex can be found in cellular processes independent of time of day, indicating a so far not appreciated cellular compartment as the place of melatonin production.

In the present study no explanation could be found for the activation of AANAT activity at night. It seems reasonable that enzyme activity is switched on at night via the cAMP-signalling pathway, possibly involving the phosphorylation of S205. This phosphorylation site needs to be analyzed in detail, and should be included in molecular modelling analyses or 3D-structure determination, as phosphorylation probably leads to conformational changes of the AANAT, thereby initiating activity. Furthermore, the cellular processes accomodating the AANAT/14-3-3/HIOMT protein complex need to be analyzed in detail to clarify their identity, including morphological and histological aspects. It is possible that these processes are a type of the recently discovered cell-cell connecting tunneling nanotubes, which would constitute the first description of this phenomenon in an animal tissue.

This study presents for the first time the detection of clock gene proteins in neuroendocrine human tissues, the pineal and the pituitary gland. Furthermore, a new regulatory mechanism for the generation of circadian rhythmicity in human peripheral tissue was determined, the so-called nucleo-cytoplasmic shuttling of clock gene products, which is depending on time of day. Together with the lack of diurnal rhythmicity in clock gene mRNA content, a post-translational regulation of rhythm generation could be postulated for the primate human, a principle that has already been shown for melatonin synthesis.

In order to retrieve the phenomenon of nucleo-cytoplasmic shuttling of clock gene proteins, it would be of interest to analyze other peripheral, non-neural human tissue. Moreover, analysis of other mammals could provide information about the question if this phenomenon is human-specific or is representative of multiple

species. To understand molecular mechanisms involved in regulation of nucleo-cytoplasmic shuttling, it would be of interest to analyze in detail post-translational modifications (e.g. phosphorylation) of clock gene proteins with time of day.

For the first time, the presence of clock gene proteins within the human SCN could be demonstrated in the present study. To obtain a more detailed picture of the total protein amount and the intracellular localization of these proteins with time of day, more specimens have to be analyzed, and methods have to be optimized to gain quantifiable results. It would be of highest interest to compare the profile of clock gene proteins of healthy subjects with that obtained from analysis of Alzheimer´s Disease patients to get a better understanding of the effects of this disease on circadian rhythm generation.

Finally, the characterization of the expression pattern of clock genes and their protein products in non- or minimally invasive human material, like blood, oral mucosa or saliva, is desirable. Thus, identification of SNPs in clock genes from patients suffering from chronobiological dysfunctions could be directly linked to an altered clock gene expression pattern, and therefore could be of great help in generating individual medical treatments.

6 References

Antle MC, Silver R. Orchestrating time: arrangement of the brain circadian clock. 2005 Trends in Neurosci 28:145-151.

Archer SN, Robilliard DL, Skene DJ, Smits M, Williams A, Arendt J, Von Schantz M. A length polymorphism in the circadian clock gene Per3 is linked to delayed sleep phase syndrome and extreme diurnal preference. 2003 Sleep 26:412-415.

Arendt J. Mammalian pineal rhythms. 1985 Pineal Res Rev 3:161-213.

Arendt J. Melatonin and the Mammalian Pineal Gland. 1995 London: Chapman & Hall, 331p.

Arendt J. Melatonin: characteristics, concerns, and prospects. 2005 J Biol Rhythms 20:291-303.

Arendt J, Skene DJ. Melatonin as a chronobiotic. 2005 Sleep Med Rev 9:25-39.

Bauer M, Gramlich I, Polzin S, Patzelt D. Quantification of mRNA degradation as possible indicator of postmortem interval – a pilot study. 2003 Leg Med 5:220-227.

Bernard M, Guerlotte J, Cogne M, Greve P, Collin JP, Voisin P. Transcriptional regulation of hydroxyindole O-methyltransferase in the chicken pineal gland : day/night changes and long-term effects of light and darkness. 1993 Biochem J 290:661-664.

Bernard M, Donohue SJ, Klein DC. Human hydroxyindole-O-methyltransferase in pineal gland, retina and Y79 retinoblastoma cells. 1995 Brain Res 696:37-48.

Bjarnason GA, Jordan RCK, Wood PA, Li Q, Lincoln DW, Sothern RB, Hrushesky WJ, Ben-David Y. Circadian expression of clock genes in human oral mucosa and skin: association with specific cell-cycle phases. 2001 Am J Pathol 185:1793-1801.

Boivin DB, James FO, Wu A, Cho-Park PF, Xiong H, Sun ZS. Circadian clock genes oscillate in human peripheral blood mononuclear cells. 2003 Blood 102:4143-4145.

Borjigin J, Wang MM, Snyder SH. Diurnal variation in mRNA encoding serotonin N-acetyltransferase in pineal gland. 1995 Nature 378:783-785.

Brownstein M, Axelrod J. Pineal gland: 24-hour rhythm in norepinephrine turnover. 1974 Science 184:163-165.

Cajochen C, Jud C, Münch M, Kobialka S, Wirz-Justice A, Albrecht U. Evening exposure to blue light stimulates the expression of the clock gene PER2 in humans. 2006 Eur J Neurosci 23:1082-1086.

Ceinos RM, Chansard M, Revel F, Calgari C, Míguez JM, Simoneaux V. Analysis of adrenergic regulation of melatonin synthesis in Siberian hamster pineal emphasizes the role of HIOMT. 2004 Neurosignals 13:308-317.

Cohen HN, Hay ID, Annesley TM, Beastall GH, Wallace AM, Spooner R, Thomson JA, Fastwold P, Klee GG. Serum immunoreactive melatonin in boys with delayed puberty. 1982 Clin Endocrinol 17:517-521.

Coon SL, Roseboom PH, Baler R, Weller JL, Namboodiri MA, Koonin EV, Klein DC. Pineal serotonin N-acetyltransferase: expression cloning and molecular analysis. 1995 Science 270:1681-1683.

Coon SL, Weller JL, Korf HW, Namboodiri MAA, Rollag M, Klein DC. cAMP regulation of arylalkylamine N-acetyltransferase (AANAT, EC2.3.1.87): a

new cell line (1E7) provides evidence of intracellular AANAT activation. 2001 J Biol Chem 275:24097-24107.

Coon SL, Del Olmo E, Young WS3rd, Klein DC. Melatonin synthesis enzymes in Macaca mulatta: Focus on arylalkylamine N-acetyltransferase (EC 2.3.1.87). 2002 J Clin Endocrinol Metab 87:4699-4706.

Debruyne JP, Noton E, Lambert CM, Maywood ED, Weaver DR, Reppert SM. A clock shock: mouse CLOCK is not required for circadian oscillator function. 2006 Neuron 50:465-477.

Dehghani F, Hischebeth GT, Wirjatijasa F, Kohl A, Korf HW, Hailer NP. The immunosuppressant mycophenolate mofetil attenuates neuronal damage after excitotoxic injury in hippocampal slice cultures. 2003 Eur J Neurosci 18:1061-1072.

Ekström P, Meissl H. Evolution of photosensory pineal organs in new light: the fate of neuroendocrine photoreceptors. 2003 Philos Trans R Soc Lond B Biol Sci 358:1679-1700.

Ferrari E, Magri F, Dori D, Migliorati G, Nescis T, Molla G, Fioravanti M, Solerte SB. Neuroendocrine correlates of the aging brain in humans. 1995 Neuroendocrinol 61:464-470.

Field MD, Maywood ES, O´Brien JA, Weaver DR, Reppert SM, Hastings MH. Analysis of clock proteins in mouse SCN demonstrates phylogenetic divergence of the circadian clockwork in resetting mechanisms. 2000 Neuron 25:437-447.

Fukuhara C, Dirden JC, Tosini G. Circadian expression of Period 1, Period 2, and arylalkylamine N-acetyltransferase mRNA in the rat pineal gland under different light conditions. 2000 Neurosci Lett 286:167-170.

Fukuhara C, Dirden JC, Tosini G. Regulation of period 1 expression in cultured rat pineal. 2002 Neurosignals 11:103-114.

Fukuhara C, Yamazaki S, Liang J. Pineal circadian clock gate arylalkylamine N-acetyltransferase gene expression in the mouse pineal gland. 2005 J Neurochem 93:156-162.

Von Gall C, Lewy A, Schomerus C, Vivien-Roels B, Pévet P, Korf HW, Stehle JH. Transcription factor dynamics and neuroendocrine signalling in the mouse pineal gland: a comparative analysis of melatonin-deficient C57BL mice and melatonin-proficient C3H mice. 2000 Eur J Neurosci 12:964-972.

Von Gall C, Schneider-Hüther I, Pfeffer M, Dehghani F, Korf HW, Stehle JH. Clock gene protein mPER1 is rhythmically synthesized and under cAMP control in the mouse pineal organ. 2001 J Neuroendocrinol 13:313-316.

Ganguly S, Gastel JA, Weller JL, Schwatz C, Jaffe H, Namboodiri MAA, Coon SL, Hickman AB, Rollag M, Obsil T, Beauverger P, Ferry G, Boutin JA, Klein DC. Role of a pineal cAMP-operated arylalkylamine N-acetyltransferase/14-3-3-binding switch in melatonin synthesis. 2001 Proc Natl Acad Sci U S A 98:8083-8088.

Ganguly S, Weller JL, Ho A, Chemineau P, Malpaux B, Klein DC. Melatonin synthesis: 14-3-3-dependent activation and inhibition of arylalkylamine N-acetyltransferase mediated by phosphoserine-205. 2005 Proc Natl Acad Sci U S A 102:1222-1227.

Gastel JA, Roseboom PH, Rinaldi PA, Weller JL, Klein DC. Melatonin production: proteasomal proteolysis in serotonin N-acetyltransferase regulation. 1998 Science 279:1358-1360.

Gauer F, Poirel VJ, Garidou ML, Simmoneaux V, Pévet P. Molecular cloning of the arylalkylamine-N-acetyltransferase and daily variations of its mRNA

expression in the Syrian hamster pineal gland. 1999 Brain Res Mol Brain Res 71:87-95.

Gerdes HH, Bukoreshtliev NV, Barroso JFV. Tunneling nanotubes: a new route for the exchange of components between animal cells. 2007 FEBS Letters 581:2194-2201.

Hastings MH, Reddy AB, Maywood ES. A clockwork web: circadian timing in brain and periphery, in health and disease. 2003 Nat Rev Neurosci 4:649-661.

Hofman MA, Skene DJ, Swaab, DF. Effect of photoperiod on the diurnal melatonin and 5-methoxytryptophol rhythms in the human pineal gland. 1995 Brain Res 671:254-260.

Hohjoh H, Takasu M, Shishikura K, Takahashi Y, Honda Y, Tokunaga K. Significant association of the arylalkylamine N-acetyltransferase (AA-NAT) gene with delayed sleep phase syndrome. 2003 Neurogenetics 4:151-153.

Hynd MR, Lewohl JM, Scott HL, Dodd PR. Biochemical and molecular studies using human autopsy brain tissue. 2003 J Neurochem 85:543-562.

Johnston NL, Cervenak J, Shore AD, Torrey EF, Yolken RH. Multivariate analysis of RNA levels from postmortem human brains as measured by three different methods of RT-PCR. Stanley Neuropathology Consortium. 1997 J Neurosci Methods 77:83-92.

Johnston JD, Bashforth R, Diack A, Andersson H, Lincoln GA, Hazlerigg DG. Rhythmic melatonin secretion does not correlate with the expression of arylalkylamine N-acetyltransferase, inducible cyclic AMP early repressor, period1 or cryptochrome1 mRNA in the sheep pineal. 2004 Neuroscience 124:789-795.

Kappers JA, Schadé JP. Sturcture and function of the epiphysis cerebri. 1965 Prog Brain Res 10.

Karolczak M, Burbach GJ, Sties G, Korf HW, Stehle JH. Clock gene mRNA and protein rhythms in the pineal gland of mice. 2004 Eur J Neurosci 19:3382-3388.

Karolczak M, Korf HW, Stehle JH. The rhythm and blues of gene expression in the rodent pineal gland. 2005 Endocrine 27:89-100.

Kennaway DJ, Stamp GE, Goble FC. Development of melatonin production in infants and the impact of prematurity. 1992 J Clin Endocrinol Metab 75:367-369.

Kennaway DJ, Lushington K, Dawson D, Lack L, van den Heuvel C, Rogers N. Urinary 6-sulfatoxymelatonin excretion and aging: new results and a critical review of the literature. 1999 J Pineal Res 27:210-220.

Klein DC, Weller JL. Rapid light-induced decrease in pineal serotonin N-acetyltransferase activity. 1972 Science 177:532-533.

Klein DC, Coon SL, Roseboom PH, Weller JL, Bernard M, Gastel JA, Zatz M, Iuvone PM, Rodriguez IR, Begay V, Falcon J, Cahill GM, Cassone VM, Baler R. The melatonin rhythm-generating enzyme: molecular regulation of serotonin N-acetyltransferase in the pineal gland. 1997 Recent Prog Horm Res 52:307-357.

Klein DC. Serotonin N-acetyltransferase. A personal historical perspective. 1999 Adv Exp Med Biol 460:5-16.

Klein DC, Ganguly S, Coon SL, Shi Q, Gaildrat P, Morin F, Weller JL, Obsil T, Hickman A, Dyda F. 14-3-3 Proteins in pineal photoneuroendocrine transduction: how many roles? 2003 J Neuroendocrinol 15:370-377.

Klerman EB. Clinical aspects of human circadian rhythms. 2005 J Biol Rhythms 20:375-386.

Koch M, Mauhin V, Stehle JH, Schomerus C, Korf HW. Dephosphorylation of pCREB by protein serine/threonine phosphatases is involved in activation of Aanat gene transcription in rat pineal gland. 2003 J Neurochem 85:170-179.

Kondratov RV, Chernov MV, Kondratova AA, Gorbacheva VY, Gudkov AV, Antoch MP. BMAL1-dependent circadian oscillation of nuclear CLOCK: posttranslational events induced by dimerization of transcriptional activators of the mammalian clock system. 2003 Genes Dev 17:1921-1932.

Konopka RJ, Benzer S. Clock mutants of Drosophila melanogaster. 1971 Proc Natl Acad Sci U S A 68:2112-2116.

Korf HW, Schomerus C, Stehle JH. The pineal organ, its hormone melatonin, and the photoneuroendocrine system. 1998 Adv Anat Embryol Cell Biol 146:1-100.

Koutcherov Y, Mai JK, Paxinos G. Hypothalamus of the human fetus. 2003 J Chem Neuroanat 26:253-270.

Kwon I, Lee J, Chang SH, Jung NC, Lee BJ, Son GH, Kim K, Lee KH. BMAL1 shuttling controls transactivation and degradation of the CLOCK/BMAL1 heterodimer. 2006 Mol Cell Biol 26:7318-7330.

Laemmli UK. Cleavage of structural proteins during the assembly of the head of bacteriophage T4. 1970 Nature 227:680-685.

Lerner A, Case JD, Takahashi Y. Isolation of melatonin, the pineal gland factor that lightens melanocytes. 1958 J. Am Chem Soc 80:2857-2865.

Lewy AJ. The dim light melatonin onset, melatonin assays and biological rhythm research in humans. 1999 Biol Signals Recept 8:79-83.

Lewy AJ, Emens JS, Lefler BJ, Yuhas K, Jackman AR. Melatonin entrains free-running blind people according to a physiological dose-response curve. 2005 Chronobiol Int 22:1093-1106.

Lewy AJ, Lefler BJ, Emens JS, Bauer VK. The circadian basis of winter depression. 2006 Proc Natl Sci U S A 103:7414-7419.

Liu T, Borjigin J. N-acetyltransferase is not the rate-limiting enzyme of melatonin synthesis at night. 2005 J Pineal Res 39:91-96.

Livak KJ, Schmittgen TD. Analysis of relative gene expression data using real-time quantitative PCR and the 2(-Delta Delta C(T)) method. 2001 Methods 25:402-408.

Lowrey PL, Takahashi JS. Genetics of the mammalian circadian system: photic entrainment, circadian pacemaker mechanisms, and posttranslational regulation. 2000 Annu Rev Genet 34:533-562.

Lynch HJ, Wurtman RJ, Moskowitz MA, Archer MC, Ho MH. Daily rhythm in human urinary melatonin. 1975 Science 17:169-171.

Magri F, Locatelli M, Balza G, Molla G, Cuzzoni G, Fioravanti M, Solerte SB, Ferrari E. Changes in endocrine circadian rhythms as markers of physiological and pathological brain aging. 1997 Chronobiol Int 14:385-396.

Maronde E, Middendorff R, Telgmann R, Muller D, Hemmings B, Tasken K, Olcese J. Melatonin synthesis in the bovine pineal gland is regulated by type II cyclic AMP-dependent protein kinase. 1997 J Neurochem 68:770-777.

Maronde E, Pfeffer M, von Gall C, Dehghani F, Schomerus C, Wicht H, Kroeber S, Olcese J, Stehle JH, Korf HW. Signal transduction in the rodent pineal organ. From the membrane to the nucleus. 1999(a) Adv Exp Med Biol 460:109-131.

Maronde E, Pfeffer M, Olcese J, Molina CA, Schlotter F, Dehghani F, Korf HW, Stehle JH. Transcription factors in neuroendocrine regulation: rhythmic changes in pCREB and ICER levels frame melatonin synthesis. 1999(b) J Neurosci 19:3326-3336.

Maronde E, Stehle JH. The mammalian pineal gland: known facts, unknown facets. 2007 Trends Endocrinol Metab 18:142-149.

Matsubara E, Bryant-Thomas T, Pacheco Quinto J, Henry TL, Poeggeler B, Herbert D, Cruz-Sanchez F, Chyan YJ, Smith MA, Perry G, Shoji M, Abe K, Leone A, Grundke-Ikbal I, Wilson GL, Ghiso J, Williams C, Refolo LM, Pappolla MA, Chain DG, Neria E. Melatonin increases survival and inhibits oxidative and amyloid pathology in a transgenic model of Alzheimer`s disease. 2003 J Neurochem 85:1101-1108.

Oxenkrug GF, Anderson GF, Dragovic L, Blaivas M, Riederer P. Circadian rhythms of human pineal melatonin, related indoles, and beta adrenoreceptors: post-mortem evaluation. 1990 J Pineal Res 9:1-11.

Pardini L, Kaeffer B, Trubuil A, Bourreille A, Galmiche JP. Human intestinal circadian clock: expression of clock genes in colonocytes lining the crypt. 2005 Chronobiol Int 22:951-961.

Potocki L, Glaze D, Tan DX, Park SS, Kashork CD, Shaffer LG, Reiter RJ, Lupski JR. Circadian rhythm abnormalities of melatonin in Smith-Magenis syndrome. 2000 J Med Genet 37:428-433.

Preece P, Virley DJ, Costandi M, Coombes R, Moss SJ, Mudge AW, Jazin E, Cairns NJ. An optimistic view for quantifying mRNA in post-mortem human brain. 2003 Brain Res Mol Brain Res 116:7-16.

Reppert SM, Perlow MJ, Tamarkin L, Klein DC. A diurnal melatonin rhythm in primate cerebrospinal fluid. 1979 Endocrinology 104:295-301.

Reppert SM, Perlow MJ, Tamarkin L, Orloff D, Klein DC. The effects of environmental lighting on the daily melatonin rhythm in primate cerebrospinal fluid. 1981 Brain Res 223:313-323.

Reppert SM. Development of circadian rhythmicity and photoperiodism in mammals. 1989 Research in Perinatal Medicine (IX). New York, Ithaca: Perinatology Press, 262 p.

Reppert SM., Weaver DR. Coordination of circadian timing in mammals. 2002 Nature 418:935-941.

Ribelayga C, Pevet P, Simonneaux V. HIOMT drives the photoperiodic changes in the amplitude of the melatonin peak of the Siberian hamster. 2000 Am J Physiol Regul Integr Comp Physiol 278:R1339-R1345.

Roseboom PH, Coon SL, Baler R, McCune SK, Weller JL, Klein DC. Melatonin synthesis: analysis of the more than 150-fold nocturnal increase in serotonin N-acetyltransferase messenger ribonucleic acid in the rat pineal gland. 1996 Endocrinology 137:3033-3045.

Rüppel R, Olcese J. Bovine pinealocytes in monolayer culture: studies on the adrenergic regulation of melatonin secretion. 1991 Endocrinology 129:2655-2662.

Scharrer E. Photo-neuro-endocrine systems: general concepts. 1964 Ann NY Acac Sci 117:13-22.

Schernhammer ES, Rosner B, Willett WC, Laden F, Colditz GA, Hankinson SE. Epidemiology of urinary melatonin in women and its relation to other hormones and night work. 2004 Cancer Epidemiol Biomarkers Prev 13:936-943.

Schomerus C, Korf HW, Laedtke E, Weller JL, Klein DC. Selective adrenergic/cyclic AMP-dependent switch-off of proteasomal proteolysis alone switches on neural signal transduction: an example from the pineal gland. 2000 J Neurochem 75:2123-2132.

Schomerus C, Laedtke E, Olcese J, Weller JL, Klein DC, Korf HW. Signal transduction and regulation of melatonin synthesis in bovine pinealocytes: impact of adrenergic, peptidergic and cholinergic stimuli. 2002 Cell Tissue Res 309:417-428.

Schramm M, Falkai P, Tepest R, Schneider-Axmann T, Przkora R, Waha A, Pietsch T, Bonte W, Bayer TA. Stability of RNA transcripts in post-mortem psychiatric brains. 1999 J Neural Transm 106:329-335.

Shibui K, Uchiyama M, Okawa M. Melatonin rhythms in delayed sleep phase syndrome. 1999 J Biol Rhythms 14:72-76.

Smith JA, Padwick D, Mee TJ, Minneman KP, Bird ED. Synchronous nyctohemeral rhythms in human blood melatonin and in human post-mortem pineal enzyme. 1977 Clin Endocrinol 6:219-225.

Smith KA, Schoen MW, Czeisler CA. Adaptation of human pineal melatonin suppression by recent photic history. 2004 J Clin Endocrinol Metab 89:3610-3614.

Spanagel R, Pendyala G, Abarca C, Zghoul T, Sanchis-Sequra C, Magnone MC, Lascorz J, Depner M, Holzberg D, Soyka M, Schreiber S, Matsuda F, Lathrop M, Schumann G, Albrecht U. The clock gene Per2 influences the glutamatergic system and modulates alcohol consumption. 2005 Nature Medicine 11:35-42.

Stehle JH, Foulkes NS, Molina CA, Simmonneaux V, Pévet P, Sassone-Corsi P. Adrenergic signals direct rhythmic expression of transcriptional repressor CREM in the pineal gland. 1993 Nature 365:314-320.

Stehle JH, von Gall C, Korf HW. Analysis of cell signaling in the rodent pineal gland deciphers regulators of dynamic transcription in neural/endocrine cells. 2001(a) Eur J Neurosci 14:1-9.

Stehle JH, von Gall C, Schomerus C, Korf HW. Of rodents and ungulates and melatonin: creating a uniform code for darkness by different signaling mechanisms. 2001(b) J Biol Rhythms 16:312-325.

Takekida S, Yan L, Maywood ES, Hastings MH, Okamura H. Differential adrenergic regulation of the circadian expression of the clock genes Period1 and Period2 in the rat pineal gland. 2000 Eur J Neurosci 12:4557-4561.

Takimoto M, Hamada A, Tomoda A, Ohdo S, Ohmura T, Sakato H, Kawatani J, Jodoi T, Nakagawa H, Terazono H, Koyanagi S, Higuchi S, Kimura M, Tukikawa H, Irie S, Saito H, Miike T. Daily expression of clock genes in whole blood cells in healthy subjects and a patient with circadian rhythm sleep disorder. 2005 Am J Physiol Regul Integr Comp Physiol 289:R1273-R1279.

Tamanini F, Yagita K, Okamura H, Van der Horst GT. Nucleocytoplasmic shuttling of clock proteins. 2005 Methods Enzymol 393:418-435.

Tamaru T, Isojima Y, Van Der Horst GT, Takei K Nagai K, Takamatsu K. Nucleocytoplasmic shuttling and phosphorylation of BMAL1 are regulated by circadian clock in cultured fibroblasts. 2003 Genes Cells 8:973-983.

Teboul M, Barrat-Petit MA, Li XM, Claustrat B, Formento JL, Delaunay F, Lévi F, Milano G. Atypical patterns of circadian clock gene expression in human peripheral blood mononuclear cells. 2005 J Mol Med 83:693-699.

Toh KL, Jones CR, He Y, Eide EJ, Hinz WA, Virshup DM, Ptácek LI, Fu YH. An hPer2 phosphorylation site mutation in familial advanced sleep phase syndrome. 2001 Science 291:1040-1043.

Touitou Y, Fevre M, Bogdan A, Reinberg A, De Prins J, Beck H, Touitou C. Patterns of plasma melatonin with ageing and mental condition: stability of nyctohemeral rhythms and differences in seasonal variations. 1984 Acta Endocrinol 106:145-151.

Travnickova-Bendova Z, Cermakian N, Reppert SM, Sassone-Corsi P. Bimodal regulation of mPeriod promoters by CREB-dependent signaling and CLOCK/BMAL1 activity. 2002 Proc Natl Acad Sci U S A 99:7728-7733.

Turek FW, Joshu C, Kohsaka A, Lin E, Ivanova G, McDearmon E, Laposky A, Losee-Olson S, Easton A, Jensen DR, Eckel RH, Takahashi JS, Bass J. Obesity and metabolic syndrome in circadian Clock mutant mice. 2005 Science 308:1043-1045.

Vondrasová D, Hájek I, Illnerová H. Exposure to long summer days affects the human melatonin and cortisol rhythms. 1997 Brain Res 759:166-170.

Vondrasová-Jelínková D, Hájek I, Illnerová H. Adjustment of the human melatonin and cortisol rhythms to shortening of the natural summer photoperiod. 1999 Brain Res 816:249-53.

Waldhauser F, Weiszenbacher G, Tatzer E, Gisinger B, Waldhauser M, Schemper M, Frisch H. Alterations in nocturnal serum melatonin levels in humans with growth and aging. 1988 J Clin Endocrinol Metab 66:648-652.

Wittkowski W, Bockmann J, Kreutz MR, Böckers TM. Cell and molecular biology of the pars tuberalis of the pituitary. 1999 Int Rev Cytol 185:157-194.

Wei N, Tsuge T, Serino G, Dohmae N, Takio K, Matsui M, Deng XW. The COP9 complex is conserved between plants and mammals and is related to the 26S proteasome regulatory complex. 1998 Curr Biol 8:919-922.

Wu YH, Feenstra MG, Zhou JN, Liu RY, Torano JS, Van Kan HJ, Fischer DF, Ravid R, Swaab DF. Molecular changes underlying reduced pineal melatonin levels in Alzheimer disease: alterations in preclinical and clinical stages. 2003 J Clin Endocrinol Metab 88:5898-5906.

Wu YH, Fischer DF, Kalsbeek A, Garidou-Boof ML, Van der Vliet J, Van Heijningen C, Liu RY, Zhou JN, Swaab DF. Pineal clock gene oscillation is disturbed in Alzheimer´s disease, due to functional disconnection from the "master clock". 2006 FASEB J 20:1874-1876.

Yagita K, Tamanini F, Yasuda M, Hoeijmakers JH, Van der Horst, GT, Okamura H. Nucleocytoplasmic shuttling and mCRY-dependent inhibition of ubiquitylation of the mPER2 clock protein. 2002 EMBO J 21:1301-1314.

Yasojima K, McGeer EG, McGeer PL. High stability of mRNAs postmortem and protocols for their assessment by RT-PCR. 2001 Brain Res Brain Res Protoc 8:212-218.

Yoo SH, Ko CH, Lowrey PL, Buhr ED, Song EJ, Chang S, Yoo OJ, Yamazaki S, Lee C, Takahashi JS. A noncanonical E-box enhancer drives mouse period2 circadian oscillations in vivo. 2005 Proc Natl Acad Sci USA 102:2608-2613.

Zeitzer JM, Daniels JE, Duffy JF, Klerman EB, Shanahan TL, Dijk DJ, Czeisler CA. Do plasma melatonin concentrations decline with age? 1999 Am J Med 107:432-436.

Zeitzer JM, Dijk DJ, Kronauer R, Brown E, Czeisler C. Sensitivity of the human circadian pacemaker to nocturnal light: melatonin phase resetting and suppression. 2000 J Physiol 526:695-702.

Zheng W, Schwarzer D, LeBeau A, Weller JL, Klein DC, Cole PA. Cellular stability of serotonin N-acetyltransferase conferred by phosphonodifluoromethylene alanine (pfa) substitution for ser-205. 2005 J Biol Chem 280:10462-10467.

7 Appendix

7.1 Specimens analyzed

Table 1: Summary of clinical data and post-mortem variables of the specimens that were used in here presented analyses (#: Immunofluorescence samples, *: Degradation Study).

Sample	sex	age [y]	PMI [h]	cause of death	group
1	m	30	48	Intoxication	night
2	m	23	91	Intoxication	night
3	m	53	16	Hypoxia	dusk
4	m	35	42	Undetermined	dusk
5	m	51	141	Heart desease	dusk
6	f	42	10	Aspiration	dawn
7	m	38	31	Intoxication?	dawn
8	f	37	67	Heart desease	day
9	f	10	45	Traffic accident	day
10	m	42	32	Intoxication	night
11	f	39	36	Drowning	night
12	f	82	31	Central collapse	night
13	m	42	10	Intoxication	night
14	m	22	47	Heart desease	day
15	f	59	63	Purler	dusk
16	m	40	54	Intoxication?	night
17	f	34	13	Bleeding	night
18	f	33	54	Intoxication	dusk
19	f	62	27	Brain death	dawn
20	m	43	61	Bleeding?	night
21	m	46	86	Hanging	night
22	m	73	25	Heart desease	day
23	f	75	40	Intoxication	night
24	m	39	24	Intoxication	dusk
25	m	76	62	Strangulation	dusk
26	f	53	46	Drowning?	day
27	f	32	48	Heart desease?	dawn
28	f	36	24	Strangulation	dusk
29	m	56	82	Heart desease	night
30	m	25	18	Intoxication?	dusk
31	m	60	16	Pneumonia	dusk
32	m	52	27	Heart desease	dawn
33	m	43	21	Bleeding	dusk
34	m	34	48	Heart desease	day
35	m	66	27	Heart desease	day
36	m	41	24	Heart desease	day

to be continued next page

continued from previous page

Sample	sex	age [y]	PMI [h]	cause of death	group
37	f	32	12	Intoxication?	night
38	m	30	36	Purler	dawn
39	m	23	43	Decapitation	dusk
40	f	84	50	Intoxication	dawn
41	m	36	77	Traffic accident	night
42	m	56	55	Heart desease	night
43	m	36	47	Bleeding	day
44	f	43	9	Heart desease	night
45	m	58	44	Hanging	dusk
46	f	60	36	Bleeding	night
47	m	25	34	Intoxication	night
48	f	63	84	Heart desease	night
49	m	57	54	Heart/Lung desease	dawn
50	m	71	26	Heart desease?	day
51	m	67	45	Pneumonia	day
52	m	52	42	Central collapse	dusk
53	m	66	92	Bleeding	dusk
54	m	34	36	Intoxication	night
55	m	29	107	Intoxication?	night
# 56	f	72	147	Heart desease	dawn
# 57	m	41	16	Heart desease	night
58	f	51	52	circulation collapse	dawn
59	f	32	19	Intoxication	dusk
60	m	31	64	Intoxication	dusk
61	m	59	88	Traffic accident	dusk
# 62	m	96	71	Heart disease	day
# 63	m	79	48	Heart disease	day
# 64	m	71	68	Traffic accident	day
# 65	f	58	18	Traffic accident	dusk
# 66	f	34	15	Intoxication	dusk
# 67	m	24	41	Heart disease	dusk
# 68	f	50	58	Purler	night
# 69	f	46	33	Bleeding	night
# 70	m	57	104	Heart disease	night
#71	m	32	29	Bleeding	dawn
#72	m	46	90	Bleeding	dusk
#73	m	39	24	Bleeding	day
#74	m	42	26	Heart disease	day
n (w):	25	47	47		MEAN
n (m):	49	2	3		SEM
*75	m	58	< 48	Bleeding	night
*76	f	40	< 19	Aspiration?	dusk
*77	f	18	47	Traffic accident	day

7.2 Primer sequences

Table 2: Primer sequences, length of PCR products and GenBank accession numbers for all genes analyzed (*: for real-time PCR only).

Gene	Primer forward 5'→3' Primer reverse 5'→3'	Base pairs	Accession Nr.
Aanat	CAGAGCACCCACCCCCTGAAAC CCTGCATGAGTCTCTCCTTGTC	310	NM_001088
Aanat*	AGATGTGGCAGCCTCTGGAG GCACCTGAGGCTGATCCTTC	53	D90041
Hiomt	CGCCTCCTTAATGACTACGCCA TTGACGCTCCAGACCTCCTG	473	NM_004043
Hiomt*	CAGGTGGTGGCATTCTGGTA CCTCGCCTGTCTTCATCCA	52	U11090
Per1	CAGTGCTCCTGTTCCTGCATC CCCGCCAACTGCAGAATCT	76	NM_002616
Cry1	TCCGCTGCGTCTACATCCT AGCAAAAATCGCCACCTGTT	76	NM_004075
Bmal1	CCAGAGGCCCCTAACTCCTC TGGTCTGCCATTGGATGATCT	79	NM_001178
Clock	TTGGCAAAATGTCATGAGCAC TTGCCCCTTAGTCAGGAACCT	78	NM_004898
Gapdh	GCACCGTCAAGGCTGAGAAC GCCTTCTCCATGGTGGTGAA	150	NM_002046
EF 1a	AAGCTGGAAGATGGCCCTAAA AAGCGACCCAAAGGTGGAT	98	J04617

7.3 Resources

7.3.1 Chemicals

^{14}C-Acetyl coenzyme A (10 mM, 60 Ci/mol)	Perkin Elmer
N-Acetylserotonin (1.3 mM)	Sigma-Aldrich
Acrylamide 4K (30% solution; mix 29:1)	AppliChem
Adenosyl-L-methionine, S-[methyl-^{14}C] (0.06 mM, 55 Ci/mol)	Perkin Elmer
Agarose (high resolution)	Roth
Ammoniumacetate	AppliChem
Ammoniumperoxodisulfate (APS)	Merck
Boric acid	Roth
Bovine serum albumine	PAA Laboratories
Bromphenol blue	Merck
Chloroform	Merck
Coomassie Brilliant Blue R-250	Fluka
Diaminobenzidine (DAB)	Merck
Disodiumhydrogenphosphate (Na_2HPO_4)	Roth
Dipotassiumhydrogenphosphate (K_2HPO_4)	Roth
Ethylenediaminetetraacetate (EDTA)	Merck
Ethanol 99,8 % p.a.	Roth
Ethidiumbromide (EtBr)	Fluka
ExtrAvidin-peroxidase	Sigma
Glycine	Roth
Glycerol (cell culture grade)	AppliChem
Hydrogenperoxide (H_2O_2)	Roth
Hexanucleotide mixture (10x)	Roche
Hydrochloric acid (HCl)	Merck
Magnesiumchloride ($MgCl_2$)	Roth
Magnesiumsulfate ($MgSO_4$)	Roth
2-Mercaptoethanol	Merck
Methanol	Merck
M-MLV reverse transcriptase	Promega

Mounting Medium (Fluorescence)	DakoCytomation
NGS/NDS	Sigma
NP 40	AppliChem
Oligo dT-primers	Roche
Orange G	Fermentas
Paraformaldehyde	Merck
Ponceau red	Sigma
Potassiumchloride (KCl)	Roth
Potassiumdihydrogen phosphate (KH_2PO_4)	Roth
Protease Inhibitor Cocktail Tablets	Roche
Protein A/G PLUS-Agarose	Santa Cruz
Phosphatase Inhibitor Cocktail Set II	Calbiochem
Rotiblock	Roth
Rotiszint eco plus	Roth
Saccharose	Fluka
Sodiumchloride (NaCl)	Sigma
Sodiumdihydrogen phosphate (NaH_2PO_4)	Roth
Sodiumdodecylsulfate (SDS)	Roth
Sodiumhydroxide (NaOH)	Roth
Sodiumtetraborate	Roth
Sudan Black	Chroma
Sulfosalicylic acid	Merck
SuperSignal West Pico Chemiluminescent Substrate	Pierce
N,N,N´,N´-Tetramethyldiamine (TEMED)	Roth
TissueTek	Sakura
Tris base	Sigma
Trichloroacetic acid	Merck
Triton X-100	Roth
Tryptamine (1 mM)	Fluka
Tween 20	Merck
Xylol	Sigma

7.3.2 Antibodies

7.3.2.1 Primary antibodies

Table 3: Primary antibodies for the detection in Western blot (WB) and in immunohistochemical/immunofluorescence (IHC) analyses.

Antibody	Host	WB	IHC	Company	Catalog
Anti-β–Actin	Rabbit	1:1.000	-	Sigma	A 2066
Anti-AANAT	Rabbit	1:1.000	1:1.000	Chemicon	AB5467
Anti-HIOMT	Mouse	1:5.000	1:4.000	Abnova	H00000438-A01
Anti-NPCP	Mouse	-	1:5.000	Covance	A488-120L
Anti-PER1	Goat	1:100	1:100	Santa-Cruz	sc-7724
Anti-CRY1	Rabbit	1:500	1:200	Abgent	AP6134a
Anti-CLOCK	Rabbit	1:500	1:200	ABR	PA1-520
Anti-BMAL1	Rabbit	1:100	1:60	Alpha Diagn.	MOP31-A
Anti-14-3-3	Sheep	1:50	1:10	AbD Serotec	7835-1009
Anti-FSH	Sheep	-	1:400	Quartett	1458105454
Anti-calbindin	Rabbit	-	1:200	Swant	CB-38a

7.3.2.2 Secondary antibodies

Table 4: Secondary antibodies used in Western blot and immunohistochemical analyses.

Antibody	Host	Dilution	Company	Catalog
Anti-rabbit IgG HRP-conj.	Goat	1:10.000	Cell Signaling	7074
Anti-goat IgG HRP-conj.	Cow	1:10.000	Santa-Cruz	sc-2352
Anti-mouse IgG HRP-conj.	Goat	1:1.000	DakoCytomation	P 0447
Anti-sheep IgG HRP-conj.	Rabbit	1:5.000	AbD Serotec	5184-2504
Alexa Fluor anti-goat 568	Donkey	1:200	Molecular Probes	A 11057
Alexa Fluor anti-rabbit 568	Goat	1:200	Molecular Probes	A 11011
Alexa Fluor anti-rabbit 488	Goat	1:200	Molecular Probes	A 11008
Alesa Fluor anti-mouse 488	Goat	1:200	Molecular Probes	A 11001
Alexa Fluor anti-sheep 488	Donkey	1:200	Molecular Probes	A 11015
Alexa Fluor anti-sheep 568	Donkey	1:200	Molecular Probes	A 21099
Anti-rabbit IgG Biotin-conj.	Goat	1:100	Sigma	B 7389
Anti-goat IgG Biotin-conj.	Rabbit	1:100	Sigma	B 7014

7.3.3 Kits

Absolutely RNA miniprep kit	Stratagene
Melatonin ELISA kit	IBL
Coomassie Protein Assay Kit	Pierce
SYBR Green PCR kit	Applied Biosystems
FastStart DNA master SYBR green 1	Roche
Taq DNA polymerase kit	Invitrogen

7.3.4 Protein and DNA standards

EZ Load Precision Molecular Mass Standard	BioRad
Precision Plus Protein Kaleidoscope Standard	BioRad

7.3.5 Equipment and miscellaneous

ABI Prism 7000 Sequence Detection System	Applied Biosystems
Centrifuges	
Biofuge pico	Heraeus
Biofuge fresco	Heraeus
Multifuge 3 L-R	Heraeus
ChemiDoc software Quantity One	BioRad
Confocal laser scanning microscope (LSM510)	Zeiss
ELISA reader (Multiscan RC)	LabSystems
Image analysis system (ChemiDoc XRS)	BioRad
Horizontal Sub-Cell System	BioRad
LightCycler 1.5	Roche
Liquid scintillation analyzer 2500 TR	Packard
Microscope slides SuperFrost Plus	Menzel
Mini-PROTEAN 3 Electrophoresis System	BioRad
Mini Trans-Blot Cell (Tank transfer)	BioRad
PowerPac HC High-Current Power Supply	BioRad
Sonifier UW 70	Bandelin
Thermocycler	Primus
UV-Vis spektrophotometer SmartSpec Plus	BioRad

7.4 Buffers and solutions

7.4.1 Agarose gel electrophoresis

TBE-buffer (1 l)

10.8 g Tris
4.0 ml EDTA (0.5 M, pH 8)
5.5 g boric acid

Gel-loading buffer (5x)

574 µl 50% glycerol (87%)
426 µl ddH_2O
0.25% Orange G (w/v)

7.4.2 SDS-PAGE

Sample buffer (2x)

2.5 ml Tris/HCl (1 M, pH6.8)
4% SDS (w/v)
10 % glycerol (v/v)
0.1 % bromphenol blue
2 % 2-mercaptoethanol (v/v)
6 ml ddH_2O

Lower gel (10%)

5.4 ml ddH_2O
2.8 ml 1.5 M Tris/HCl pH 8,9
2.8 ml Acrylamide (30%; Acrylamide:Bisacrylamide = 29:1)
112 µl SDS (10%)

Upper gel

1.4 ml ddH_2O

0.75 ml Bromphenol blue

37 µl SDS (10%)

560 µl Acrylamide (30%, Acrylamide:Bisacrylamide = 29:1)

1313 µl 0.5 M Tris pH 6,8

Running buffer (1 l)

6 g Tris

28.8 g glycine

10 ml 10% SDS (w/v)

7.4.3 Immunoblotting

Blotting-buffer (1 l)

5.8 g Tris

2.9 g glycine

0.37 g SDS

Ponceau Red (10x)

2 g Ponceau Red

30 g trichloroacetic acid

30 g sulfosalicylic acid

TBS (10x, 1 l)

24.2 g Tris

80 g NaCl

TBS-Tween (1 l)

100 ml 10x stock TBS

1 ml Tween 20

7.4.4 Immunohistochemistry and Immunofluorescence

PBS (0.02 M, pH 7.4, 1 l)

2.27 g Na_2HPO_4

0.54 g KH_2PO_4

9.0 g NaCl

Phosphate buffer (0.2 M, pH 7.4, 1 l)

22.7 g Na_2HPO_4

5.4 g KH_2PO_4

9.0 g NaCl

PFA (4 %, pH 7.4, 1 l)

40 g paraformaldehyde

500 ml 0.2 M phosphate buffer

500 ml dd H_2O

Acknowledgment

First of all I would like to express my gratitude to Prof. Dr. Jörg H. Stehle for the opportunity to work in his group and under his supervision. He provided excellent working conditions and all kinds of scientific support necessary for carrying out my doctoral studies. Furthermore, he offered me a more than fascinating topic for my thesis, and the possibility to accomplish my studies with a lot of freedom. Thanks to him for fruitful discussions and continuous support, and for the opportunity to get a deep insight into human chronobiology.

I am thankful to Prof. Dr. Jürgen H. Bereiter-Hahn as my 'Fachbereichs-supervisor' for continuous help and support.

Prof. Gerold Kauert must be thanked for his support that constituted the basis for my doctoral studies, namely providing autoptic human tissue.

I thank Prof. Dr. H. Zimmermann for accepting me as a member of the graduate school 'Neuronal plasticity', giving me the chance to meet other highly motivated doctoral students in a stimulating atmosphere.

Next, I am thankful to Prof. Erik Maronde for his continuous help, for inspiring discussions and his patience in answering all of my questions.

PD Dr. Faramarz Dehghani is thanked for his great support, and for the 'dark hours' at the confocal microscope, as well as for interesting and motivating discussions. Importantly, Prof. Dr. Maronde and PD Dr. Dehghani always had a cup of coffee for me.

I am also grateful to PD Dr. Abdelhaq Rami for introducing me into immunofluorescence microscopy.

Special thanks to Dr. Magdalena Karolczak, who has left the group in the middle of my studies. She introduced me into methods of molecular biology and spent more than one evening with me sitting at the Main river.

I am grateful to Antje Jilg for inspiring debates, and for her help in many different situations, and her patience in teaching me knitting socks.

I am grateful to Dr. Marco Koch for inspiring debates about the AANAT project and the kind supply of rat pineal glands. Together with PD Dr. Christof Schomerus, they must be thanked for introducing me in the measurement of enzyme activities.

I thank Sina Kühne and Florian Wunderer for experimental help with processing human pituitaries.

I am thankful to Dr. Estifanos Ghebremedhin and PD Udo Rüb for their valuable help with statistical questions.

I thank Dr. Tamás Sebestény and Bernd vom Schemm for help with the generation of figures.

Next, I am grateful to the technical support team, namely Gaby Sties, Angelika Langhagen and Natalie Peruzki, for their invaluable help and support during my studies.

All members of the Institute of Anatomy III are thanked for the nice time, interesting discussions, continuous support, photo-sessions, cheerful evenings, nice chats about books and cooking and whisky... All of this made work really enjoyable.

Members of the Institute for Forensic Medicine, University Frankfurt, and in particular the assistants performing autopsies, namely R. Bux, H. Auer, S. Eckhold, and M. Enders are thanked for their continuous help and support during tissue collection.

I am grateful to Dr. David Hazlerigg for the kind supply of sheep pineal sections, and to Prof. Dr. Wilfred Den Dunnen for the kind supply of human hypothalami.

Thanks for the financial support of my studies, namely grants from Riese-, Ebert-, and Scheidel-Stiftung, and Stiftung Forensisches Forum.

I am much obliged to my parents who laid the basis for my ‘scientific career’ by enabling me to study biochemistry without having to bother much about unimportant things. Thanks for your continuous support.

This thesis is espcially dedicated to my longtime companion, Bela Ernest Bode - for consoling me, or calming me down if necessary, for motivation, fruitful discussions and for any help and backing I needed. He also shared my happiness whenever possible and gave me the strength to go on.

Lebenslauf

Name:	Ackermann
Vorname:	Katrin
Adresse:	J.W. Goethe-Universität
	Dr. Senckenbergische Anatomie
	Institut für Anatomie III
	Theodor-Stern-Kai 7
	60590 Frankfurt am Main
	Tel: 069-6301-6426
	Fax: 069-6301-6920
	email: Kat.Ackermann@med.uni-frankfurt.de
Privat:	Carl-Goerdeler-Str. 5
	60320 Frankfurt am Main
	email: K@trinsche.de

Geboren am:	26.04.1977
Geburtsort:	Neunkirchen/Saar
Persönlicher Statut:	ledig
Staatsangehörigkeit	deutsch

Ausbildung und wissenschaftlicher Werdegang:

1987 – 1996 Privates staatlich anerkanntes Gymnasium “Albertus-Magnus” in St. Ingbert, Erwerb der Allgemeinen Hochschulreife (Abitur) 1996

1996 – 1998 Ausbildung zur Chemielaborantin am Institut für Rechtsmedizin, Universität des Saarlandes, Homburg/Saar; Abschluß der Ausbildung mit Auszeichnung 1998

1998 – 2003 Biochemiestudium an der Universität von Bayreuth (erstes und zweites Semester) und an der J.W. Goethe-Universität Frankfurt am Main

01/02 2003 Biochemie-Diplom-Prüfungen
Fächer: Biochemie, Biophysikalische Chemie, Zellbiologie

03-09 2003 Diplomarbeit über "NMR-spektroskopische Untersuchungen einer Lysozym-Mutante sowie eines neu entwickelten Lanthanide-bindenden Peptid-Tags". Betreuer: Professor Harald Schwalbe, Institut für Organische Chemie und Chemische Biologie, BMRZ Niederursel

09/2003 Erwerb des Grades der Diplom-Biochemikerin (Gesamtnote: sehr gut)

01-03/2004 Stipendium im Rahmen des EU-Projektes „Structural Proteomics in Europe" bei Prof. Harald Schwalbe, Institut für Organische Chemie und Chemische Biologie, BMRZ Niederursel

2004-2008 Promotion am Institut für Anatomie; Betreuer: Prof. Dr. J.H. Stehle, Prof. Dr. J. Bereiter-Hahn

Akademische Lehrer

J. Bereiter-Hahn, W. Brüggemann, E. Egert, H. Fasold, M. Göbel, C. Griesinger, S. Hashmi, B. Ludwig, H. Rüterjans, O. Schiemann, H. Schwalbe, R. Tampé, H. Zimmermann.

Publikationen

Original-Artikel in Peer-reviewed Journals:

Christian Schlörb, Katrin Ackermann, Christian Richter, Julia Wirmer, Harald Schwalbe (2005). Heterologous expression of hen egg white lysozyme and resonance assignment of tryptophan side chains in its non-native states. **Journal of Biomolecular NMR** 33:95-104.

Katrin Ackermann, Roman Bux, Udo Rüb, Horst-Werner Korf, Gerold Kauert, Jörg H. Stehle (2006). Characterization of human melatonin synthesis using autoptic pineal tissue. **Endocrinology** 147(7):3235-3242.

Katrin Ackermann, Faramarz Dehghani, Roman Bux, Gerold Kauert, Jörg H. Stehle (2007). Day-night expression patterns of clock genes in the human pineal gland. **Journal of Pineal Research** 43(2):185-194.

Katrin Ackermann, Erik Maronde, Faramarz Dehghani, Gerold Kauert, Jörg H. Stehle. New aspects in regulation of melatonin synthesis in the human pineal gland. (*in preparation*)

Katrin Ackermann, Sina Kühne, Florian Wunderer, Gerold Kauert, Jörg H. Stehle. Clock genes in the human pituitary gland. (*in preparation*)

Reviews:

Katrin Ackermann, Jörg H. Stehle (2006). Melatonin synthesis in the human pineal gland: advantages, implications and difficulties – a mini-review. **Chronobiology International** 23 (1&2):369-379.

Jörg H. Stehle, Tamás Sebestény, Katrin Ackermann. Rhythm and blues of the human pineal gland. **Progress in Brain Research**. (*in preparation*)

Katrin Ackermann, Jörg H. Stehle. Clock genes and the mammalian pineal gland: a remnant left-over, ticking away, or timely regulators, clocking ahead? **Journal of Pineal Research**. (*in preparation*)

Abstracts und Kongressbände:

Katrin Ackermann, Roman Bux, Faramarz Dehghani, Gerold Kauert, and Jörg H. Stehle (2007). Clock genes in the human pineal gland. **European Journal of Cell Biology** 86S1 (Suppl. 57):14.

Katrin Ackermann, Jörg H. Stehle (2007). Genetische Grundlagen der Chronobiologie – zirkadiane Rhythmogenese und Uhrengene im Menschen. Zitierfähiger Kongressband der GSAAM-Tagung 2007. (*in press*)

Poster

Gordon Research Conference on Pineal Cell Biology, Buellton, Kalifornien, 15.01.2006-20.01.2006:
Katrin Ackermann, Gerold Kauert, Jörg H. Stehle. Characterization of human melatonin synthesis using autoptic pineal tissue.

Abschluß-Symposium des Graduiertenkollegs "Neuronale Plastizität: Moleküle, Strukturen, Funktionen", Frankfurt/Main, 22.09.2006:
Katrin Ackermann, Roman Bux, Udo Rüb, Horst-Werner Korf, Gerold Kauert, Jörg H. Stehle. Melatonin synthesis in the human pineal gland.

23. Arbeitstagung der Anatomischen Gesellschaft, Würzburg, 27.09.2006-29.09.2006:
Jörg H. Stehle, Roman Bux, Udo Rüb, Horst-Werner Korf, Gerold Kauert, Katrin Ackermann. Characterization of human melatonin synthesis using autoptic pineal tissue.

Annual meeting of the Study Group Neurochemistry (Gesellschaft für Biochemie und Molekularbiologie, GBM): Molecular pathways in health and disease of the nervous system, Witten, 28.09.2006 – 30.09.2006:
Katrin Ackermann, Gerold Kauert, Jörg H. Stehle. Melatonin synthesis in the human pineal gland.

Annual meeting of the German Society for Cell Biology, Frankfurt/Main, 14.03.2007-17.03.2007:
Katrin Ackermann, Roman Bux, Faramarz Dehghani, Gerold Kauert, and Jörg H. Stehle. Clock genes in the human pineal gland.

ICN (Interdisciplinary Center for Neuroscience) Kurzsymposium, Frankfurt/Main, 13.04.2007:
Katrin Ackermann, Roman Bux, Faramarz Dehghani, Gerold Kauert, and Jörg H. Stehle. Clock genes in the human pineal gland.

Vorträge

X. Congress of the EPBRS (European Pineal and Biological Rhythms Society, jetzt EBRS), Frankfurt am Main, 01.09.2005-05.09.2005,
Katrin Ackermann, Roman Bux, Udo Rüb, Christof Schomerus, Horst-Werner Korf, Gerold Kauert, Jörg H. Stehle. Characterization of diurnal patterns in *Aanat* mRNA, AANAT activity and melatonin content in autoptic human pineal tissue.

7. Konferenz der GSAAM (Deutsche Gesellschaft für Prävention und Anti-Aging Medizin e.V.), München, 10.05.2007-12.05.2007,
Katrin Ackermann. Genetische Grundlagen der Chronobiologie – zirkadiane Rhythmogenese und Uhrengene im Menschen. (*Invited talk*)

Förderung

Januar bis März 2004: Stipendium im Rahmen des EU-Projektes "Structural Proteomics in Europe"

2005: Stiftungsmittel: Arthur und Margarete Ebert-Stiftung (6.000 Euro)

2006: Gordon Research Conference on Pineal Cell Biology, Buellton, Kalifornien: Übernahme der Teilnahmekosten (Registrierungsgebühr, Unterbringung und Verpflegung) durch den Vorsitzenden (Chair's fund; 895 $)

2006: Stiftungsmittel: August Scheidel-Stiftung (1.305,37 Euro); Heinrich und Fritz Riese-Stiftung (7.694,63 Euro); Stiftung Forensisches Forum (1.000 Euro)

Sonstiges

Mitglied des Graduiertenkollegs "Neuronale Plastizität: Moleküle, Strukturen, Funktionen" ab April 2006.